

Preface

The Finnish Defence Forces Logistics Command, Joint System Centre (FDFLOGCOM JSC) initiated and supported this work. The editors are indebted to the following individuals who helped in the preparation of the review (organizations and individuals in alphabetical order):

Aalto	<i>Aalto University, School of Engineering, Department of Mechanical Engineering: Olli Saarela, Iikka Virkkunen;</i>
AFCOMFIN	<i>Air Force Command Finland: Kalle Vaaraniemi (PoC);</i>
ARCOMFIN	<i>Army Command Finland: Ville Siiröpää (PoC);</i>
Areca	<i>Areca Ltd: Arto Mattila;</i>
Elomatic	<i>Elomatic Ltd: Jarkko Aakkula, Juho Ilkko, Risto Kallinen, Matti Palin, Esa Salminen, Timo Siikonen, Jaakko Sotkasiira;</i>
Emmecon	<i>Emmecon Ltd: Risto Hedman;</i>
Eurofins ES	<i>Eurofins, Expert Services Ltd: Markku Hentinen, Perttu Hintikka, Juha Juntunen, Samuli Korhikoski, Sebastian Segercrantz, Antti Sivonen, Kari Vähävaara, Aki Vääntinen (Compite);</i>
FDFLOGCOM JSC	<i>Finnish Defence Forces Logistics Command, Joint Systems Centre: Riku Lahtinen (PoC);</i>
FINAFSAC ACC	<i>Satakunta Air Command, Air Combat Centre, Flight Test Section: Pasi Greus (PoC);</i>
Insta ILS	<i>Insta ILS Oy: Tuure Hakavuori, Mikko Vesa;</i>
Patria	<i>Patria Aviation Oy, RTD & Aeronautical Engineering: Jarno Havusto, Jaakko Hoffren, Toivo Hukkanen, Henri Kauppila, Mika Keinonen, Jussi Kettunen, Yrjö Laatikainen, Miika Laulajainen, Mirve Liius, Janne Linna, Juha Lähteenmäki, Simo Malmi, Matias Mattila, Antero Miettinen, Mikko Orpana, Jorma Patronen, Jouni Pirtola, Tuomo Salonen, Jarkko Tikka, Kari Vertanen, Marko Ylitalo, Markus Wallin;</i> <i>Patria Aviation Oy, Systems / Avionics: Tini Mäkelä, Marika Vuori;</i>
TAU	<i>Tampere University, Plastics and Elastomer Technology: Mikko Kanerva, Jarno Jokinen, Olli Orell;</i>
Trano	<i>Trano Ltd: Harri Janhunen;</i>
Trueflaw	<i>Trueflaw Ltd: Iikka Virkkunen;</i>

VTT

VTT Technical Research Centre of Finland Ltd: Jouni Alhainen, Esko Arilahti, Pertti Auerkari, Juha-Matti Autio, Samuli Eskola, Antti Forsström, Elisa Isotahdon, Oskari Jessen-Juhler, Petteri Kokkonen, Jukka Koskela, Keijo Koski, Tuomas Koskinen, Risto Laakso, Timo Lehti, Taru Lehtikuusi, Esa Leskelä, Sebastian Lindqvist, Sauli Liukkonen, Johanna Lukin, Maija Marja-aho, Jukka Maunumäki, Sakari Merinen, Jarkko Metsäjoki, Jukka Mäkinen, Vesa Nieminen, Arto Nyholm, Matti Okkonen, Pasi Puukko, Juhani Rantala, Kalle Raunio, Joni Reijonen, Jari Rinta-aho, Mikko Savolainen, Aslak Siljander, Tuomas Teittinen, Antti Tuhti, Antti Vaajoki, Piritta Varis, Tomi Viitanen.

Espoo, 24 June 2021

Editors

Contents

Preface	2
Contents	4
1 Introduction.....	5
1.1 Valmet L-70 Vinka	8
1.2 Grob G 115E.....	10
1.3 Hawk Mk.51/51A and Mk.66.....	11
1.4 F/A-18C/D Hornet	13
1.5 HX Fighter Program.....	17
1.6 Scope of the review	19
2 Current activities: ASIMP 2017-2020 and ASMIP 2021-2022.....	21
2.1 Loads and stresses	21
2.1.1 Recent helicopter flow simulations at Patria Aviation.....	21
2.1.2 Enhancement of the Hawk Mk.66 flow simulation model	22
2.1.3 Wing Root and Wing Fold load computations for the Hornet	22
2.1.4 Flow simulations for the Hornet engine inlet duct	23
2.1.5 Applications and enhancements of Grob G 115E CFD model.....	24
2.1.6 Computational Fluid Dynamics at Elomatic Ltd.	26
2.1.7 Hornet FE modeling - update.....	27
2.1.8 Flight simulations - update for the F/A-18C aircraft mass model.....	28
2.2 Loads monitoring and fatigue tracking systems	29
2.2.1 The FINAF HOLM aircraft in routine squadron service	29
2.2.2 Parameter based fatigue life analysis - update	31
2.2.3 Operational spectra for Hornet Wing Root and Wing Fold loads	32
2.2.4 Modal testing of Vertical Tail of the F/A-18C Hornet	36
2.2.5 The effect of A/G training on the structure of the FINAF Hornet	38
2.2.6 Research efforts towards Hawk structural integrity management.....	41
2.2.6.1 Hawk Structural Health Monitoring (SHM) update.....	41
2.2.7 The FINAF Grob Mini-OLM	44
2.2.8 Fatigue and damage tolerance test of Gripen Rudder	45
2.3 Structural integrity of metallic materials	46
2.3.1 Risk Level Assessment for Structural Integrity Management.....	46
2.3.2 Update of study of small cracks growth	47
2.3.3 NDE reliability evaluation with POD round-robin	48
2.3.4 Fatigue testing of bolted joints with solid shims and blind fasteners.....	49
2.3.4.1 Introduction	49
2.3.4.2 Test specimens	49
2.3.4.3 Test setup	50
2.3.4.4 Test results.....	50
2.3.4.5 Comparison of predictions and test results.....	51
2.4 Structural integrity of composite materials.....	54
2.4.1 Structural integrity of composite structures and adhesively bonded joints.....	54
2.5 Repair technologies.....	58
2.5.1 Composite repair of the Wing Root Step Lap Joint	58
2.5.2 VCCT analysis of the Step Lap Joint.....	60
3 Related activities	62
3.1 EDA Patchbond I project.....	62
3.2 EDA Patchbond II project.....	62
3.3 Quantification of optical distortions near industrialization and the follow-on project to quantify scratches and dents on aircraft transparencies and their repair instructions near successful completion.....	63
References	67

1 Introduction

The coordinated aeronautical life cycle support research in Finland - and its embodiment: the national research network - has over the decades been solely advocated and supported by the Finnish Air Force (FINAF). Their vision is that while the FINAF is concentrating to carry out its primary objectives, the national research network help FINAF to optimize the use of their prevailing fleet in a cost-effective way, and to make the most of their asset. The assigned research activities by the FINAF are of two kinds: on the one hand, the tasks are related to finding pragmatic solutions to be applied with only slight effort in every day's routine, but on the other hand, the tasks feature a more scientific flavor such that the possible solution goes beyond the obvious and requires more time to mature. The FINAF has also found it advantageous that Finland belongs to the core of the international community of aeronautical fatigue research, being a member nation in the International Committee on Aeronautical Fatigue and Structural Integrity (ICAF). This commitment is manifested in the multiple ICAF National Reviews since 2001. [25], [26], [27], [28], [29], [30], [31], [32], [33], [34]

The FINAF is one of the oldest independent air forces in the world. It all began 103 years ago when the Swedish Count, Eric von Rosen, donated to the FINAF its first aircraft: A Thulin typ D reconnaissance plane. In the beginning, the aircraft inventory of the Service comprised a miscellany of donated or procured aeroplanes. For example, in the early 1920s, the focus of the FINAF development was on maritime aviation, since it was then considered that the primary task of the Finnish air arm was, with procured floatplanes, to conduct surveillance and reconnaissance operations relying on Finland's territorial waters and thousands of lakes. In 1921, Finland obtained the manufacturing license from Germany for the Hansa-Brandenburg W.33 seaplane, which thus became the first industrially manufactured aircraft in Finland, called as IVL A.22 Hansa (**Figure 1**). Beginning from 1922, the company "Ilmailuvoimien Lentokonetehtäs", Air Force Aircraft Factory, predecessor of what is today known as Patria, built as many as 122 Hansas. [1]



Figure 1: *The Hansa-Brandenburg reconnaissance aircraft were the mainstay of the Finnish Air Force during the 1920s and 1930s when the focus was on maritime air operations. Figure courtesy of the FINAF. [1]*

The Finnish Defence Forces (FDF) has clearly set tasks to maintain a credible and preventive defence capability that secures Finland’s territorial integrity. Finland as a militarily non-allied country is responsible for its own defence, despite the increased international cooperation. Responsibility for Finland's air defence and air operations is with the Air Force. The observance of active air policy mission aims to secure Finland’s airspace on a 24/7 basis, throughout the year, and react to airspace violations if necessary. It can be concluded that the primary objective of the FINAF has remained unchanged over the time, but the tools to implement the objective are somewhat more capable - and considerably more complicated systems - than back in the old days. The current fixed wing aircraft inventory of the FINAF is summarized in **Figure 2**.

This year will be a remarkable milestone for Finland’s future air defence capability. The service life of the Finnish F/A-18C/D Hornet fleet comes to an end by 2025-2030 as the aircraft will reach the end of their planned 30-year service life. In parallel, the replaced capabilities must be phased in and be fully operational in service in 2030. The Government of Finland will decide on the procurement for replacing the F/A-18C/D fleet by the end of 2021. Replacing the capabilities of the Hornet fighters significantly affects Finland’s security and defence policy relations and standing. The procurement will be the biggest arms trade in Finland’s history: the projected cost of the program is EUR 7...10 billion. The impact of the HX Fighter Program is monumental in creating a credible defence capability. The replacement of the Hornet fleet will define the Air Force’s entire combat capability into the beginning of the 2060s.

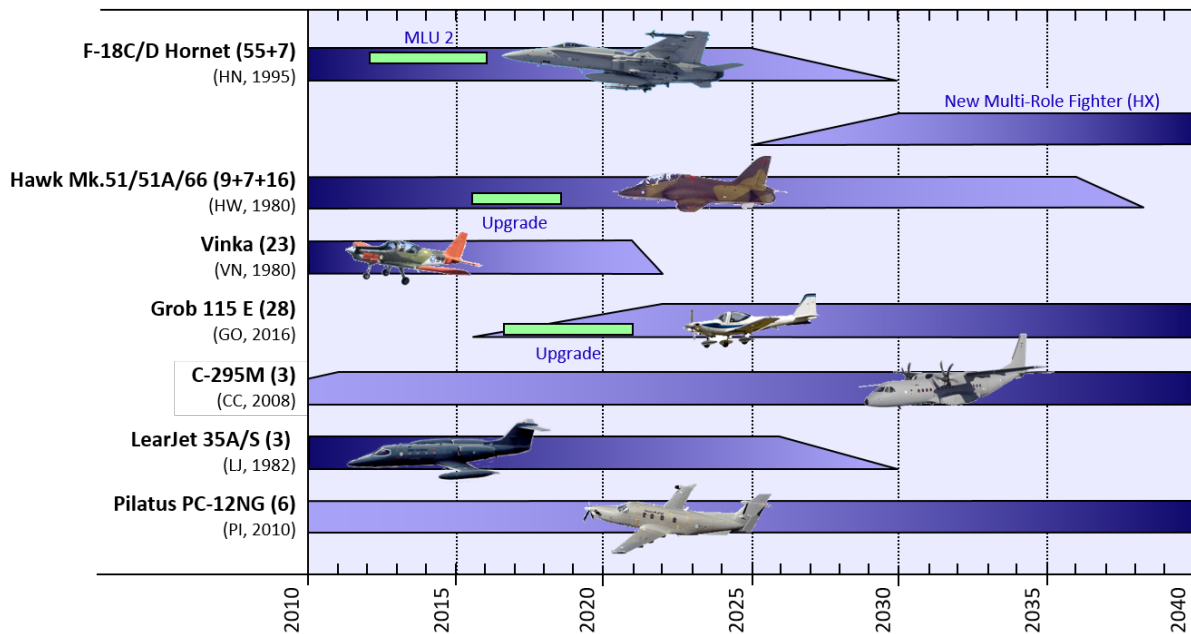


Figure 2: An overview of the fixed wing aircraft inventory of the Finnish Air Force (FINAF). Figure courtesy of the Joint Systems Centre.

The 20 TTH/SAR NH90 helicopters purchased earlier by the FDF were retrofitted (by Patria Aviation) and reached the Full Operational Condition (FOC) status. The retrofits (including the platform and various systems therein) started in 2014, and were completed in 2019.

Presently, the MD500 fleet is going through a cockpit modification project in which avionics will be upgraded. The result will increase the MD500s’ operative performance, improve their interoperability with the other branches, and facilitate pilot transitions into the NH90 platform.

The current rotary wing aircraft inventory of the FDF is summarized in **Figure 3**.

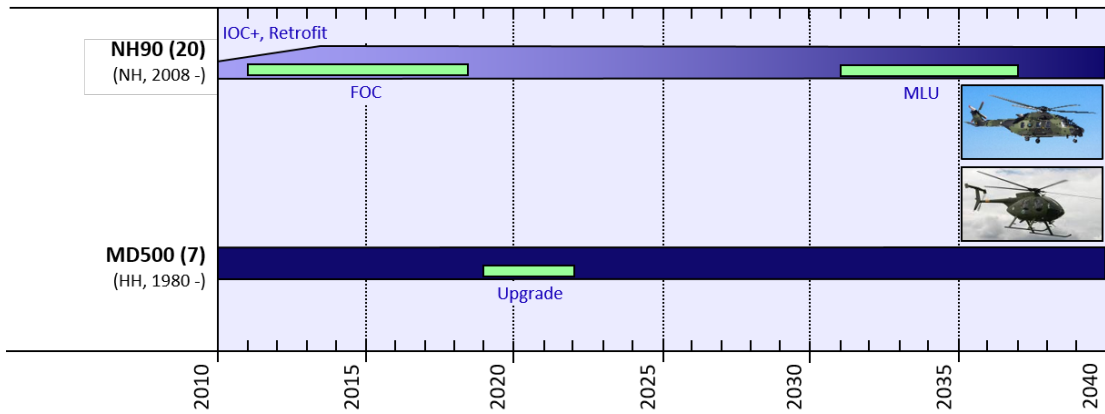


Figure 3: An overview of the rotary wing aircraft inventory of the Finnish Defence Forces (FDF). Figure courtesy of the Joint Systems Centre.

Before proceeding into the highlights of the structural integrity management activities, a brief update of the FINAF's fighter aircraft and associated pilot training aircraft is provided next.

1.1 Valmet L-70 Vinka

The Valmet L-70 Vinka (the FINAF military designation VN) is a three-seat piston-engine aircraft of Finnish design and manufacture (**Figure 4**). Since 1980, the FINAF military pilots have started their career at the controls of the indigenous Vinka primary trainer. Due to its long service life, the Vinka fleet has undergone several minor structural reinforcements and other modifications. By now 23 of the original 30 Vinkas remain in service with the FINAF. The German-built Grob G 115E will replace the Vinka aircraft in the primary and basic training role in the coming years (Chapter 1.2). [2]



Figure 4: Valmet L-70 Vinka primary trainer aircraft (VN-5). Figure courtesy of the FINAF.

Previous activities related to the Valmet Vinka primary trainer of the FINAF were outlined in e.g. [34] Chapter 1.1. During the Life Extension Program (LEP) of the Vinka primary trainer fleet, each aircraft was equipped with a g counter. The structural life consumption and severity of the usage is monitored by Patria Aviation from the g counter data. Patria also issues recommendations on a yearly basis regarding the rotation of the Vinka fleet to obtain a more even rate of structural life expended.

Based on the g counter information, the severity of usage is more benign compared to the basis of the LEP analyses and tests, see **Figure 5**.

The first fleet leader was removed from operation in September 2015 after logging 7100 FH (it was given 100 FH extension to the official 7000 FH limit). After that the plane was disassembled for structural inspections. Most of the inspections were done visually but the most critical locations were inspected using NDT. No cracks or loose rivets were found. Based on the inspection results, and the fact that originally three fleet leaders were selected as a precaution, it was decided that the two other fleet leaders do not any more need to log hours differently compared to the rest of the fleet. In late 2018 loose rivets were found from the lower surface of the wing of the fleet aircraft. This finding could not be predicted based on the fleet leader inspection.

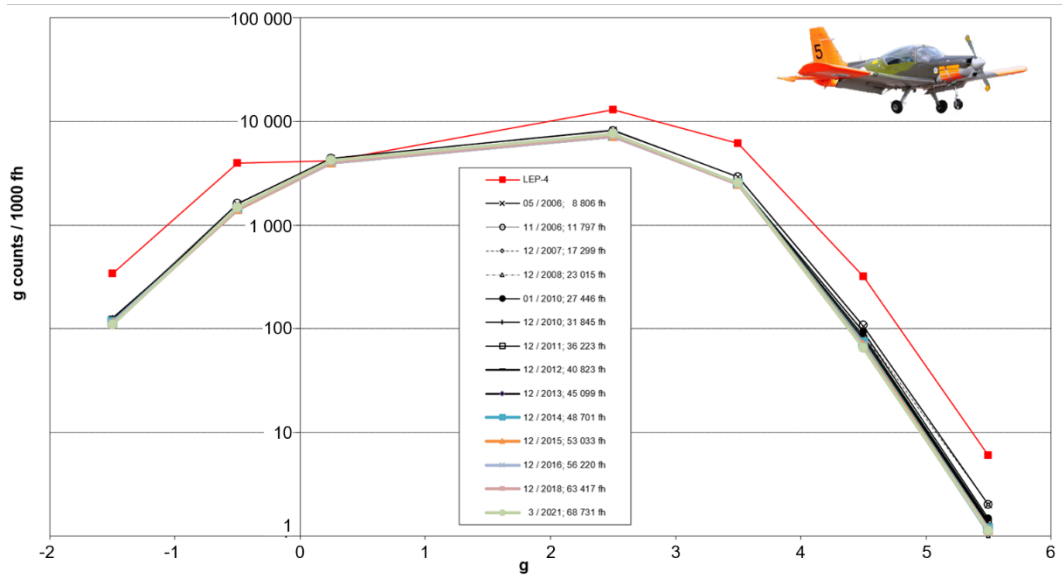


Figure 5: The g counts per 1000 FH of the Valmet Vinka. From top to bottom: The spectrum representing the LEP design assumptions (LEP-4); the post LEP g counter spectrum as of May 2006; as of November 2006; as of December 2007; as of December 2008; as of January 2010; as of December 2010; as of December 2011; as of December 2012; as of December 2013; as of December 2014; as of December 2015; as of December 2016; as of December 2018; and the update from the previous review: as of March 2021 including a total of 68 731 FH. All curves (excluding the red LEP-4) represent the fleet average from all Vinkas, as ranked according to the aircraft center of gravity normal acceleration. Figure courtesy of Patria Aviation.

1.2 Grob G 115E

The Grob G 115E is a small, lightweight, two-seat piston-engine aircraft built in Germany by Grob Aircraft. In October 2016, the FINAF procured 28 pre-owned Grob G 115Es for the Defence Forces to supersede Valmet L-70 Vinkas (Chapter 1.1) in primary and basic training roles. The aircraft were purchased from Babcock Aerospace Limited, which had previously operated them as a training platform for the Royal Air Force. [3]

The Finnish Grobs are allocated GO-series military registrations and were delivered to Finland in 2016-2018. Before handover to the customer, the Grob fleet will receive an avionic and communication systems upgrade. State-of-the-art digital displays will be fitted in order to bring the cockpit layout compatible with the other aircraft operated by the Defence Forces.

On the contrary to its predecessor (Vinkas), the structure of Grob G 115E is manufactured of composite materials. It is constructed predominantly from carbon fiber reinforced composites, has a tapered low wing, a 180 hp engine with a 3-bladed variable-pitch propeller, a fixed tricycle undercarriage, fixed horizontal and vertical stabilizers and conventional flight control surfaces. The large glass canopy renders clear all-round visibility to the crew (**Figure 6**).



Figure 6: Grob G 115E primary trainer aircraft. Figure courtesy of the FINAF.

1.3 Hawk Mk.51/51A and Mk.66

The BAE Systems Hawk is a British single-engine two-seat advanced jet trainer. The FINAF Hawks bear the military designation HW and are operated by the Air Force Academy, primarily in advanced and tactical training roles. The Hawk is also flown by the Air Force's official display team the Midnight Hawks. [4]

The Finnish Air Force became the first export customer of the type, and the first fifty Hawks, Mk.51s, entered Finnish service in 1980-1985. In 2020 was the 40th anniversary for the Finnish Hawk, thus becoming gradually the oldest aircraft type in the FINAF history (Figure 7).



Figure 7: *The first FINAF Hawk Mk.51 (HW-302) in a test flight over Dover, UK in 1980 (left). The Hawk (HW-340) in festive blue and white livery commemorating the 40 years of service in the FINAF (right, realized by Patria Aviation). Figures courtesy of the FINAF.*

In 1993, the FINAF ordered an additional batch of seven Hawk Mk.51As that contain minor improvements in structure and avionics compared with the Hawk Mk.51. Finland augmented its Hawk fleet in 2007 by sourcing 18 low-hour Hawk Mk.66s from Switzerland. Externally, the former Swiss Hawks stand out from the grey legacy Hawks owing to their red-and-white paint scheme (see Figure 8). However, in 2021 the first Mk.66 aircraft will receive a grey livery similar to older model aircraft, and the rest are expected to follow during the next couple of years.



Figure 8: *BAE Systems Hawk advanced jet trainer variants in the FINAF fleet (from left to right): Hawk Mk.51, Hawk Mk.51A, and Hawk Mk.66. Figure courtesy of the FINAF.*

Due to increasing signs of metal fatigue, a major structural reinforcement program (SRP) was performed to extend the operational life of Finland's Hawks. The Hawk SRP was

completed for the Mk.51 and Mk.51A fleet during the late 1990s, and started for the Mk.66 fleet in 2020. Along with the Mk.66s, the Finnish Hawks underwent an extensive cockpit upgrade program carried out by Patria Aviation. The glass cockpit upgrade program included the replacement of analogue cockpit instruments with modern displays which narrows the gap between the instrument layout of the Hawk and F/A-18C/D Hornet (see Chapter 1.4). In the first phase, all Mk.66s, seven Mk.51As, and one Mk.51 received the cockpit modification and were delivered to the FINAF by January 2018. Later, eight additional Mk.51s were modernised in 2016-2020 based on the refined Hawk life cycle plans and to compensate the loss of two already modernized Mk.66 aircraft. Thus, the 2021 fleet consists of 32 upgraded Hawks: 9 Mk.51s, 7 Mk.51As and 16 Mk.66s. They are expected to remain in service until the late 2030s.

The inherent fatigue tracking of each FINAF Hawk aircraft relies on counting g level exceedances and calculating a usage index i.e. Fatigue Index (FI) by the variant specific equations on a flight-by-flight basis. This method is adequate for monitoring the structural locations mainly influenced by aircraft normal acceleration (multiplied by weight). However, the FI tracking does not take into account of buffet loading which is the main driver for the structural fatigue issues e.g. in the empennage of the Hawk aircraft. The Fatigue Index summary of the Finnish Hawk fleet is shown in **Figure 9**.

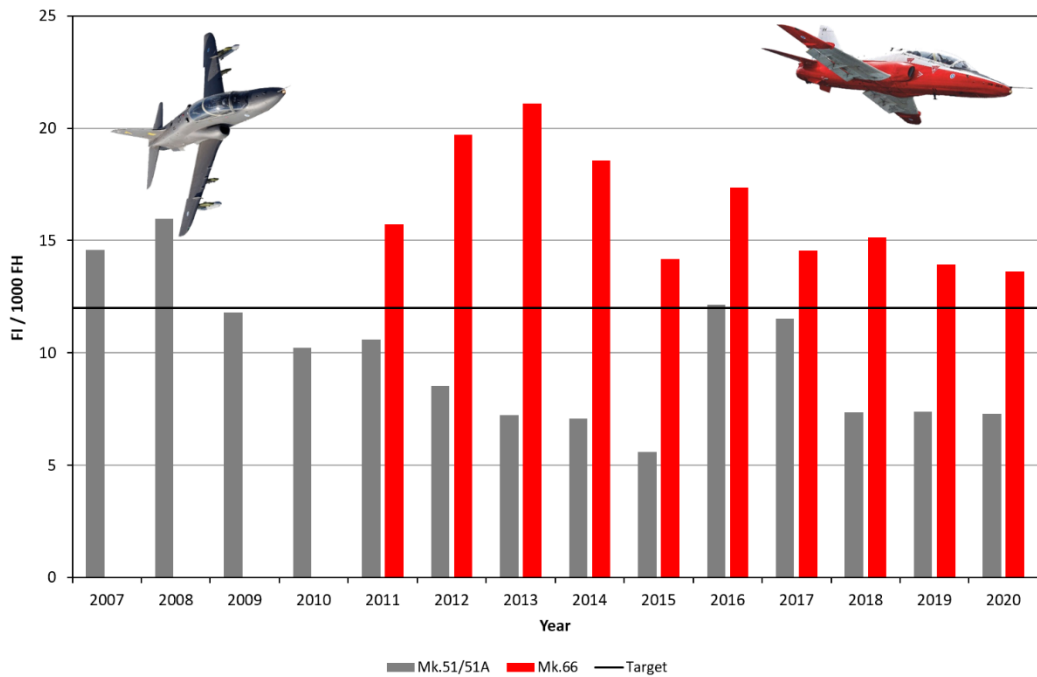


Figure 9: Annual Fatigue Index (FI) development of the FINAF Hawk aircraft (Mk.51/51A in grey; Mk.66 in red) in the end of 2020. The annual target, average of all the variants, is 12 FI/1000 FH. Figure courtesy of the FINAF.

1.4 F/A-18C/D Hornet

The Boeing F/A-18C (single seat) and F/A-18D (two seat) Hornet are twin-engine, mid-wing, carrier-capable, multirole jet fighters, that form the nucleus of the Finnish air defence. In 1992, Finland selected the Hornet to replace its aging Saab J35 Draken and MiG-21bis fleets. The late-production Lot 17 aircraft entered Finnish service in 1995-2000, bearing the military designation HN. The Finnish two-seaters were built in the United States by McDonnell Douglas which later merged with Boeing, while the single-seat aircraft were assembled at Patria Finavitec (nowadays Patria Aviation) facility in Finland. [5]

The FINAF Hornet fleet consists of 62 aircraft: 55 C-models (**Figure 10**), and 7 D-models (**Figure 11**). Most of the fleet is divided between two operational fighter wings: Lapland Air Command (Fighter Squadron 11) at Rovaniemi Air Base and Karelia Air Command (Fighter Squadron 31) at Kuopio Rissala Air Base.



Figure 10: Boeing F/A-18C Hornet multirole jet fighter. Figure courtesy of the FINAF.



Figure 11: Boeing F/A-18D Hornet multirole jet fighter. Figure courtesy of the FINAF.

It was recognized already in the planning stage of the Hornet program that technology of the 1990s would be obsolete way before the planned withdrawal date of the type, 2025-2030 time frame. Therefore, in order to keep the Hornet fleet at their highest level of performance, the fleet needs to be subjected to planned and systematic updates over its life span. On the heavier end of the spectrum have been the full-scale upgrades. The Finnish Hornets have undergone two mid-life upgrades, designated as Mid-Life Update 1 (MLU 1) and Mid-Life Update 2 (MLU 2) which were incorporated between 2006-2010, and 2012-2016 respectively. The partners in the upgrades were Boeing, Naval Air Systems Command as an upgrade design organization and equipment supplier, and Patria Aviation as a life cycle support service provider for the aircraft. [6], [7]

The focal point in MLU 1 was to enhance the FINAF Hornets' air-to-air (A/A) capability. The upgrade involved the incorporation of a helmet-mounted sighting system mated with the state-of-the-art AIM-9X Sidewinder infrared guided missile for improved close-in air combat performance. MLU 1 also introduced features to better the pilot's situational awareness and joint operation capabilities.

The primary objective in MLU 2 was to enable the FINAF Hornets' air-to-ground (A/G) capability by integrating various types of weapons (the short range guided bomb JDAM, medium-range glide bomb JSOW and the long-range JASSM standoff missile), and modern self-protection, communication, navigation and information distributions systems which make the aircraft more interoperable in joint operations. Other examples of MLU 2 upgrades were the cockpit upgrades with new displays and the BOL countermeasures dispensers.

From structural point of view, the MLU 2 upgrade included structural strengthening and a purchase of Line Replaceable Units (LRU) and other spares to ensure the safe and reliable performance until the sundown of the aircraft type. All structural MLU 2 modifications were carried out by Patria Aviation, and the MLU 2 preparation work was done in cooperation with the Swiss Air Force.

There are special arrangements to manage the C and D model differences between the USN and the FINAF in the MLU 2 induced configurations: The software testing will be done in Finland by the FINAFSAC ACC (Satakunta Air Command, Air Combat Centre, Flight Test Section) and Patria Aviation's STIC laboratory (Software Test and Integration Centre). For the first time in the history of the Hornet, there is a foreign (Finnish) organization approved as a part of the approval process of the US software.

Along with the MLU 2 upgrade, the FINAF F/A-18C/D Hornet has finally reached its Full Operational Capability (FOC) that expands the operational envelope for a true multi-role aircraft. The Finnish pilots are now enabled to exercise the full potential of the Hornet in joint and combined operations with a wide range of air-to-air and air-to-ground capabilities. The new type of mission capability reflects on training programs and the use of the aircraft and thus, also the airframe stressing.

Fatigue tracking of the FINAF Hornet fleet is currently based on: 1. Flight Hours (FH), 2. Wing Root Fatigue Life Expended (WR FLE) -value, and 3. T*-value (time spent in a buffet-dominating Point In The Sky, PITS) for the Vertical Tail [53]. Summary of the wing root fatigue life expended (WR FLE) of the FINAF F/A-18C/D fleet is presented in **Figure 12**.

It is known that the WR FLE is primarily dependent on the aircraft normal acceleration, so it does not provide useful fatigue information about the structural locations prone to the buffeting. As the Vertical Tail of the F/A-18 aircraft is typically buffeting-strained structure, a more useful usage index, developed by the international F/A-18A/B/C/D Hornet user's community, has been put into practice in the FINAF. A T* (T star) value indicates time spent [h] in the PITS that contributes most of the fatigue damage for the Vertical Tail. Summary of the T*-values of the FINAF F/A-18C/D fleet is presented in **Figure 13**.

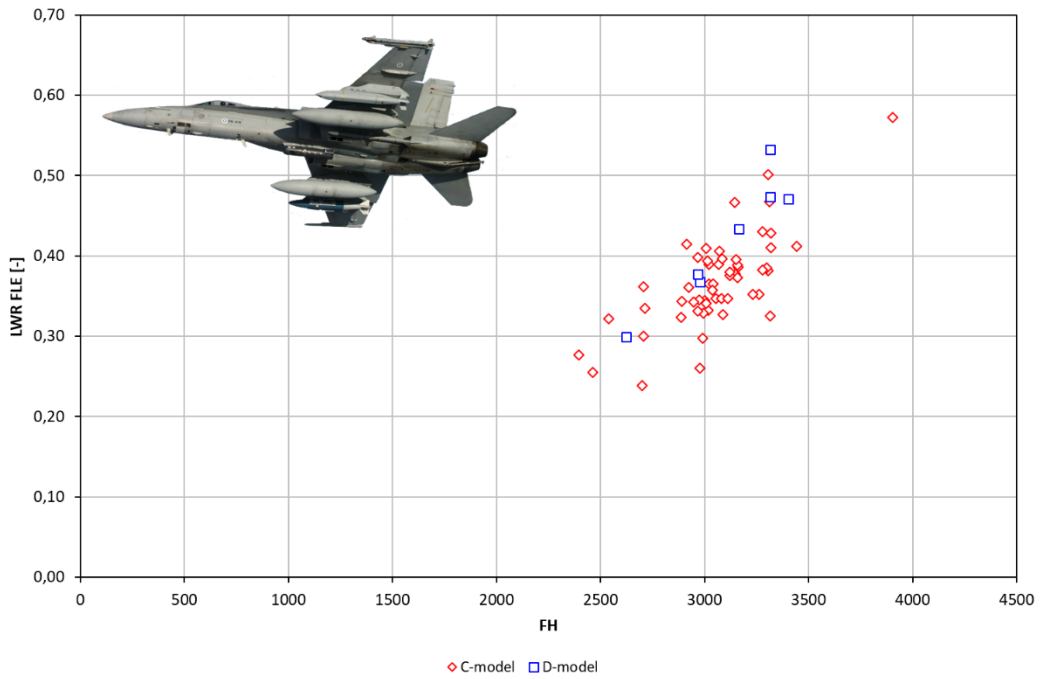


Figure 12: Summary of the Left Wing Root Fatigue Life Expended (LWR FLE) of the FINAF F/A-18C/D fleet at the end of 2020. The data is from all 62 aircraft included [53]. Figure courtesy of the Joint Systems Centre.

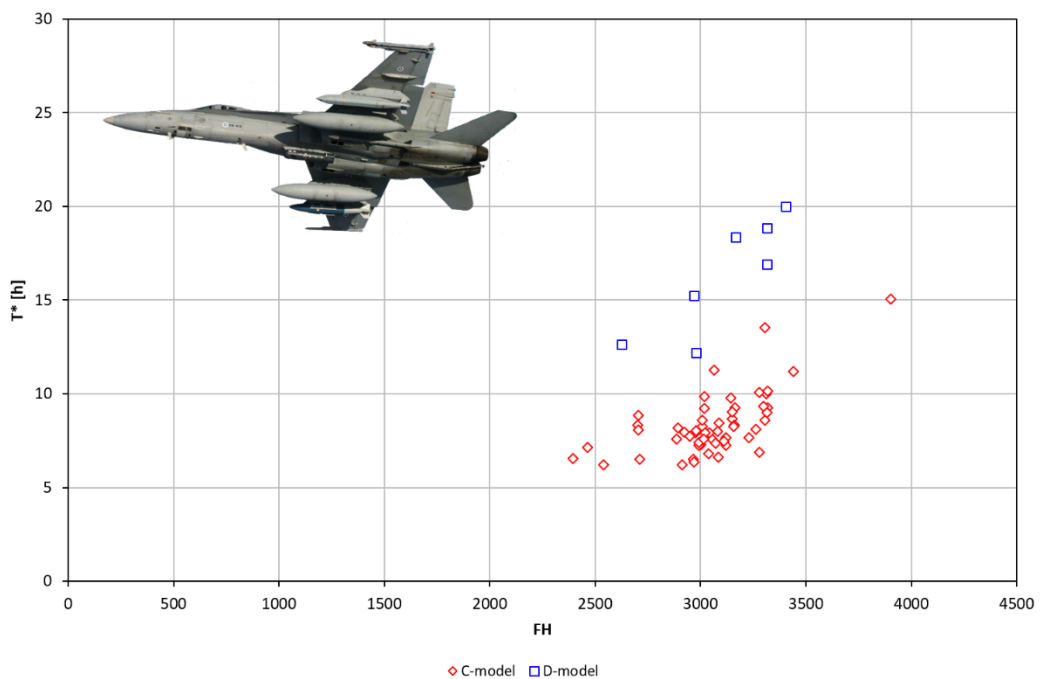


Figure 13: Summary of the Vertical Tail fatigue tracking (T*-value) of the FINAF F/A-18C/D fleet at the end of 2020. The data is from all 62 aircraft included [53]. Figure courtesy of the Joint Systems Centre.

The FINAF mission readiness requires flight training syllabi that include a great deal of air combat maneuvering, which stresses the structures of the aircraft - sometimes more than originally planned. Throughout the service history of the Hornet fleet the FINAF has

been analysing its flight training syllabi with respect to structural life-limiting aspects and come to a conclusion that several structural modifications are required in order to achieve the targeted flight hours. The present service life model is based on an adjusted operations profile which together with structural modifications enables the Hornet fleet safe usage until 2030.

However, the combined benefit of MLU 1 and MLU 2 will not extend the service life of the airframe from the planned withdrawal date. According to the structural analysis, and evidenced by the recorded structural response data from operational conditions, the FINAF Hornets will reach their expected service life without a need for further airframe work as planned.

In the post-MLU 2 era, the Hornet will not be given new capabilities. Only updates and modifications to systems that are essential for the maintenance of flight safety and operational performance will be carried out.

The Finnish F/A-18C/D fleet is capable of accomplishing its operations safely and reliably until the mid-2020s. The decommissioning of the Hornet fleet will start in 2025. Phasing out the aircraft becomes a reality when they are about to reach their structural flight hour limits between 2025 and 2030. Then new multi-role fighters to be purchased through the HX Program will replace an obsolescent fleet (see Chapter 1.5).

1.5 HX Fighter Program

The service life of the Finnish F/A-18C/D Hornet fleet comes to an end by 2025-2030 as the aircraft reach the end of their planned 30-year service life. In parallel, the replaced capabilities must be phased in and be fully operational in service in 2030. The aim of the HX Fighter Program is to replace the nationwide air defence capability of the Finnish Air Force F/A-18C/D fleet with the most cost-effective manner to Finland's state economy. This comprises a comprehensive solution that introduces a capable multi-role fighter. The major factors that limit the service life of the FINAF Hornet fleet are [8], [9]:

1. Structural fatigue,
2. Expiring system support, and
3. Weakening comparative capabilities.

Extending the lifespan of the FINAF Hornet fleet into the 2030s, contrary to the present plans, would increase expenses in life-cycle management and increase the cost risks of system support. The relative capabilities of the Hornet fleet will degrade in the 2020s and the most significant degradation falls on its interdiction capability: the next generation multi-role fighters in Finland's neighborhood will technologically surpass the Hornet's capabilities. Extending its structural life and implementing a new, sizeable midlife upgrade would make it possible to delay the decision to replace the Hornet capabilities by five years, at most. It is estimated that the capability would be fully available no earlier than eight years after the financial decision is taken. As a result, substantial additional costs would be incurred in case of the service life of the Hornet fleet would be extended. This is neither a cost-effective solution nor would it be sufficient in terms of Finland's defence.

The Request for Information (RFI) for replacing the FINAF Hornet fleet capabilities was sent out in spring 2016, and based on the responses in April 2018, the Defence Forces sent a Request for Quotation (RFQ) to the governments of France, Great Britain, Sweden and the United States, to be forwarded to five manufacturers of multi-role fighters in these countries. The aircraft types in question are: Boeing F/A-18 Super Hornet (United States), Dassault Rafale (France), Eurofighter Typhoon (Great Britain), Lockheed Martin F-35 (United States) and Saab Gripen (Sweden) (**Figure 14**).



Figure 14: The multi-role fighter candidates of the HX program. Figure courtesy of Ministry of Defence.

The Finnish Defence Forces Logistics Command received replies from the five aircraft manufacturers, and after initial evaluation, a more specific RFQ was sent in the second half of 2019; this was followed by the second phase of negotiations during which the

content of procurement packages were finalized. The second phase of negotiations ended in 2020, after which the Request For the Best and Final Offer (RFBAFO) was sent to the tenderers in January 2021.

As a part of the HX capability evaluation, all five HX fighter candidates underwent cold weather trials in the ‘Operation HX Challenge’ in Finland. (Figure 15). The HX Challenge was defined in the RFQ as one out of the three opportunities for the candidates to demonstrate their capabilities and the validity of the information presented in their responses to the RFQ. The purpose of the HX Challenge was not to rank the candidates, but to make sure that the performance values reported in the responses to the call for tenders actually apply in the Finnish operating environment. Each contender got seven days for evaluation starting from 9th of January and ending at 26th of February 2020. [10]



Figure 15: The HX Challenge logo. Figure courtesy of the FINAF.

By set deadline, at the end of April 2021, the Finnish Defence Forces Logistics Command received the final and legally binding quotations (also known as BAFO: Best and Final Offer) from all the five fighter manufacturers [11]. Next, the quotations will be evaluated in line with the invitation for tenders and the programme’s decision model to make a procurement proposal. The evaluation of quotations will be completed in autumn 2021, after which the Finnish Government will decide on the procurement, on proposal by the Ministry of Defence. It has been estimated that the COVID-19 pandemic has caused approximately 6 months delay on the program schedule, but the Government of Finland will decide on the procurement at the end of 2021, as originally planned. The timetable and phasing of the HX Program in 2018-2021 time frame is presented in Figure 16.

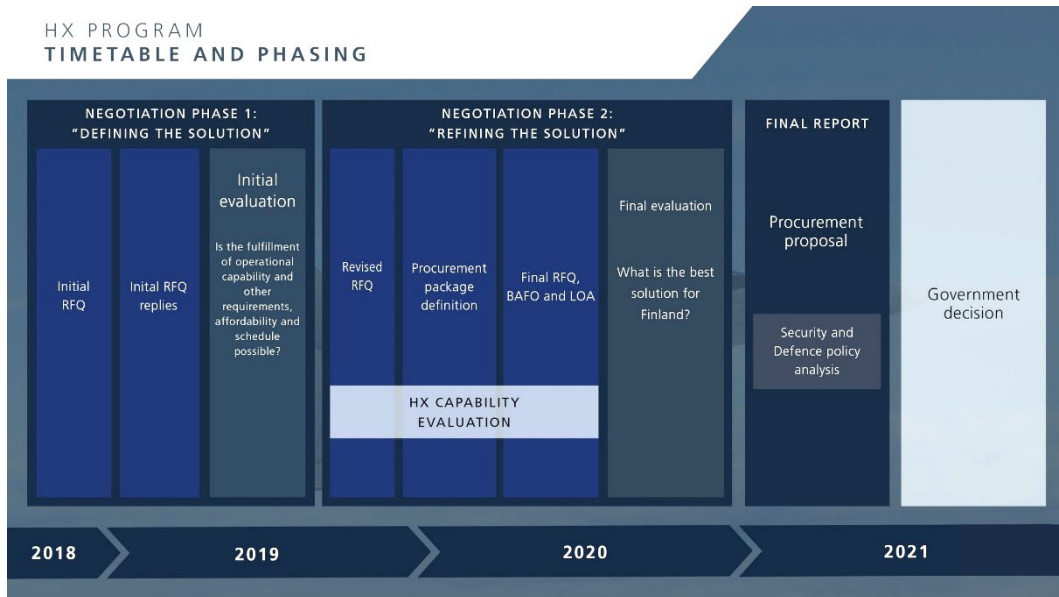


Figure 16: The HX program’s timetable and phasing in 2018-2021 time frame. Figure courtesy of Ministry of Defence.

The procurement will be the biggest arms trade in Finland’s history: the projected cost of the program is EUR 7...10 billion. The impact of the HX Fighter Program is monumental in creating a credible defence capability. The replacement of the Hornet fleet will define the Air Force’s entire combat capability into the beginning of the 2060s. The acquired defence capability must also be constantly sustained and developed i.e. kept up-to-date within coming decades on the grounds of assessed development potential of the product.

1.6 Scope of the review

This national review on aeronautical fatigue concentrates on the fixed wing aircraft of the FINAF related to fighter aircraft and associated pilot training aircraft. The FINAF inventory includes: 62 F/A-18C/D Hornet fighters, 9 Hawk Mk.51, 7 Mk.51A and 16 Mk.66 jet trainers, 23 Valmet L-70 Vinka primary trainers, and 28 Grob G 115E primary trainers. By now, approx. 195 000 FH have been flown with the Hornets, 271 000 FH with the Hawks, and 191 000 FH with the Vinkas.

No FINAF aircraft of these type designations have been lost due to structural issues.

The severity of the Finnish usage in view of structural fatigue with the aircraft of noteworthy maneuvering capability (**Figure 9** (Hawk) and **Figure 12, Figure 13** (Hornet)) clearly demonstrates the need to maintain, further develop and apply concrete and systematic efforts to cope with the structural deterioration effects.

In 2005, the International Committee on Aeronautical Fatigue and Structural Integrity (ICAF) formally welcomed Finland as a full member of the ICAF, making Finland the 13th member nation. The 9th national review as a full member about the aeronautical fatigue investigations in Finland April 2019 - April 2021 was compiled by Tomi Viitanen and Aslak Siljander (VTT).

The review comprises inputs from the organizations listed below (in alphabetical order):

Aalto	Aalto University, School of Engineering, Department of Mechanical Engineering, P. O. Box 14300, FI-00076 Aalto, Finland (http://appmech.aalto.fi/en/).
AFCOMFIN	Air Force Command Finland, Plans Division A5, Programmes Coordination Section, P. O. Box 30, FI-41161 Tikkakoski, Finland.
ARCOMFIN	Army Command Finland, Plans Division C2, P. O. Box 145, FI-50101 Mikkeli, Finland.
Arecap	Arecap Ltd, Toivolantie 4, FI-04800 Mäntsälä, Finland (https://arecap.fi/).
Elomatic	Elomatic Ltd, Vaisalantie 2, FI-02130 Espoo, Finland (https://www.elomatic.com/en/).
Emmecon	Emmecon Ltd, Tammitie 12, FI-53810 Lappeenranta, Finland (https://www.emmecon.fi/).
Eurofins ES	Eurofins Expert Services Oy, P. O. Box 47, FI-02151 Espoo, Finland (https://www.eurofins.fi/expertservices/).
FDFLOGCOM JSC	Finnish Defence Forces Logistics Command, Joint Systems Centre, P. O. Box 69, FI-33541 Tampere, Finland (https://puolustusvoimat.fi/en/about-us/logistics-command).
Insta ILS	Insta ILS Oy, Sarankulmankatu 20 (P.O. Box 80), FI-33901 Tampere, Finland (https://www.insta.fi/en/en/).
Patria	Patria Aviation Oy, Lentokonetehtaantie 3, FI-35600 Halli, Finland (http://www.patria.fi/).
TAU	Tampere University, Plastics and Elastomer Technology, FI-33014 Tampere, Finland (https://www.tuni.fi/en).

Trano	Trano Oy, Vetikonkuja 13, FI-04300 Tuusula, Finland.
Trueflaw	Trueflaw Ltd, Tillinmäentie 3 Tila A113, FI-02330 Espoo, Finland (http://www.trueflaw.com/).
VTT	VTT Technical Research Centre of Finland Ltd. P. O. Box 1000, FI-02044 VTT, Finland (http://www.vtt.fi/?lang=en).

2 Current activities: ASIMP 2017-2020 and ASMIP 2021-2022

The Aircraft Structural Integrity Management Program (ASIMP) 2017-2020, as briefly outlined in [34], has been completed. The follow-on program, ASIMP 2021-2022, with its various sub-programs is about to begin. On contrary to the previous four-year research periods, the incipient research period covers two years only. The reason for halving the span is connected to the HX candidate selection (Chapter 1.5) during the transitional period. An attempt is provided below to provide highlights of the ASIMP 2017-2020 achievements.

2.1 Loads and stresses

2.1.1 Recent helicopter flow simulations at Patria Aviation

In the ICAF 2019 report (Chapter 2.1.1 of Ref. [34]), flow simulations related to the NH90 heavy store carriers (HSC) and external fuel tanks were described. Since then, no actual helicopter CFD model extensions have been realized at Patria. However, the existing NH90 model was utilized in 2019 in a practical design project to compute the aerodynamic loads acting on the cockpit door in critical flight conditions. The aim of the project was to replace the original three-pane door window by a single-pane window offering better view for the pilots.

The computed pressure coefficient distribution on the NH90 forward fuselage in a sideslip load condition is illustrated in **Figure 17**. The area of the door window of interest on the side opposite to the sideslip is marked by a white grid. The computational loads were utilized in the documentation of the modification to obtain a supplemental type certificate based on CS-29 airworthiness requirements.

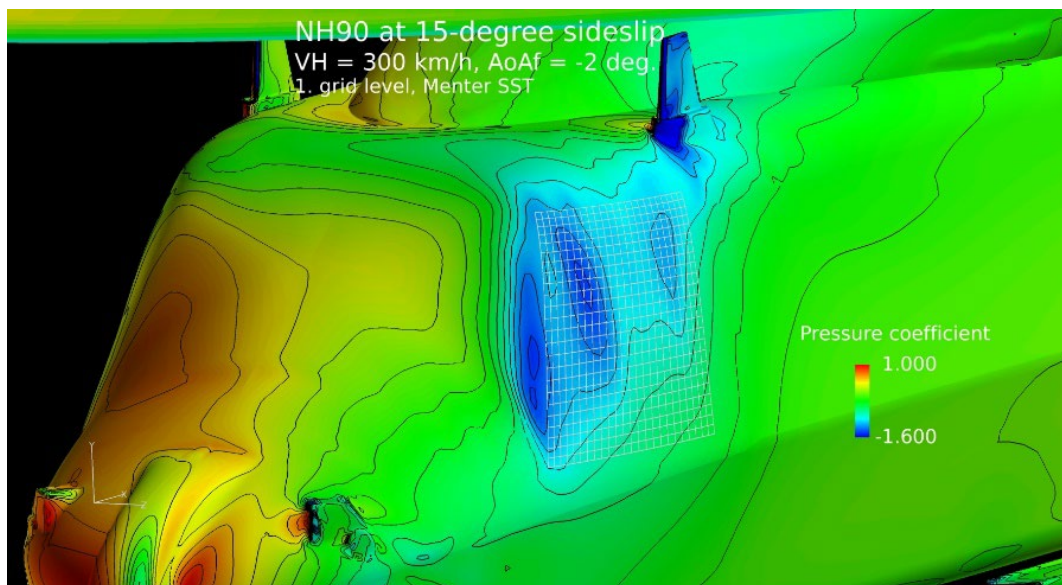


Figure 17: Pressure coefficient distribution on the NH90 forward fuselage in a 15-degree sideslip as computed by FINFLO. Figure courtesy of Patria Aviation.

2.1.2 Enhancement of the Hawk Mk.66 flow simulation model

In the ICAF 2019 report (Chapter 2.1.2 of Ref. [34]), updates of the BAe Hawk CFD model were described. These included the addition of deflecting capability for the ailerons, rudder and airbrake via applying overset grid blocks, while the earlier model version already had a tailplane that could be deflected. During 2020, a new version of the Hawk model with flap deflections was created to complete the modelling of control surfaces. The double-slotted design of the flap involves a vane that penetrates deep into the wing in cruise configuration, but the model version with flap deflections does not include such a large cavity to enable full flap retraction. The minimum flap deflection allowed by this low-speed model is 20 degrees, but with the takeoff setting of 25 degrees the available range is sufficient. In addition to the main flap and the shortened vane of the relevant Hawk version, the model includes flap hinge brackets below the wing.

An example of test simulations with the flaps in the landing setting computed with the updated model using the FINFLO flow solver is shown in **Figure 18**. Even with a flap deflection of 50 degrees, the flow appears to remain essentially attached to the main flap behind the vane, whereas behind the removed vane portion the flow separates. The computed lift behavior at different flap settings is realistic, but the model has not been systematically validated.

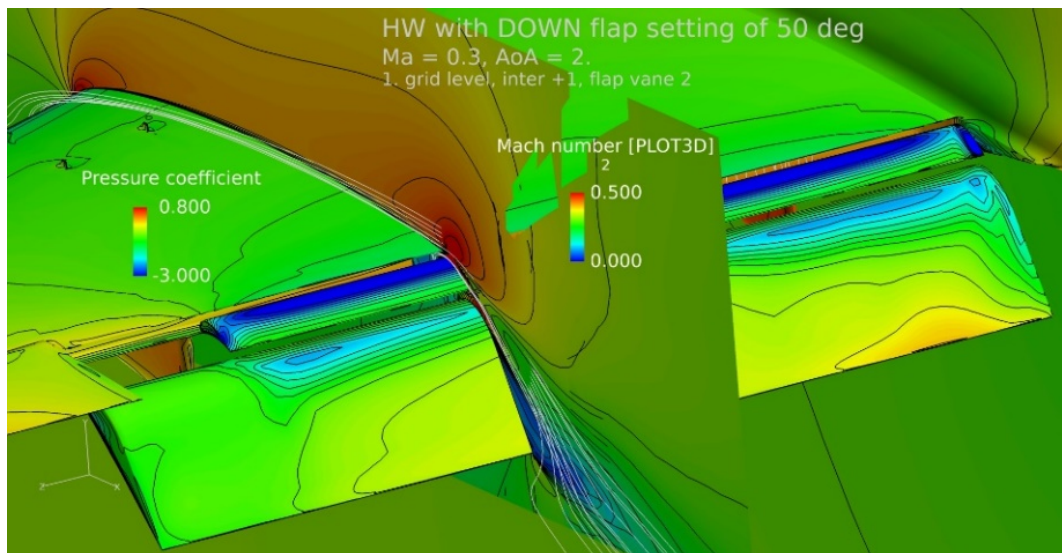


Figure 18: Flow solution around the Hawk flap in the landing configuration as computed by FINFLO. Figure courtesy of Patria Aviation.

2.1.3 Wing Root and Wing Fold load computations for the Hornet

Related to the aging of the Hornet fleet of the FINAF, operative load spectra for the Wing Root and Wing Fold were to be determined in 2020 to enable enhanced fatigue studies. As building blocks of the spectra, the shear, torque and bending moment at the defined wing locations as functions of flight parameters are required. However, the structural load reports from the OEM (Boeing) available in Finland do not cover the wing loads of the F/A-18C/D variants, but represent the early F-18 prototype wing with significant geometric and structural differences. Therefore, the manufacturer's data was partially useless and had to be replaced by loads representing the actual Finnish Hornet fleet.

The wing loads consist of inertial and aerodynamic components, the latter of which are more challenging to determine. The missing aerodynamic data to augment the outdated Boeing data were created at Patria Aviation by computations with the FINFLO flow solver. The computations covered systematic deflections of ailerons and leading edge flaps for the F/A-18C/D models at varying Mach numbers and angles of attack, as well as the

effects of roll rate at different Mach numbers [21]. In addition, the effects of the wing-tip missile status were computed, as they are important for the wing fold loads. The modelled configurations included an empty launcher and the launcher with the AIM-9M or with a completely new model of the AIM-9X currently in use.

Two examples of the computations are illustrated in **Figure 19**. The left image is related to the determination of the aileron effects on the wing loads, where just the left aileron was fictively deflected in an otherwise static level flight condition with other control surfaces in the neutral position. In the right image, the AIM-9M missile is present only at the left wing tip, and no control surfaces are deflected. A comparison of results between the left and right wing half gives the desired load increments at each situation. Altogether, the computations performed to determine the aerodynamic wing load increments of the control deflections, roll rate and missile status included 50 different FINFLO runs.

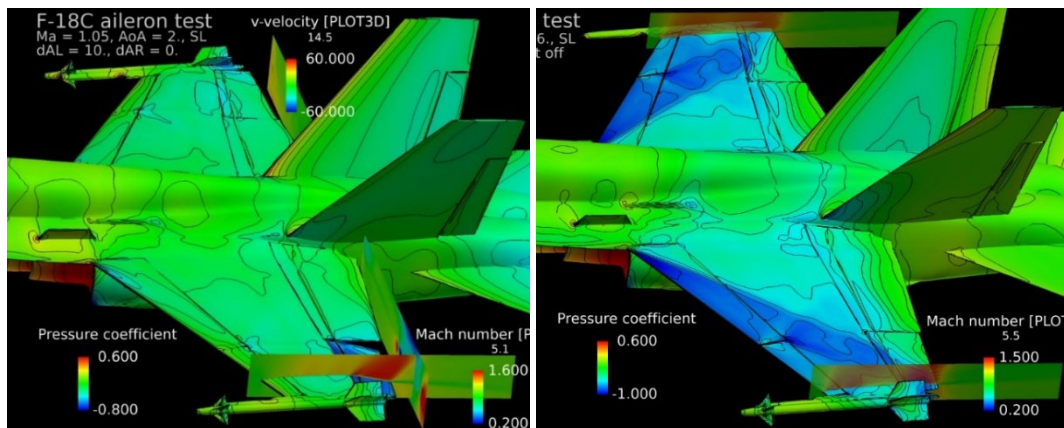


Figure 19: FINFLO flow solutions for the Hornet at $Ma = 1.05$ and $AoA = 2^\circ$ with a deflected left aileron, and at $Ma = 0.95$ and $AoA = 6^\circ$ with an AIM-9M just on the left wing tip. Figure courtesy of Patria Aviation.

2.1.4 Flow simulations for the Hornet engine inlet duct

A new kind of CFD campaign was performed at Patria Aviation in 2020 [22] to study the potential flow distortions in the Hornet engine inlet duct caused by a necessary structural crack repair that caused a small bulge on the duct surface of an individual aircraft. To focus on the potentially critical operating conditions, three rather extreme computational cases were selected on the basis of Boeing reports. In two of the cases, the angle of attack was 45 degrees with a 5 degree sideslip at Mach number of 0.45 and altitude of 30000 ft. The thrust setting was either flight idle or Military power, i.e. maximum without the afterburner. In the third case, the angle of attack was just 2 degrees and there was no sideslip, but the Mach number was 1.5. At such a supersonic speed and at the lowest possible thrust setting, the inlet flow is close to an instability.

The three cases were computed by FINFLO with the repair bulge and without it to see the differences. A special Hornet grid version with an enhanced resolution in the engine ducts and with a simplified external modelling was employed. Representative boundary conditions for the fan inlet surface were defined on the basis of a realistic engine simulator. The computations of the subsonic cases were rather straightforward, but the supersonic flight condition required a development of a special run strategy to establish the realistic overall flow pattern with subsonic flow in the inlet duct downstream of a shock wave at the inlet mouth.

As an example of the results, **Figure 20** illustrates the pressure coefficient distribution on the left inlet duct surface computed at Military power with the 1.6 mm high smooth repair bulge in place. The left image covers the whole duct with the inlet mouth at the

lower right corner, and the right image is a close-up around the repair on the forward upper section of the duct with a different colour scale. As in this figure, the effects of the repair on the duct flow appeared to be negligible, and the repair was deemed acceptable for service.

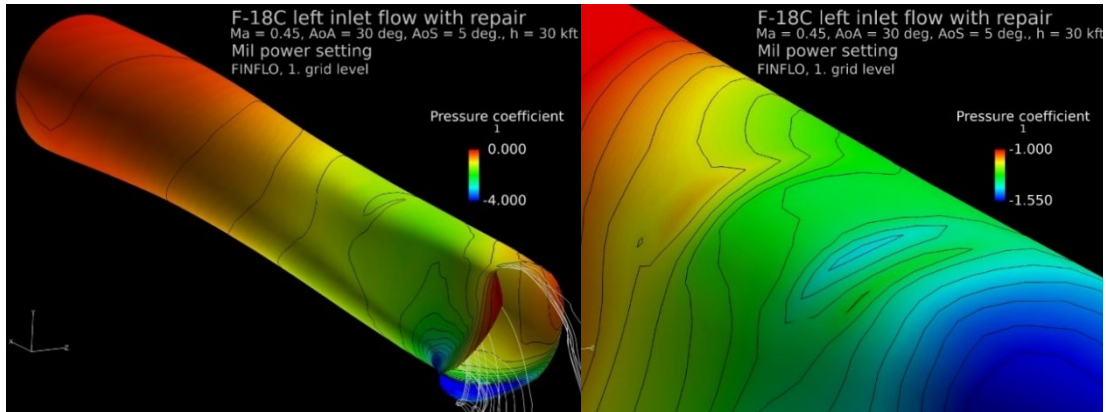


Figure 20: Pressure coefficient distribution for the Hornet left engine inlet duct with a repair at an extreme low-speed flight condition as computed by FINFLO. The full duct is on the left and a close-up of the repair area is on the right. Figure courtesy of Patria Aviation.

2.1.5 Applications and enhancements of Grob G 115E CFD model

In the ICAF 2019 report (Chapter 2.1.4 of Ref. [34]), the CFD models created for the Grob G 115E were described. One version assumes symmetry and is suitable for limited use, and a full model with an asymmetric nose and a propeller actuator disk can be applied to any flight condition at an added computational expense. The purpose of the modelling is to facilitate the support of the fleet acquired by the FINAF from the UK by enabling flight-mechanical studies and determination of aerodynamic structural loads and their distributions, as needs emerge.

As initial applications of the Grob model, the aerodynamic loads acting on the control surfaces in different conditions have been computed. All control surfaces have been studied to assess the hinge loads, and the results have been compared with flight test data. For the elevator, extreme deflections have been applied, and the maximum flap deflection of 60 degrees has also been employed, as seen in the example of **Figure 21**. This case was computed as symmetrical using the half grid. As expected, the flow over the flap separates immediately behind the hinge line at this deflection.

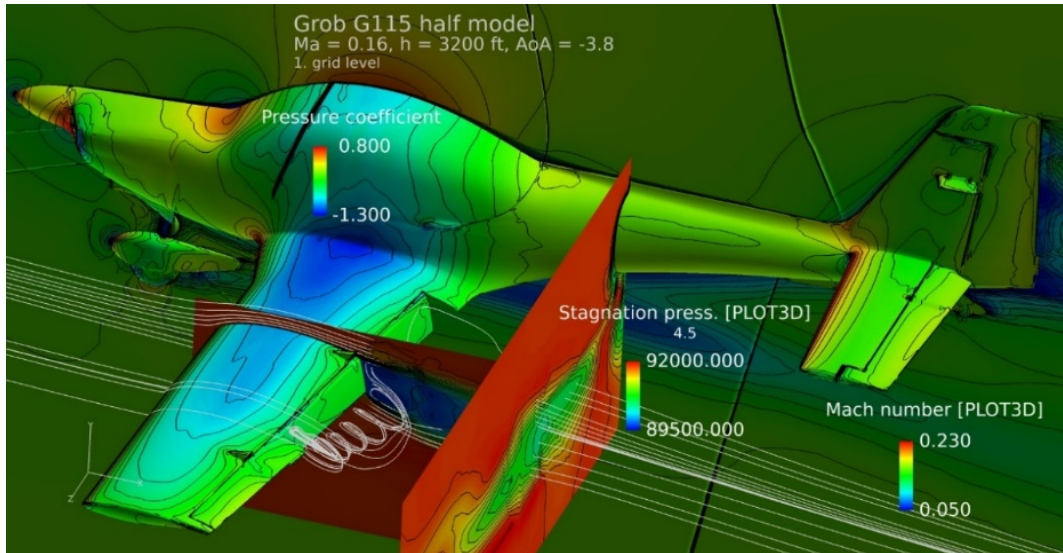


Figure 21: Flow solution for the half Grob G 115E with a flap deflection of 60 deg in a flight-tested condition. Figure courtesy of Patria Aviation.

Another recent application of the G 115E CFD model was to determine the critical loads for the windscreen. The related computations involved the full model with the skew propeller actuator disk producing a rotating slipstream, which results in asymmetric load distributions on the windscreen even in nominally symmetric flight conditions.

In addition to the applications, the Grob model itself was further enhanced in 2019 by adding a movable trim tab to the left elevator via an overset grid block. As the tab involves only the left half of the aircraft, this feature makes sense only in the context of the full model. **Figure 22** illustrates a pressure distribution on the Grob tail obtained with the deflected trim tab. On the left tailplane lower surface, also the flow disturbance caused by the modelled trim tab mechanism tube along the elevator hinge line near its root is clearly visible.

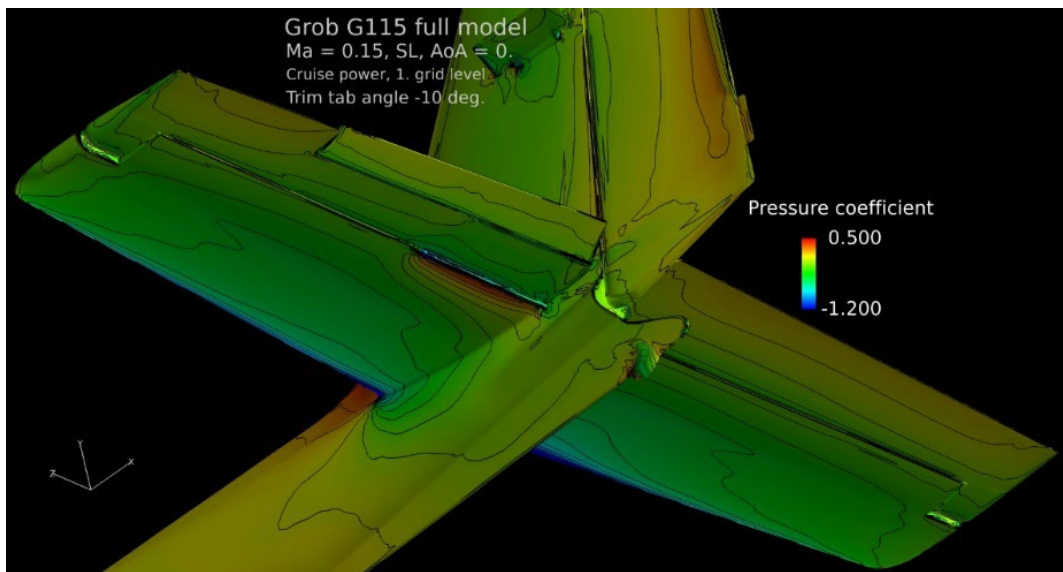


Figure 22: Pressure coefficient distribution on the Grob G 115E tail with the elevator trim tab deflected upwards by 10 deg as computed by FINFLO. Figure courtesy of Patria Aviation.

2.1.6 Computational Fluid Dynamics at Elomatic Ltd.

Computational fluid dynamics (CFD) research at Elomatic Ltd. is based on the in-house flow solver FINFLO. Our F/A-18C related research has been made in collaboration with Patria Aviation and VTT who also utilize the FINFLO solver.

Non time-accurate Hornet simulations with deforming structures have been completed using the FINFLO flow solver over the past years [81]. In addition to the coupling with the MSC Nastran code, in these Fluid-Structure Interaction (FSI) calculations a simplified structural model was coupled with the FINFLO. The coupling was done manually, since only a few couplings are usually required in steady-state cases.

In 2019-2021, time-accurate simulations were further developed and the utilized weak coupling between the fluid mechanics and the structural model was automatized. The FSI calculation system executes the structural modelling in a non-time-accurate manner at every time step, whereas the fluid mechanics is modelled time-accurately. First a single physical time step with the previous geometry is run by the FINFLO flow solver. After the FINFLO run, the simplified structural model is applied to create a new deformed geometry. In the next phase, the updated geometry is read inside the FINFLO code, and the new physical time step is started in the CFD side.

Because of the steady structural part, the basic assumptions were not correct. Despite of shortcomings in the FSI coupling, several simulations were made. The sample case was completed in the same way as it was reported in the ICAF 2019 report (Chapter 2.1.5 of Ref. [34]). The case is a maneuvering aircraft (F/A-18C) flying along a pre-determined path. An instantaneous deformed shape of the aircraft is compared to the rigid geometry in **Figure 23**. It can be stated that the results with the deformation have been more realistic than without the deformation. Owing to the steady-state assumption on the structural side, the biggest problem has been a too high deformation speed, thus artificial damping factors were needed in the simulation system. A more sophisticated methodology for the structural analysis will be pursued in the future.

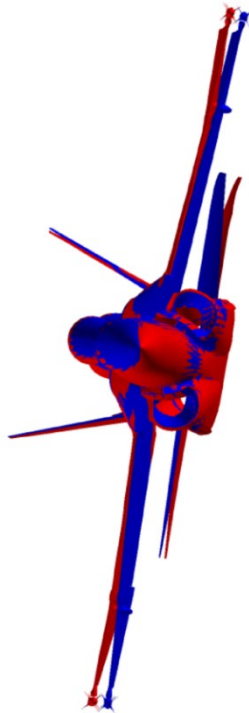


Figure 23: The geometry of the studied F/A-18C aircraft model with deformation (red) and without deformation (blue) during 6 G Rolling Pull-Out at $Ma = 1.09$, Figure courtesy of Elomatic Ltd.

CFD collaboration between Switzerland and Finland has contained regular meetings of persons who work with the F/A-18C CFD models and develop the FINFLO (FIN) and NSMB (SWISS) flow solvers. In 2020, a large project concentrating on code validation as well as on developments in FSI and Chimera-grid technique was started. A goal is to achieve a better understanding of the differences in the results predicted by the CFD codes and to investigate the effects of FSI in the simulations.

2.1.7 Hornet FE modeling - update

In the ICAF 2019 report (Chapter 2.1.6 of Ref. [34]), previous development phases of the global and detailed finite element (FE) modeling of the FINAF F/A-18C Hornet were outlined. Since then, new detailed FE models and crack initiation analyses based on the FINAF fleet usage representative FINAF Basic Operational Spectrum, ver 2 (BOS2) (Ref. [33], Chapter 2.2.5) have been prepared for the following structural locations: Aft Closure Rib, FS233 Former, Dorsal Longeron (Center/Aft Fuselage and FS557.7 Splice Plate) [50], MLG Duct Longeron, Inner Wing Front Spar Fasteners [49], FS508 Shear Tie (extension to previous analysis) [54], [57] and Center Fuselage Dorsal Deck Area FS453-557.5 [42] (Figure 24).

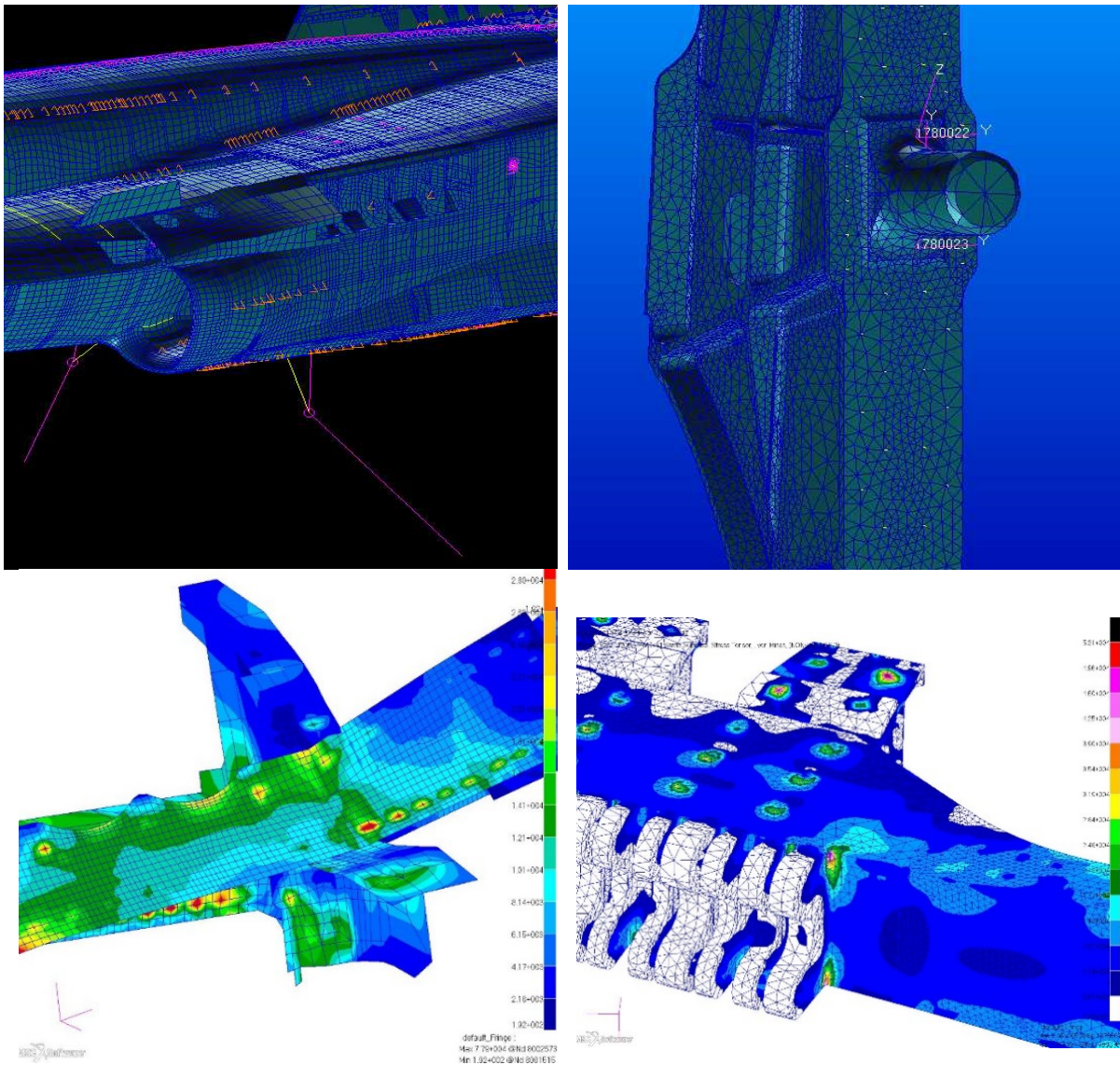


Figure 24: Detailed FE model of FS508 Shear Tie (analysis extension, up), and results of the Dorsal Longeron (FS557.5 Splice plate, lower left) and Inner Wing Front Spar (fastener holes, lower right). Figure courtesy of Patria Aviation.

2.1.8 Flight simulations - update for the F/A-18C aircraft mass model

HUTFLY2 is a generic, MATLAB/Simulink®-based flight simulation software for engineering solutions, including an atmospheric model, nonlinear six degree-of-freedom rigid-body flat-earth equations of motion, determination of forces and moments and other common routines (like visualizations) required by the simulation. Modular design allows different aircraft models to be implemented into simulations. One important example is the F/A-18C Hornet aircraft model, describing the aerodynamic properties, Flight Control System (FCS), mass distribution and propulsion system that has been incorporated into the HUTFLY2 simulation as a subsystem. The recorded HOLM data (Chapter 2.2.1) has also been utilized in the VER/VAL process of the Hornet aircraft model.

Over the years, the HUTFLY2 flight simulations have supported structural fatigue life management of the FINAF fleet in various ways, like by inverse flight simulations, providing input values (aircraft initial state) for CFD analyses, and providing realistic approach paths to support functional troubleshooting in the Hornet Main Landing Gear (MLG) plaining link issues of the FINAF F/A-18C/D aircraft [67]. Former flight simulation activities have been highlighted in various ICAF National Reviews, like in Chapter 4.5 of Ref. [27], Chapter 13.6.3.1.1 of Ref. [28], Chapter 13.2.1.2 and Chapter 13.3.3 of Ref [29], and Chapter 13.2.1.2 and Chapter 13.2.1.2.3 of Ref. [30].

The associated elements (software/hardware) have been upgraded when needed in order to maintain the simulation capability in a level corresponding to the actual flying of the FINAF aircraft. Last updates for the F/A-18C aircraft model have been the upgrade of the Flight Control System (FCS) model (Chapter 13.2.1.2 of Ref. [31]), and most recently, the mass model update [66] (**Figure 25**) along with the A/G training capability (see also Chapter 1.4). VTT completed all the updates, but the mass model update was also supported by the Joint Systems Centre and Air Combat Centre/Flight Test Section of the FINAF. The updated data/model has been utilized in the revised Hornet MLG study (Chapter 3.1 of Ref. [34]), and in trajectory comparisons for the external store separation simulations done by Elomatic Ltd [71].

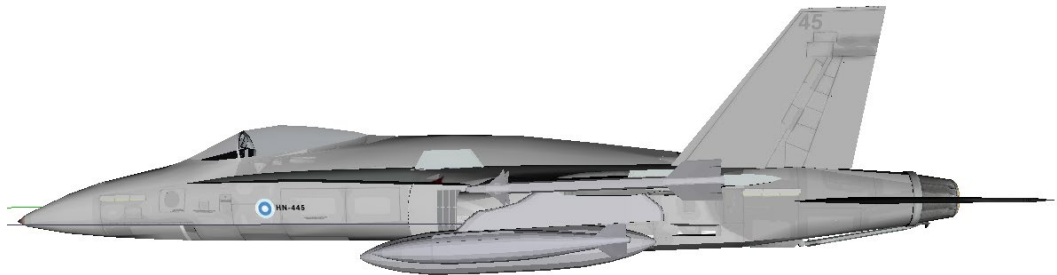


Figure 25: The FINAF F/A-18C aircraft model with a JDAM store in the HUTFLY2 flight simulation software. Visualization module updated by Trano Ltd. Figure courtesy of VTT.

2.2 Loads monitoring and fatigue tracking systems

2.2.1 The FINAF HOLM aircraft in routine squadron service

The FINAF has routinely been running the Hornet Operational Loads Measurement (HOLM) program since 2006 [28]. The goal in this program is to quantify the effects of operational loads on the structure of the F/A-18 Hornet aircraft and thus support the national aircraft structural integrity efforts. The HOLM program employs two Boeing F/A-18C Hornet aircraft (HN-416 and HN-432) with originally identical, but afterwards diverged onboard data acquisition systems (**Figure 26**) and instrumentation (Ref. [33] Chapters 2.2.2, 2.2.4). 44 strain sensors, in all, have been fitted on globally important locations as well as in the vicinity of structural locations addressed to be fatigue critical. In addition, four accelerometers have been installed in top of the Vertical Tails. Concurrently the HOLM system monitors and records 250+ flight parameters from the MIL-STD-1553 data buses of the aircraft. The optimized sampling rates of the strains vary from 1280 Hz in the highly vibrating structural locations (e.g. Vertical Tail) to 640 Hz elsewhere. The sampling rate of the accelerometers is 2560 Hz.

The master plan is that the recorded high fidelity structural response information from two extensively instrumented aircraft can be merged with data obtained from Artificial Neural Network (ANN, Chapter 2.2.2) enabling to evaluate the structural life consumption of the entire Hornet fleet with adequate reliability.

After 15+ years of service in harsh environment, the hardware is still working great, and the quality of the recorded HOLM data has remained outstanding, that is, the HOLM data forms a good basis for all the subsequent analyses and data sets needed, like in Ref. [72].



Figure 26: HOLM DAU Master Unit. Figure courtesy of VTT.

To date, VTT has analyzed in the HOLM ground analysis environment more than 3300 flights from routine fleet operations, and thus prepared several annual or semi-annual fatigue analysis reports, from which the newest was dated 2020 [76]. The report presents fatigue life estimates of the critical and the instrumented locations of the HN structure in a versatile way, such as from a syllabus, a sub-assembly, and from buffeting point of view. A remarkable advantage is the possibility to compare the results on a flight-by-flight basis in between different sources (SAFE and HOLM), and as recurring process, track the trends of the analyses.

Within this research period, the structure and contents of the HOLM fatigue analysis database have been updated. The database works seamlessly with the data from the HOLM ground analysis environment. In addition to data from the fatigue tracking system the database includes all the information needed from the data analysis process. [75]

During the period of this report there has not been any notable finished HN related updates to the HOLM ground analysis environment, like new transfer functions or fitting factors, but commissioning of the crack growth analysis module is ongoing at VTT [43]. AFGROW, a fracture mechanics and fatigue crack growth analysis software, is integrated into a part of HOLM ground analysis environment. This is possible by means of COM (Component Object Model) automation interfaces that allows AFGROW to interface with other Windows® applications to perform repetitive tasks or control AFGROW from these applications [13].

The onboard HOLM instrumentation is periodically calibrated by VTT. The annual electrical calibrations of HN-416 and HN-432 reveals if any changes in the measuring chain have occurred or if the calibration coefficients need to be adjusted. Based on the calibration results, the quality of the system has remained outstanding: the quality of the strain signals is good and all the recordable strain data has been captured (minimal missing data). This all forms a solid base for all the analyses that are made based on the HOLM data. [51], [69], [73], [74]

As highlighted in Chapter 2.2.5 of Ref. [33], a representative FINAF F/A-18 usage spectrum, Basic Operational Spectrum ver 2 (BOS2), was compiled on the basis of HOLM and SAFE data in co-operation with VTT and Patria. To this point, VTT has analyzed HOLM data from many air-to-ground (A/G) missions, too (Chapter 2.2.5). To investigate the significance of the A/G flights to the BOS2 flight data set (BOS2), where this kind of flights were not included yet, VTT conducted a brief sensitivity analysis [77]. The sensitivity analysis focused mainly on the fatigue effects of the flights, which is one of the two primary aims when formulating a BOS spectrum. In this connection, it is significant to take the FINAF's current operating syllabus spectrum, but also all relevant flights and all other available aspects of the fatigue calculations, into account.

Achieved results showed that thus far absent A/G flights can be seen as a shortage and should be included in a BOS spectrum. It is noteworthy that a BOS spectrum is always a syllabus spectrum of flight hours, and not a syllabus spectrum of the amount of flights nor fatigue distribution. Due to all these above-mentioned aspects, the lack of the A/G flights in any BOS version should be considered as a distortion of the BOS spectrum.

Since the previous ICAF National Review, the store configurations of the BOS2 spectrum flights have been summarized in [68], and provided to the FINAF.

Since the previous National Review, the HN structural damage database has also been updated. The database has been used e.g. in screening the fatigue critical structural locations of the FINAF F/A-18C/D configurations and to help focusing the proactive maintenance planning activities. The latest update includes observations from the OEM's component level Vertical Tail fatigue test reports. The database together with its graphical user interface has been updated into version GUI 5.0. [70]

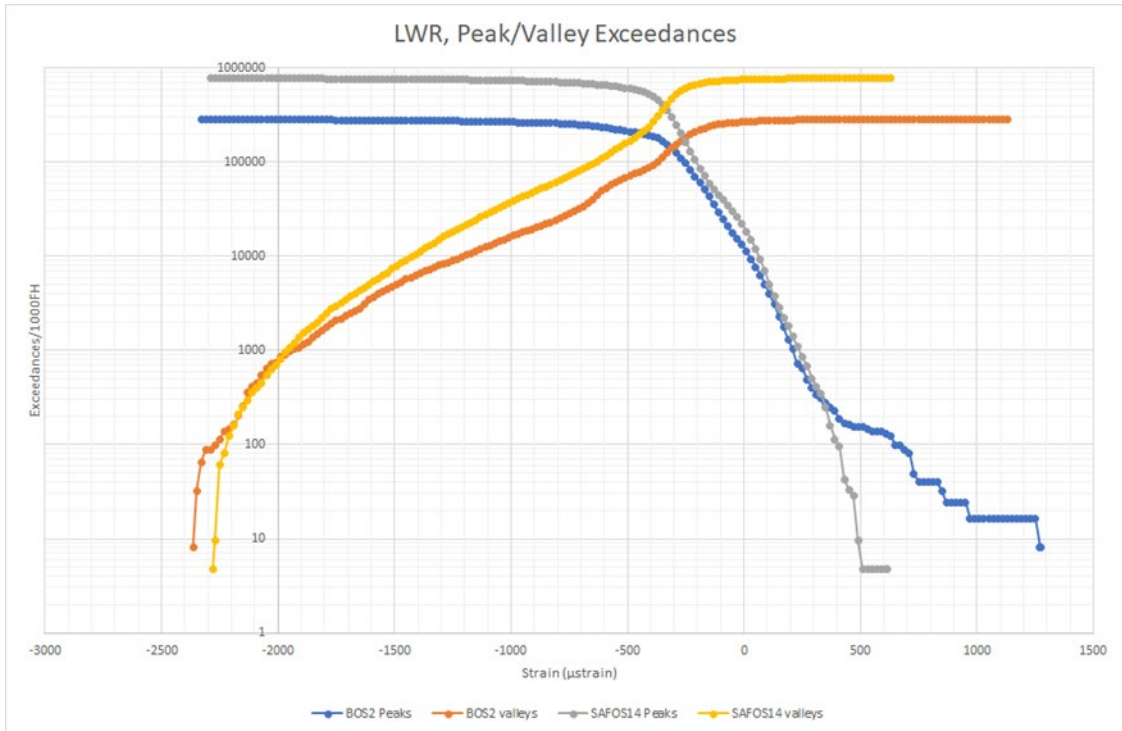


Figure 28: An example of strain signal peak/valley exceedance comparison in between the Swiss SAFOS14 spectrum and Finnish BOS2 spectrum. Figure courtesy of Patria Aviation.

Although both spectrums were only analysed partially due the problems of missing flight parameter data, some valuable information from the differences of the spectrums were obtained. This kind of information can be useful if fatigue life estimates of the different structural location are further compared.

2.2.3 Operational spectra for Hornet Wing Root and Wing Fold loads

Related to the aging F/A-18C/D Hornet fleet of the FINAF, operational load spectra for the Wing Root and Wing Fold were formed and studied in 2020 [56] to enable enhanced fatigue studies and comparisons with the other F/A-18 users. The loads of interest are the shear, torque and bending moment at locations specified in **Figure 29**. The work combined the flight parameter and strain gage data recorded from a representative block of operational flights (BOS2) with a parameter-based load model. The applied Finnish BOS2 operational spectrum covers 161 flights and approximately 140 flight hours recorded from two HOLM-instrumented aircraft (Chapter 2.2.5 of Ref. [33]).

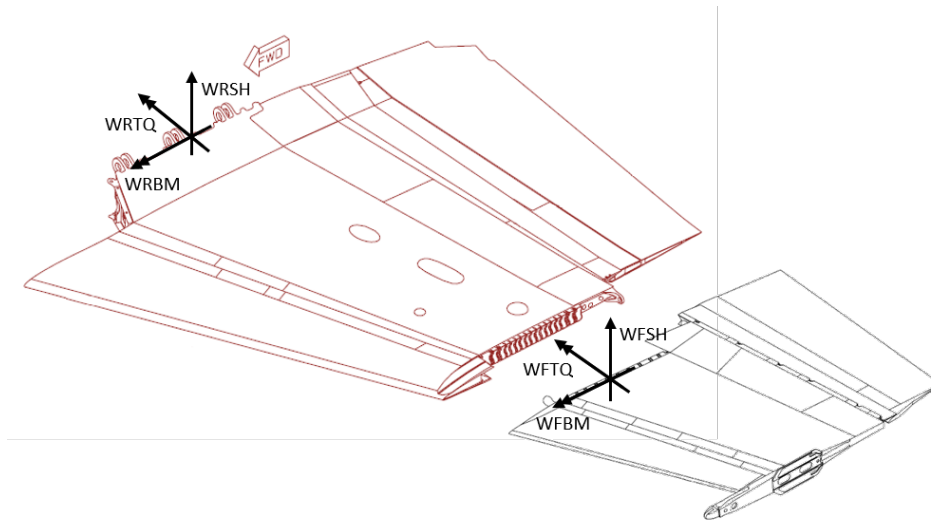


Figure 29: Definitions and reference locations for the Hornet Wing Root Shear (WRSH), Wing Root Torque (WRTQ), Wing Root Bending Moment (WRBM), Wing Fold Shear (WFSH), Wing Fold Torque (WFTQ), and Wing Fold Bending Moment (WFBM).

The wing maneuvering loads as functions of flight parameters and aircraft store configuration could partially be modelled on the basis of the OEM (Boeing) supplied reports, but the CFD computations with FINFLO solver were also required to obtain a model to represent the relevant F/A-18C/D variant data instead of the early F-18 prototype wing covered by the OEM data. These computations were described separately in Chapter 2.1.3. As an example of the maneuvering load modelling, the left hand side of **Figure 30** shows the aerodynamic bending moment coefficients at different angles of attack at selected Mach number with and without the wing tip missile. The right hand side in turn illustrates the composition of the Wing Fold loads with the two store configurations in selected flight condition.

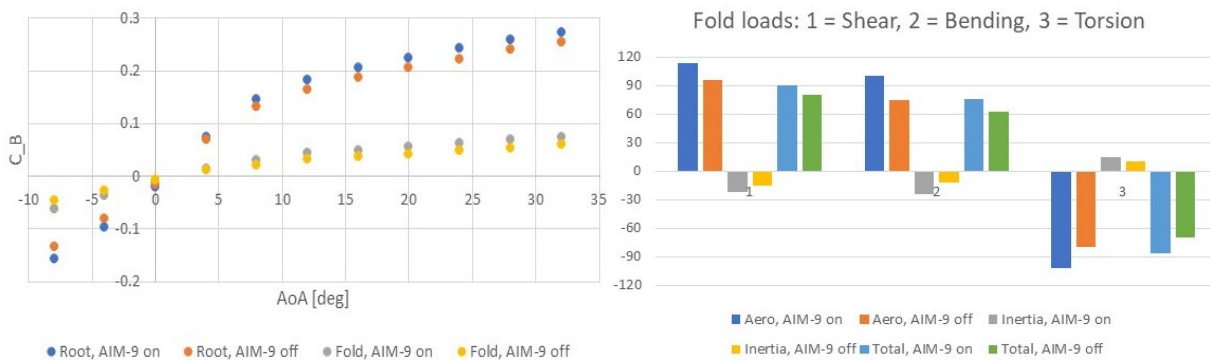


Figure 30: Wing Root and Wing Fold aerodynamic bending moment coefficients as a function of angle of attack at $Ma = 0.95$ (left) and the composition of all three maneuvering loads at the wing fold in one flight condition (Steady State Pull-Up, SSPU, $Ma = 0.95$, $\alpha = 8.9^\circ$, $h = 15$ kft, $n_z \approx 7.5$) (right) with and without the tip missile. Figure courtesy of Patria Aviation.

In addition to the maneuvering loads, the total fatigue critical loads are increased in certain flight conditions by the buffeting (flow separation). These highly dynamic load increments must be taken into account. To formulate a general model, suitable filtering of the HOLM-recorded strain gage signal histories can be applied to separate the high-frequency buffeting components from the deterministic maneuvering load components.

A rainflow analysis can be applied to these additions, and the resulting essential dynamic load amplitudes and frequencies can be related to the flight parameters. However, such generalized modelling of buffeting loads could not be realized in 2020, and the high-frequency load variations were studied just in the context of BOS2 data based directly on the recorded strains.

To generate histories of the Wing Root and Wing Fold loads from the BOS2 flights, two methods were applied. One method involved the maneuver load modelling based on the recorded flight parameters. In the second method, the filtered strain histories collected from several wing locations were firstly correlated with the modelled maneuver loads. When the unfiltered high-frequency strain signals were then fed into the correlations, total loads with the buffeting additions were obtained. A difficulty in the correlations was caused by the fact that the HOLM gages do not match the load locations defined in **Figure 29** very well, and the directions of the measured strains also were not necessarily optimal to capture the essential phenomena.

Figure 31 shows examples of time histories for the maneuvering bending moments (BM) at Wing Root (WRBM) and Wing Fold (WFBM) based on the maneuver load model directly and on correlations applying different strain gages (like S12a and S20a) during a 30-second period of a BOS2 flight. It is seen that for the Wing Root the four different variants to model the load agree quite well, but at the Wing Fold the curves deviate at low load levels. The reason for the deviation may be related to the recorded angle of attack that is a strong factor in the load model. The most problematic load of the six turned out to be the Wing Root Torque (WRTQ), for which no useful strain based correlation could be formed.

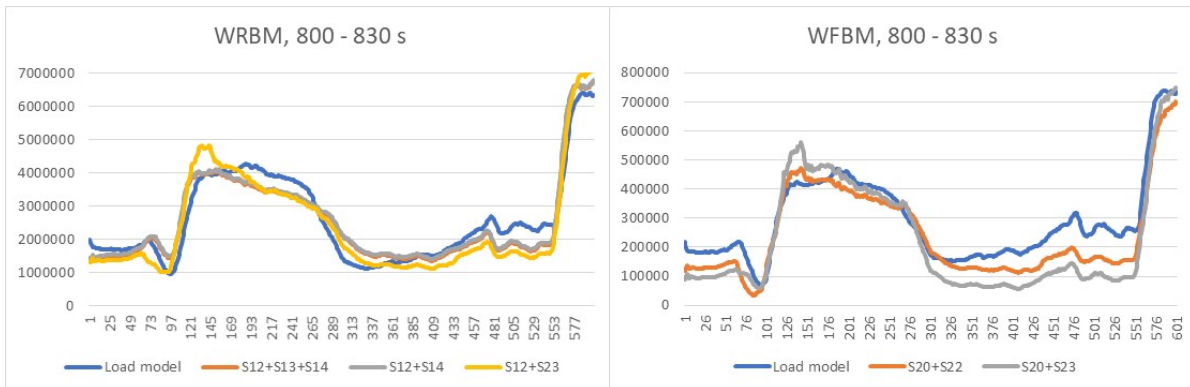


Figure 31: Wing Root and Wing Fold maneuvering bending moments [lb-in] modelled in different ways during a 30-second period of a BOS2 flight. Figure courtesy of Patria Aviation.

Figure 32 depicts the mutual correlations of different Wing Root and Wing Fold maneuvering bending moment estimates from five BOS2 flights with more than 250000 data points. It is seen that the overall agreement of loads based on the flight parameters and the maneuvering load model and based on the selected strain gage data with their formed correlation with the load model is not particularly good. There is a lot of noise and some systematic deviations exist. The point clouds for other loads than the bending moments are even more dispersed.

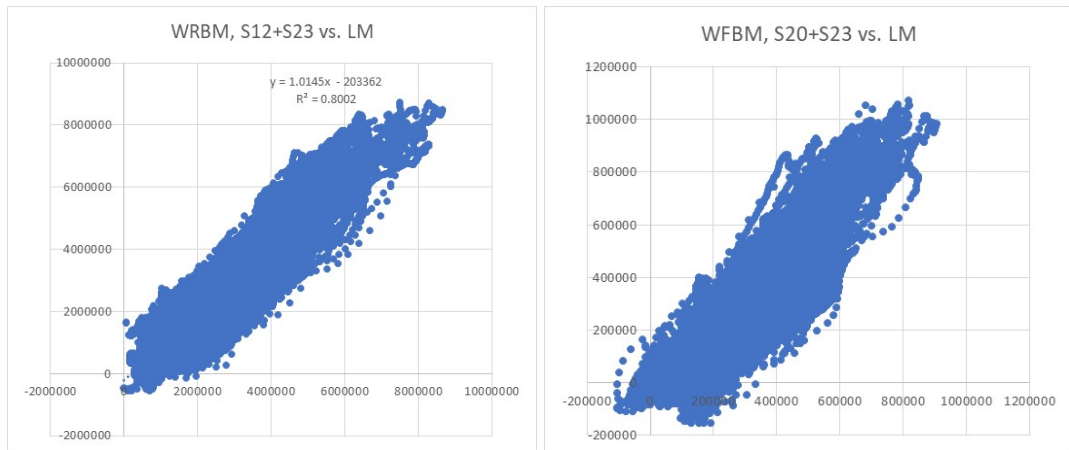


Figure 32: Mutual correlations of Wing Root and Wing Fold bending moments from five BOS2 flights. The horizontal axes represent loads determined via the maneuvering load model (LM), and the vertical axes represent values based on selected sets of strain gage data. Figure courtesy of Patria Aviation.

Eventually, the load histories generated for the BOS2 flights in three ways were utilized to estimate the structural fatigue lives at the Wing Root and Wing Fold. In this phase, LifeWorks program [48] was applied to predict crack initiation and growth using the load histories and related local stresses. **Figure 33** shows the computed fatigue life curves for aluminium alloy 7050-T74 based on the bending moment histories at the Wing Root and Wing Fold and on practical stress levels. The horizontal axes represent flight hours, and the vertical axes give the stress levels at which the crack growth limits the fatigue life. The blue curves are based on the load histories obtained from the flight parameter based maneuvering load model. The yellow curves relate to loads based on the strain data histories but filtered down to a frequency of 4 Hz, which should represent maneuvering loads, too. The black curves are based on the strain data histories analyzed at a high frequency of 80 Hz, which corresponds to total loads including the buffeting effects.

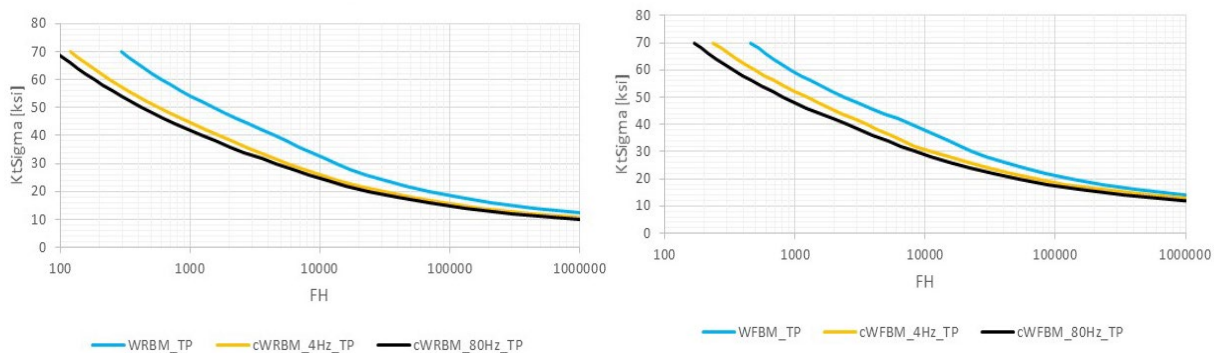


Figure 33: Fatigue life curves computed on the basis of complete BOS2 data for the Wing Root and Wing Fold at practical stress levels related to bending moment variations. Figure courtesy of Patria Aviation.

It is seen from **Figure 33** that the curves based on different versions of the load spectra differ from each other markedly. The spectrum based directly on the maneuvering load model is the most benign, and the predicted fatigue lives based on it are typically more than double of the lives based on the recorded strain data. These differences are larger than expected and suggest inaccuracies in the different types of load models. As expected, the high-frequency load spectrum is the most severe one, but the additional effects of buffeting do not appear significant.

Until now, the determination of the load histories for the Wing Root and Wing Fold based on the BOS2 flight data is not entirely successful, which leads to suspicious wing fatigue life estimates. There are some uncertainties in the definitions of recorded flight parameters, and the available set of HOLM strain gages do not completely determine the prevailing load conditions. Improved correlations could probably be formulated, but presently the work is not continuing. Furthermore, the generalization of the buffeting load model as a function of flight parameters is tempting, because it would enable individual fatigue studies for each standard aircraft of the fleet - not instrumented with the specific HOLM data acquisition system.

2.2.4 Modal testing of Vertical Tail of the F/A-18C Hornet

The goal of this study was to identify experimentally dynamic vibration characteristics of the Vertical Tail (VT) of the FINAF F/A-18C Hornet (here HN-416). Vibration properties, i.e. natural frequencies, modal damping factors and mode shapes were determined experimentally by impact testing [58]. Special focus was on the modes around 15 Hz and 45 Hz. Based on earlier analysis of the measured (in-flight) acceleration and strain data, it has been found that the VT experiences high vibration levels around these frequencies due to flow-induced excitations.

The measurements were conducted by VTT at Lapland Air Command (Rovaniemi) on June 2019, following the HOLM system electrical calibrations (Chapter 2.2.1). The aircraft was standing on the landing gears. The VT (L/H and R/H tails separately) was excited by instrumented impact hammer having a soft plastic tip. Responses were measured by 18 triaxial IEPE-type accelerometers. In total, 50 acceleration response points were measured, all locations in three directions. Measurement points were located on the Vertical Tails, stabilators, wings and engine cover, see **Figure 34** and **Figure 35**. Both VTs were excited separately and responses from both VTs and other locations were measured during all tests. Due to limited number of accelerometers, measurements were repeated three times and locations of the accelerometers (except two reference points) were shifted between the tests in order to cover all the locations. Averaged Frequency Response Functions (FRFs) were calculated between measured input excitation force and acceleration responses. Poly-reference least squares complex frequency domain estimation method (PolyMAX) was used for modal parameter estimation. In addition, maximum likelihood modal model-based (MLMM) estimator was used for improve the initial PolyMAX modal parameter estimates, i.e. improving modal model fit to the measured FRFs.

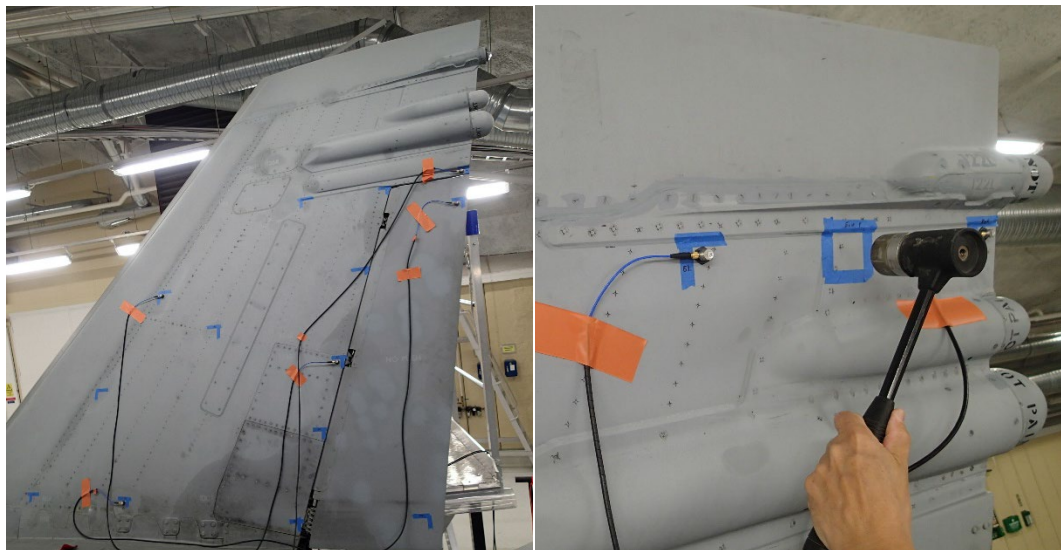


Figure 34: A set of measurement points (left) and a reference excitation location (right) during the impact testing of the FINAF F/A-18C Vertical Tail. Figure courtesy of VTT.

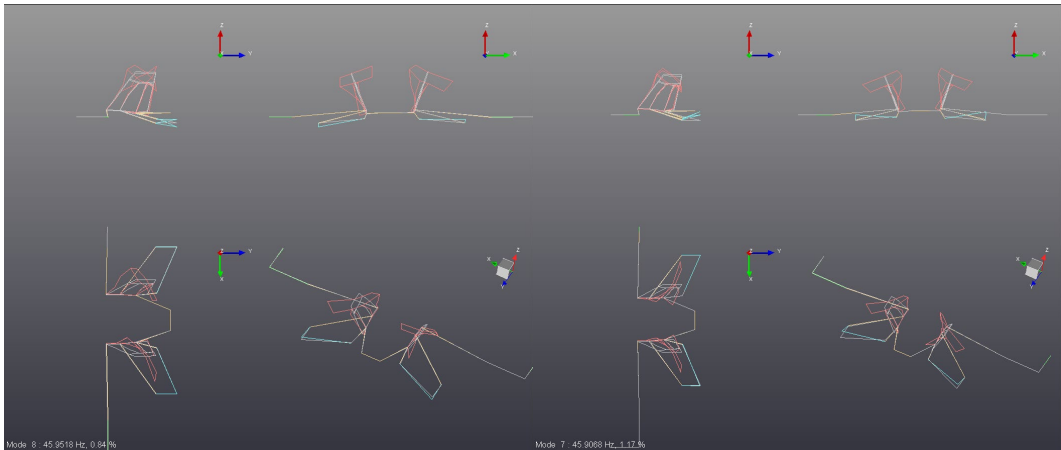


Figure 37: Measured FINAF F/A-18C Vertical Tail mode shapes (torsion) around 45 Hz. Antisymmetric mode, 45.95 Hz (left) and symmetric mode, 45.91 Hz (right). Figure courtesy of VTT.

It could have been tempting to measure reference accelerations with the HOLM system (Chapter 2.2.1), as it incorporates acceleration transducers installed on tip of the Vertical Tails (two per VT) of this FINAF HOLM aircraft (HN-416). Unfortunately the idea was not practicable in the impact testing, since the aircraft engines had to be running while recording structural responses by means of the HOLM system.

2.2.5 The effect of A/G training on the structure of the FINAF Hornet

Along with commenced air-to-ground mission training of the FINAF Hornet fleet (Chapter 1.4), it had, in process of time, become topical to study the effects of a new Syllabus from the structural point of view - and the rugged HOLM-system (Chapter 2.2.1) in conjunction with its analysis environment was a perfect tool for the purpose.

Although the FINAF started A/G training sorties with the fully operational HOLM aircraft in 2015, not until 2020 the number of recorded flights was estimated sufficient that VTT in collaboration with Trano Ltd. could conduct systematic evaluation and draw initial conclusions about the effect of A/G training on the structure of the FINAF Hornet aircraft. [77]

In the selected time frame, 6 % of the flights were categorized as A/G training. The fatigue analyses based on the HOLM strain data indicated that the effect of A/G training on the structure had been mild: the share of cumulative fatigue damage accrued from the A/G training was approx. 5.3 % at most. The most strained structural details were in the center fuselage and wing-to-fuselage joint. Structural fatigue on the aft fuselage or Vertical Tail were almost negligible. This indicates that the A/G training akin to the evaluated flights has no detrimental effect on the structure from fatigue point of view. The analyzed fatigue damage rates of the HN-416 aircraft are presented as an example in **Figure 38**. It can be seen that the emphasized air-to-ground training is relatively insignificant for the structure, and there exists more straining sorties in the training repertoire. Flight training and exercises include, in accordance with the FINAF mission requirements, a great deal of air combat maneuvering which stresses the aircraft's structure more than air-to-ground training.

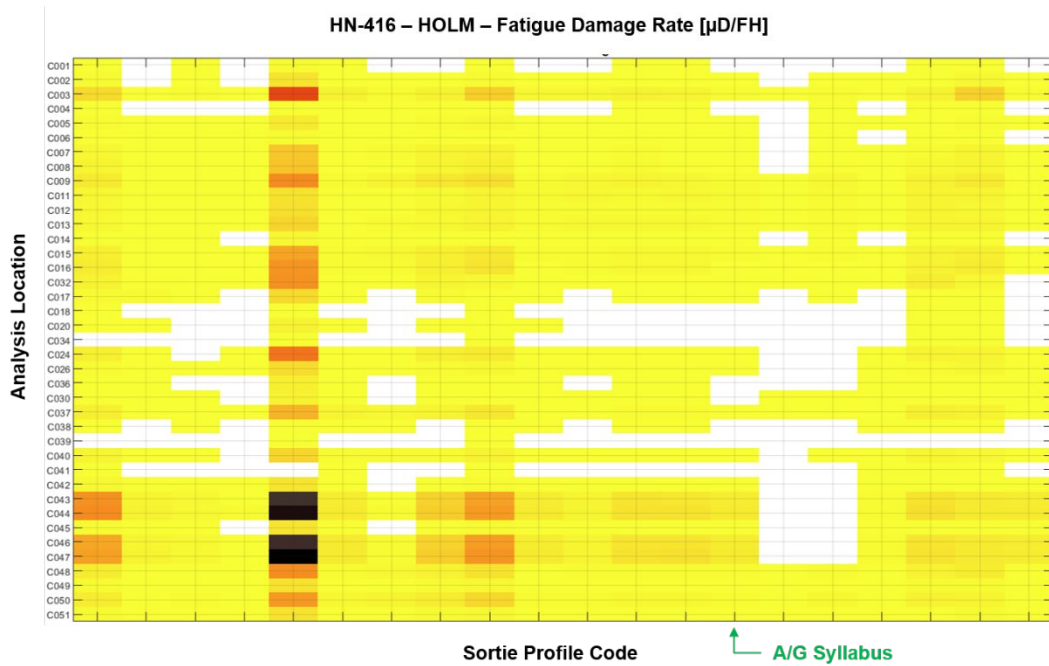


Figure 38: Calculated fatigue damage rates of the FINAF HOLM aircraft (HN-416) as a heatmap. A/G syllabus results at the tick mark are emphasized in the figure. White color indicates negligible damage rates, which are clipped out from the scale. Figure courtesy of VTT.

Thus far recorded A/G flights were also analyzed in the view of their significance to the BOS2 flight data set (Chapter 2.2.1), and grouped according to their flight profiles to see if there existed a trend in between specific flight profiles and calculated fatigue damage of the corresponding flights.

Since introducing the air-to-ground capability, the new ordnance has been subjected to operational testing and evaluation, including live drops, in a dedicated test range in Finland. Sometimes there can form an unfavorable in-flight pressure distribution in the vicinity of store that hinders the released store from entering the air stream and falling properly to the target. To overcome this unwanted phenomenon and to ensure a safe release, the bomb ejector rack ejects the store from the bomb rack with sufficient force. The ejection of a conventional store is thus a transient event that causes a so-called g-jump i.e. sudden counter-reaction of the platform. Obviously the structure must withstand the imparted loads during the ejection of a store from pylon.

The HOLM system records a good number of flight parameters - like weapon code/count - in a synchronized time history format from the MIL-STD-1553 buses of the FINAF F/A-18 Hornet. Among other things, the recorded HOLM data can be utilized to track and analyze structural responses from the store ejection events.

In addition to getting an overall view of the structural effects from A/G training, the secondary objective of the study was to quantify the effects of a store ejection to the structure of the FINAF Hornet.

Among the recorded A/G flights only few ejections/launches were identified. At the time, the state of the aircraft was analyzed from signal time histories, and the interesting time segments were also confirmed with a handy visualization tool (see also Chapter 2.1.8).

In one example, a 250 lb JDAM (short range guided bomb) was ejected from the station #8 (R/H wing) in a level-flight (Figure 39).



Figure 39: Screenshots from visualization of the analyzed drop event. The store was released from the station #8, R/H wing. Figure courtesy of VTT.

From fatigue damage point of view the store ejection did not play any role in this example. Instead, it was interesting to analyze the structural responses from the in-flight dynamic event. The structural response from ejection impulse can be seen in **Figure 40**. The store was ejected from the R/H wing, and the response was recorded at the L/H Wing Fold. Transient impulse was strong enough to excite the lowest natural frequencies of the structure, but transient vibrations decayed quickly, within one second. Structural responses could be observed in all the HOLM measurement points.

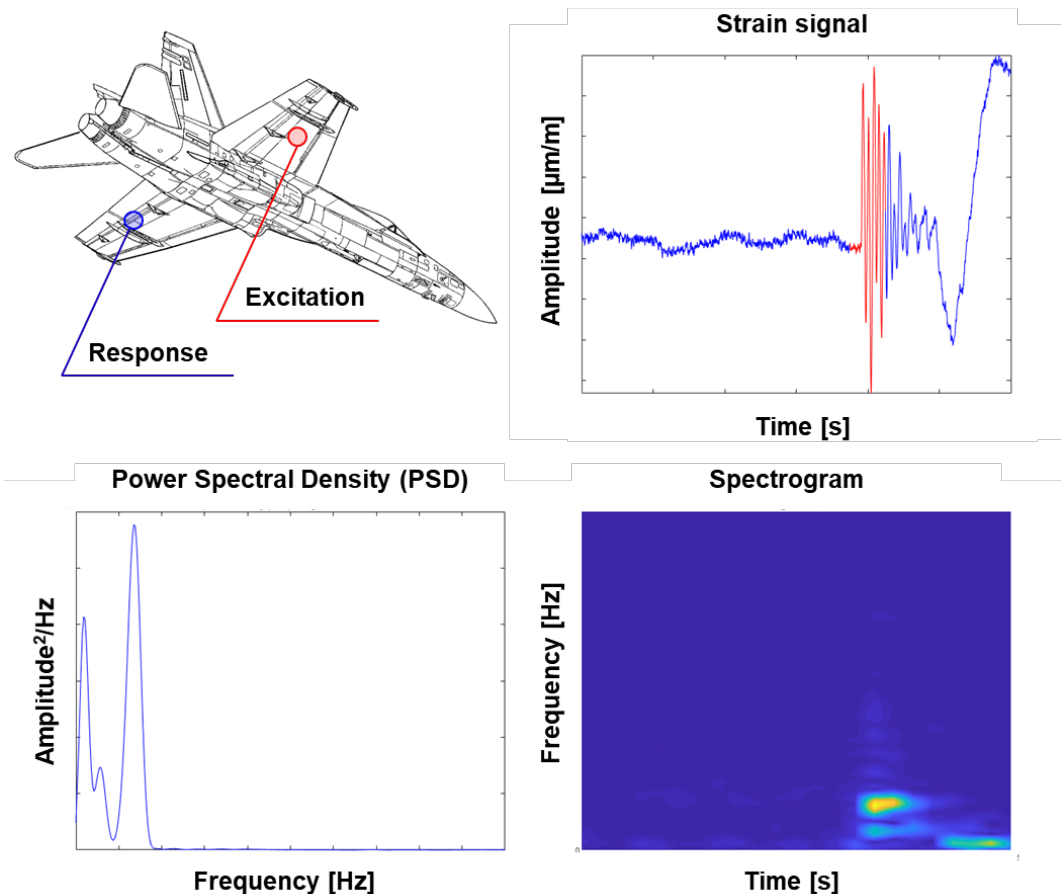


Figure 40: An example of the structural responses from ejector impulse. In this case, a 250 lb JDAM was ejected from the station #8, R/H wing, and recorded at the L/H Wing Fold measurement point. Transient vibrations decayed within one second. Figure courtesy of VTT.

2.2.6 Research efforts towards Hawk structural integrity management

The FINAF flight training syllabi changed significantly some years ago. For example, glass cockpit modification (see Chapter 1.3) enables practising some training flights with the Hawk aircraft which earlier were flown solely by the Hornet. These changes may reduce the life of some critical structural components or locations well known from the older FINAF Hawk Mk.51/51A fleet.

The inherent fatigue tracking system for each FINAF Hawk aircraft has solely been based on counting g level exceedances and calculating a usage index i.e. Fatigue Index (FI) by the variant specific equations. This method is adequate for monitoring the structural locations mainly influenced by aircraft normal acceleration (multiplied by weight). However, current FI tracking does not take buffet loading into account which is the main driver for the fatigue issues e.g. in the empennage of the Hawk aircraft, thus additional structure-specific fatigue tracking indices have been developed.

2.2.6.1 Hawk Structural Health Monitoring (SHM) update

The Structural Health Monitoring (SHM) related Neural Network (NN) investigations for the FINAF Hawks were already explained to some extent in the previous ICAF 2019 report (Chapter 2.2.3.2 of Ref. [34]).

To reliably track the structural integrity of the Hawks' tail with the NN system, the application must be trained (the specific virtual stress data channels, i.e. digital twins must be created) with real flight data measured from the instrumented aircraft. Also, the NN system maintenance needs data from the instrumented strain gauges later in the tracking phases, but the training data set must be different from the tracking data set; i.e., the sets are from different flights. [55]

The first NN version was based on HW-368 mini OLM flights (Chapter 2.2.3.1 of Ref. [34]). There were 434 measured flights in all, from which 149 were chosen for NN training and 238 for validation. Previous studies have shown that vibration is the main contributor for fatigue in Hawks' tailplane. The lowest natural frequencies that are effective on fatigue were found as 15 Hz and 90 Hz. That was why stress modelling was divided to three NN components: static (below 5 Hz), frequency and amplitude components.

The NN input parameters are: pitch rate, normal acceleration, Mach number, angle of attack, roll acceleration, pitch acceleration and dynamic pressure, which are recorded in each FINAF Hawk by a mission data recorder. At the first stage, the data from the chosen flights was imported to the NN "training environment" and 7000 data points were filtered from it for NN training and validation. The NN training program establishes correlation figures in between stresses obtained from the NN analyses and flight measurements, shown as an example in **Figure 41**. Correlation in static component was rather linear (Subfigure a) but amplitude (Subfigure b) and frequency (Subfigure c) components were more scattered. This is typical behaviour. The correlation in validation data points are not shown here but they were very similar to the NN training data points.

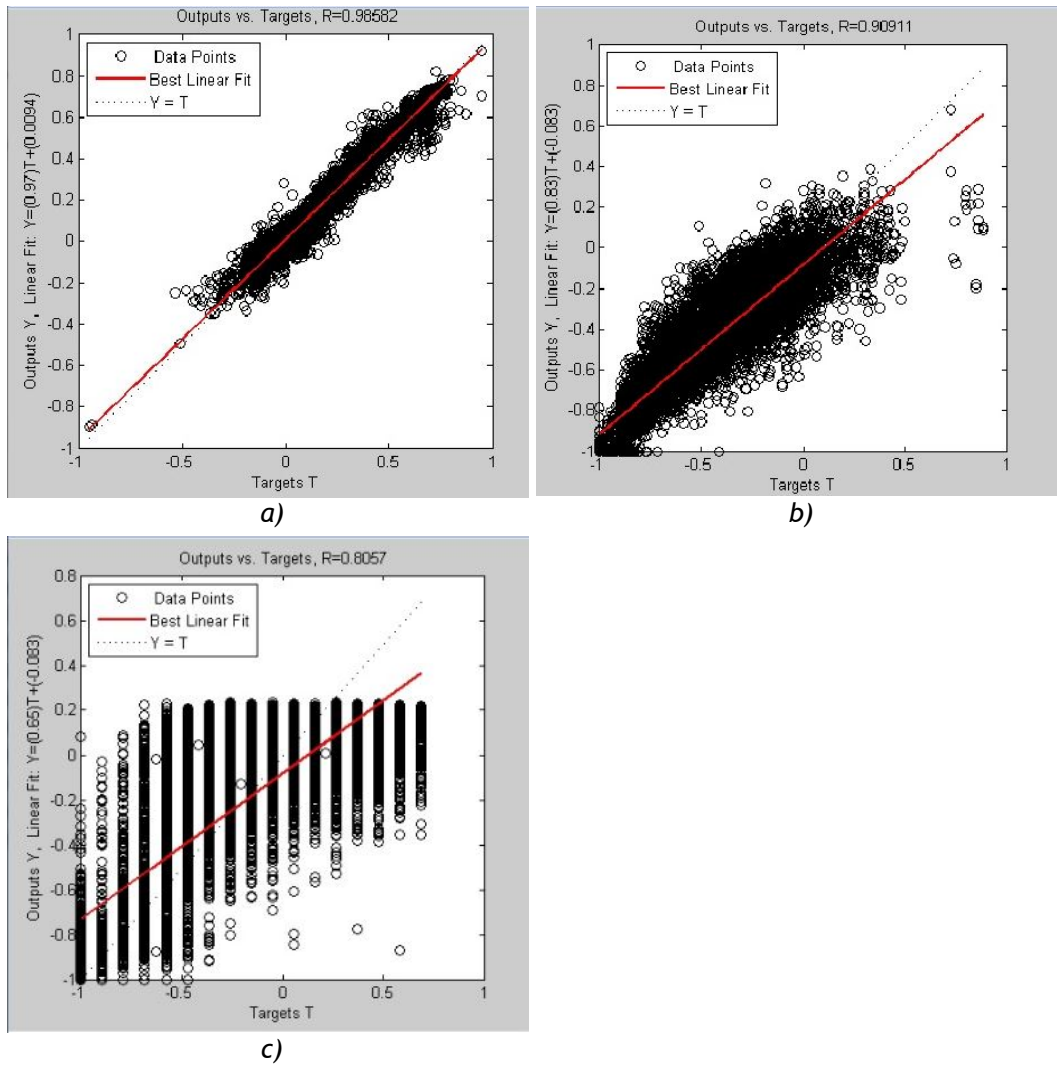


Figure 41: Subfigure a: Scatter of training static (low-pass filtered data) component (correlation 98,6%), b: amplitude component (correlation 91.0%), and frequency component (correlation 80.6%). Figure courtesy of Patria Aviation.

In **Figure 42**, stress time histories generated by the NN simulation, and measurements obtained from the same flight are compared. It can be seen that the NN simulation corresponds rather well to the flight measurements - even in dynamic events. The difference in calculated fatigue damage based on data from NN simulations and flight measurements was approx. 3% for this specific flight. It is obvious, that not for all flights the correspondence would be as good. For all the analyzed flights, the ratio between calculated damage from NN simulation and flight measurements was approx. 1.6 (the NN simulation being conservative).

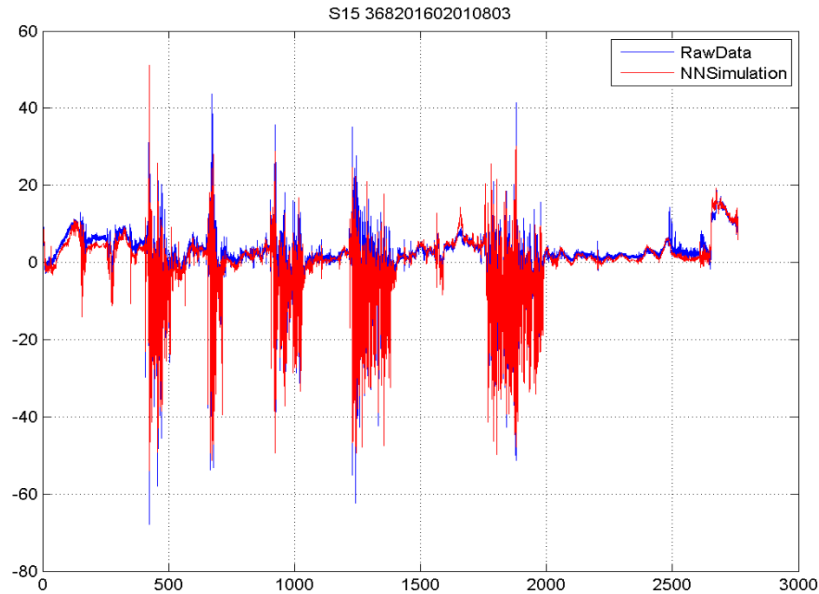


Figure 42: Stress [MPa] time history generated by the NN analyses (NNSimulation) compared with the data obtained from the flight measurements (RawData). Figure courtesy of Patria Aviation.

The created neural network based on recorded mini-OLM data was used to calculate fatigue damage of the empennage for the FINAF Hawk fleet, and the first results seemed reasonable. However, the NN will further be developed with more training data from five SHM-instrumented aircraft (Chapter 2.2.3.2 of Ref. [34]). The onboard instrumentation consists of five strain sensors of which three are installed on the tailplane, one in the fin root, and one in the fuselage top longeron, left-hand side. The fuselage measurement location is highly influenced by the aircraft g-loads (times the weight of aircraft), and is therefore used for synchronising the strain gauge data with the flight parameter data.

The training and the tracking data sets are acquired with Emmecon's Data Acquisition Unit (DAU). The time history and turning point data is stored as an ASCII file format for further processing. Before actual training of the neural network, the data set must be quality checked, which is ongoing at VTT [46].

Updated data checking modules of VTT's ground analysis environment are used to convert, and pre-check the recorded data, and to show the signal time histories to analyst, who visually makes final checks, and decides the status of the data integrity. Each flight is checked e.g. for drop-outs and spurious data points (spikes), flat responses, limit exceedings, start/stop levels, and completenesses. A decision is then made, whether to accept the data quality or not for the NN training set using also flight log data, operating syllabus, and aircraft parameter data as an interpretation backing.

It is noteworthy that the data quality check helps develop Emmecon's SHM (EMM-SHM) data processing software modules too. Due to this, the ongoing data quality check is an exceptionally iterative process.

The first neural network based on data acquired from the five aircraft with the EMM-SHM system is planned to be created until the end of the year 2021.

2.2.7 The FINAF Grob Mini-OLM

Related to the domestic support of the Grob G 115E fleet an aerodynamic model of the plane has been created (Chapter 2.1.4 of Ref. [34]). As a step towards a more profound understanding of the aircraft type, one plane has been instrumented as a collaboration of the FINAF, Patria Aviation and VTT, to get detailed strain, load and flight mechanical data [52], [47].

The onboard instrumentation consists of 40 strain sensors installed at structurally significant locations. Following the strain sensor installation, electrical calibrations, ground (mechanical) calibrations, and EMI/EMC tests were performed, prior to test flights.

Two separate onboard Data Acquisition Units are used. The main system records data from the above-mentioned strain sensors. Most of them have been mechanically calibrated to indicate loads (for instance control surface hinge moment or wing bending and shear (**Figure 43**), and some of them measure local strains. In addition, airspeed, altitude and normal acceleration are collected. The additional system is a standalone gyro platform, which records for instance attitude, angular velocities and accelerations, in addition of airspeed and altitude.

The flight test program started in September 2020 and will be completed in spring 2021. During the program, all the normal and acrobatic maneuvers of the plane will be flown covering the whole flight envelope and varying the mass and center of gravity. During the test program approx. 20 flights and 20 hours will be flown.

Even though the test program is not yet completed and reported, utilization of the results has already started. This applies mainly to control surface hinge moments, as some control system problems have been encountered.

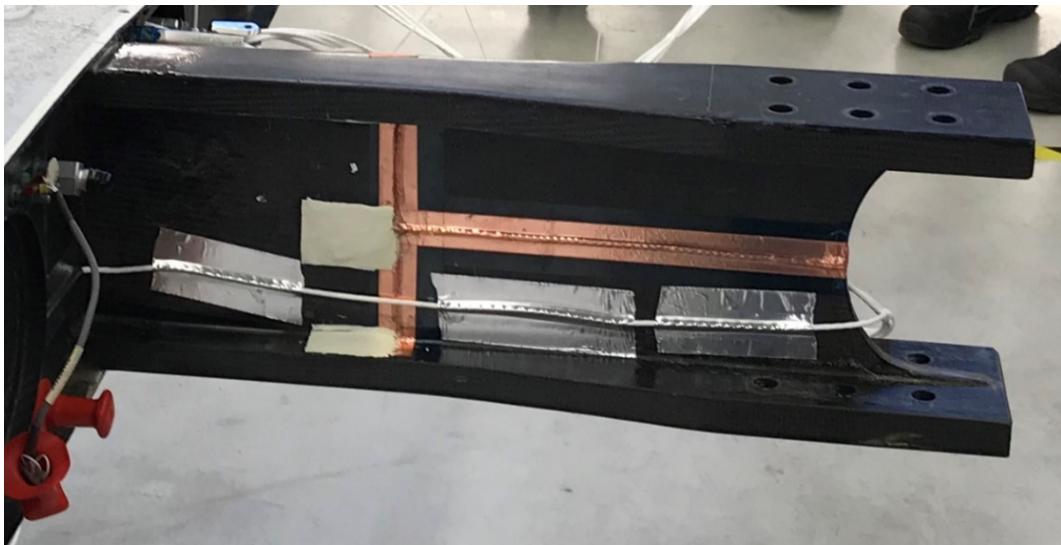


Figure 43: Main spar instrumentation in the wing root area. Figure courtesy of Patria Aviation.

2.2.8 Fatigue and damage tolerance test of Gripen Rudder

This chapter highlights the international cooperation research activities in between Saab Aeronautics (Sweden) and VTT (Finland). The authors of the chapter are Jan-Erik Lindbäck, Zlatan Kapidzic (Saab AB) and Risto Laakso (VTT).

The Rudder fatigue and damage tolerance (DT) test will be performed in 2021 in Finland in collaboration with VTT Technical Research Centre of Finland Ltd and its partners Eurofins Expert Services Ltd and Arecap Ltd. **Figure 44** shows the test set-up, which is the result from a close cooperation between the parties. Actuators will apply the air-loads to the pads on the Rudder via a simple whiffle tree. The rig contains the actuators as a floating and free-standing unit, i.e. the actuators are integrated in the rig itself. All support reactions, actuator loads, and actuator displacements will be measured. There will also be a number of strain gauges and displacement transducers attached to the Rudder. At the time of writing the review, manufacturing of the rig parts is almost finished, and the data acquisition system is assembled. The Rudder is expected to be in the rig in late June, the test readiness review is expected in August, and the project is awaited to finish in April 2022 at VTT [45].

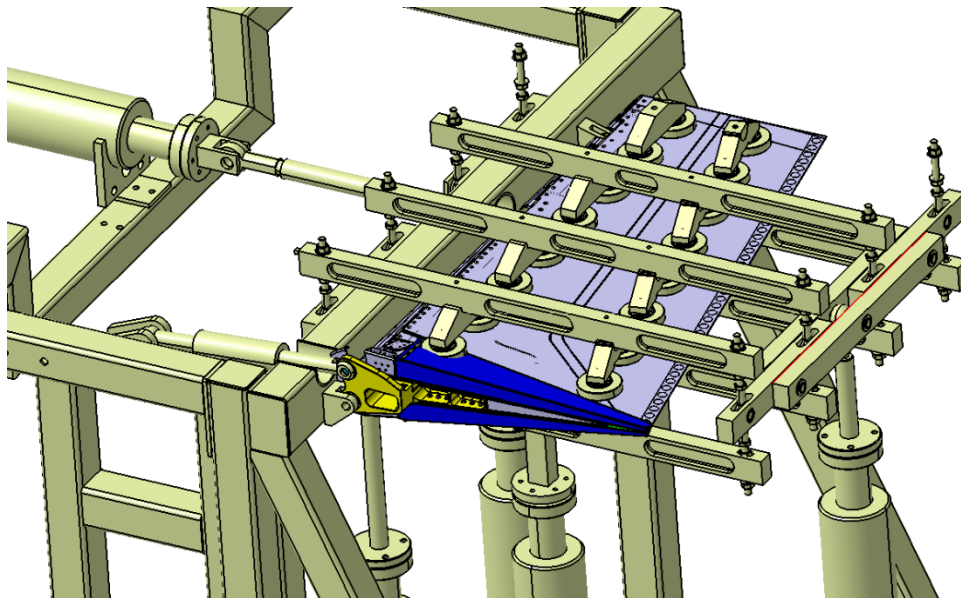


Figure 44: Rudder fatigue and DT test object and test rig. Figure courtesy of Saab Aeronautics.

Spectrum loading representing two design lifetimes will be applied initially as the fatigue test part. Then, artificial defects will be introduced at locations with the lowest strength margins based on the DT analysis, and another two design lifetimes of loading will be applied. This will be followed by a residual strength test (RST) to 120 % LL (Limit Load). There is an option to increase both spectrum loads and residual strength loads another 20 % after the initial test campaign and to run another design lifetime, provided that no findings are observed after the initial DT test. Periodic non-destructive eddy current, ultrasonic, and visual inspections will take place at critical locations throughout the test campaign. Strain gauge results will be recorded also for the sequence loading. The big data gauge results will be used to check for local stiffness variations in the structure that can indicate a crack initiation and/or growth.

2.3 Structural integrity of metallic materials

2.3.1 Risk Level Assessment for Structural Integrity Management

The need for estimation of risk level in aircraft structural integrity management is evident when plans and decisions for different inspection actions and/or modifications for flight safety critical structures are made. As the amount of structural inspections and need for modifications increase with aging aircraft fleet the effect of all actions to the total cumulative risk and failure rate must be evaluated. A simplified tool for understanding the risk levels and to provide support for decision making in the structural integrity management activities was developed at Patria Aviation. [23], [24]

The risk level of a structural detail depends on:

- Material properties - deviation in material fatigue properties and initial flaw sizes
- Uncertainty in known damage history - accuracy in analysis of the structural detail, deviation in local fatigue load spectrum and accuracy in fatigue monitoring system of the aircraft
- Mitigation actions - overall life of the component, structural inspection program and structural modifications.

Based on experience and known indications from the fleet together knowledge obtained from international collaboration, different parameters and factors affecting the fatigue life can be estimated realistically. By combining the POD-curves of the selected inspection method and the effect of possible structural modifications the inspection interval can be optimized to obtain required level of total cumulative risk over the life of the component as well as failure rate (risk/flight hour). The analysis process and an example of the results are illustrated in **Figure 45**. The work for improving the analysis method will be continued.

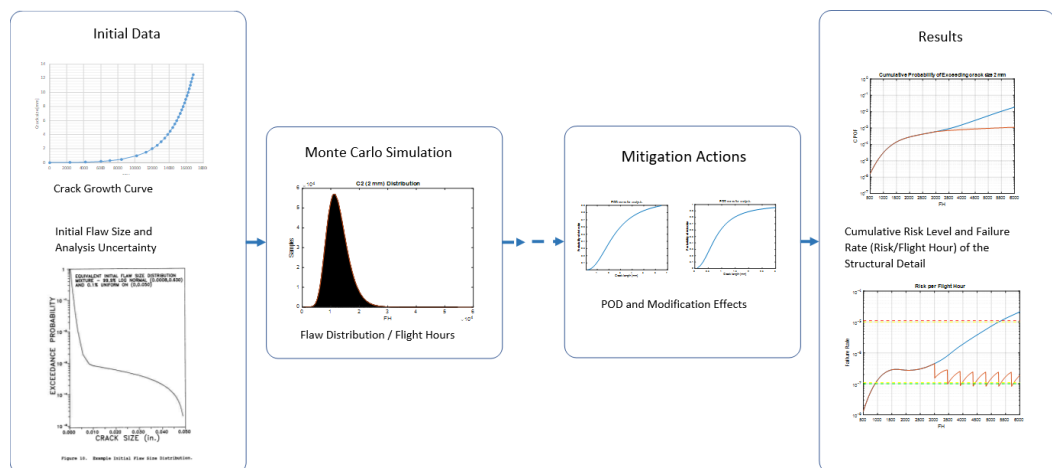


Figure 45: Analysis process to determine the risk level for a structural detail. Figure courtesy of Patria Aviation.

2.3.2 Update of study of small cracks growth

The growth of small cracks have been studied experimentally by fatigue tests, and was introduced in Chapter 2.3.2 of Ref [34]. The objective of the study was to find out the effect of selected parameters (load spectrum, surface working methods, fastener hole tolerances and preparation methods) on small crack growth. Test matrix included two kinds of test specimens: Al 7050-T7451 dogbone type specimens with shoulders in test section, and Al 7075-T76 double lap shear joint specimens.

The applied life improvement methods were shot peening, polishing and reaming of the fastener holes. The effect of the three different fastener hole fittings together with the oversize hole modification were also tested.

The implementation of the life improvement modifications took place after pre-cycling at 40 % or 60 % of the average lifetime of the specimen and spectrum in question. After the modifications, all the specimens were cycled until fracture.

The quantitative fractography (QF) was carried out to some of the specimens in order to determine the small crack growth rates. The fracture surfaces were investigated in more detail with a scanning electron microscope (SEM). The applied load spectra included so called markers whose function was to improve the tracking of the crack growth. The crack growth was determined along one track per one fracture surface.

Excerpted from the accomplished study [65], relative total lifetimes of the different life improvement modifications are shown in **Table 1** and **Table 2** for the dogbone and the double lap shear joint specimens, respectively.

Table 1 reveals that the shot peening of the dogbone specimens clearly extended the lifetime. According to **Table 2**, the interference fit resulted the best lifetime extension. However, the oversize hole modification with the interference fit did not seem to improve the lifetime of the pre-cycled specimens. The best lifetime extension was achieved by the Class 2 fit for the pre-cycled specimens.

Table 1: *The effect of polishing and shot peening on the normalized fatigue life for the dogbone specimens. [65]*

Test/Method	Polished	Shot peened
Basic ¹⁾		1.0
Pre-cycling at 40 %	– ²⁾	2.5
Pre-cycling at 60 %	1.3	3.1

¹⁾ The specimens without any modifications.

²⁾ The specimens did not fracture from target location.

Table 2: *The effect of the different fittings and oversize hole modifications on the normalized fatigue life for the double-lap shear joint specimens. [65]*

Test	Class 2 fit	Interference fit	Cold worked + Class 2 fit
Basic ¹⁾	1.0	3.0	1.7
Pre-cycling at 40 %	1.7	2.9	2.0
Pre-cycling at 60 %	2.4	3.2	2.8

¹⁾ The specimens without any modifications.

2.3.3 NDE reliability evaluation with POD round-robin

Reliable non-destructive evaluation (NDE) is important in maintaining safe and effective operation of aircraft. The reliability of NDE is usually studied in terms of probability of detection (POD) - a statistical metric designed to find the smallest cracks that can still be reliably found or the largest crack that could still be left in the structure after a given inspection.

Previous POD activities in Finland were highlighted in the ICAF2019 National Review (Chapter 2.3.3 of Ref. [34]). Since then, the work has been continued. To evaluate and to improve the reliability of NDE, a round-robin study of POD was completed among the Finnish operators. The round-robin included altogether 10 participants from both the military and civil companies, including Patria, GA Telesis and VTT. The round-robin focused on fluorescent penetrant inspection (FPI), and the POD analysis was executed according to the ASTM E2862-18 standard [15]. The round-robin was organized and facilitated by Trueflaw Ltd. A POD curve generated from the round-robin is illustrated in Figure 46. [79]

The round-robin offered a rare opportunity for the participating organizations and inspectors to benchmark their performance within the group. The overall POD performance was very good and the process allowed organizations to identify several points of further improvements. It is expected, that the practice will be extended to other inspection methods in the future.

Other examples of POD studies within the research period supported by the FINAF can be found from Refs. [78] and [80].

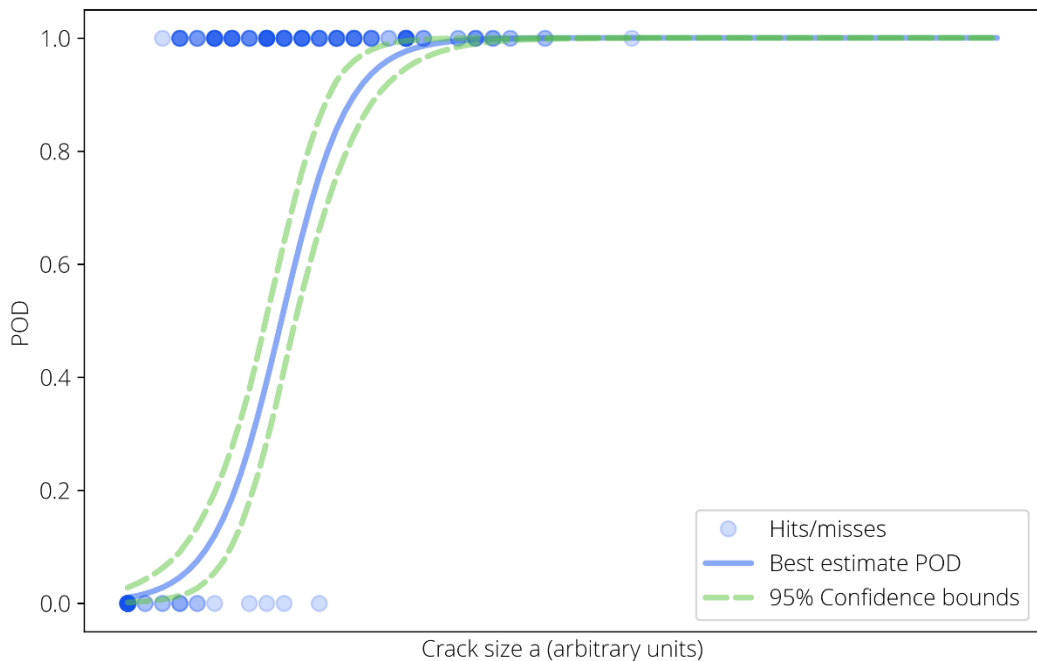


Figure 46: Example results from round robin. Figure courtesy of Trueflaw Ltd.

2.3.4 Fatigue testing of bolted joints with solid shims and blind fasteners

This chapter highlights the international cooperation research activities in between Saab Aeronautics (Sweden) and VTT (Finland). The authors of the chapter are Zlatan Kapidzic (Saab AB) and Keijo Koski (VTT).

2.3.4.1 Introduction

A fatigue sizing method for bolted joints in AA7050-T7451 and AA2050-T84 was earlier developed at Saab based on testing of joint specimens performed at VTT [44], see also chapter 2.3.7 of Ref [34]. The method is based on results from constant amplitude (CA) testing of six different specimen geometries at different load ratios and with different amounts of secondary bending. The test data was fitted to an equation representing the Haigh diagram on which the cumulative damage calculation is based. Some spectrum tests were performed for purposes of validation and further comparisons to the results from the literature were done with satisfactory results. Since the publication of the results in [34], the method was expanded to include joints with low clamping force. Such applications may include joints with small fasteners, relatively large clamping lengths, blind fasteners, rivets or liquid shims although there is not much test data available for systematic categorization of joint fatigue life based on the clamping force.

The current study was focused on evaluating the fatigue life of joints with solid shims and Ti-screws, and joints with three types of blind fasteners: B-bolt, Visu-lok and ZJQ.

2.3.4.2 Test specimens

Totally 36 single shear butt joint specimens were tested. The plate material in all specimens was AA7050-T7451 and all specimen types had two columns of countersunk fasteners but different fastener types. Six specimens of each of the following specimen types were tested in spectrum loading:

- Type D, three row specimen with 6 mm Ti-screws
- Type D-S, three row specimen with 6 mm Ti-screws and a shim plate
- Type C, two row specimen with 5 mm Ti-screws
- Type C-B, two row specimen with ~5 mm B-bolts MS21140
- Type C-V, two row specimen with ~5 mm Visu-lok fasteners NAS1672
- Type C-Z, two row specimen with ~4.1 mm ZJQ fasteners, CR7774S Cherry Maxibolt.

Specimen type D was the reference for D-S and specimen type C was the reference for C-B, C-V and C-Z. Refer to **Figure 47** where the drawing of D-S specimen type plates are shown. The drawings of the other specimen types are not shown in this report but apart from the absence of the shim plate and different number of fastener rows, they had a similar configuration as the D-S type.

The bolt holes in specimens with Ti-screws, D, D-S and C, were made with H10 tolerance according to the "Near Full Size" (NFS) procedure. No deburring or surface treatment was applied. Pretension torque was applied on the Ti-screws according to standard aerospace recommendations (6.3 Nm for M6 and 4.1 Nm for M5).

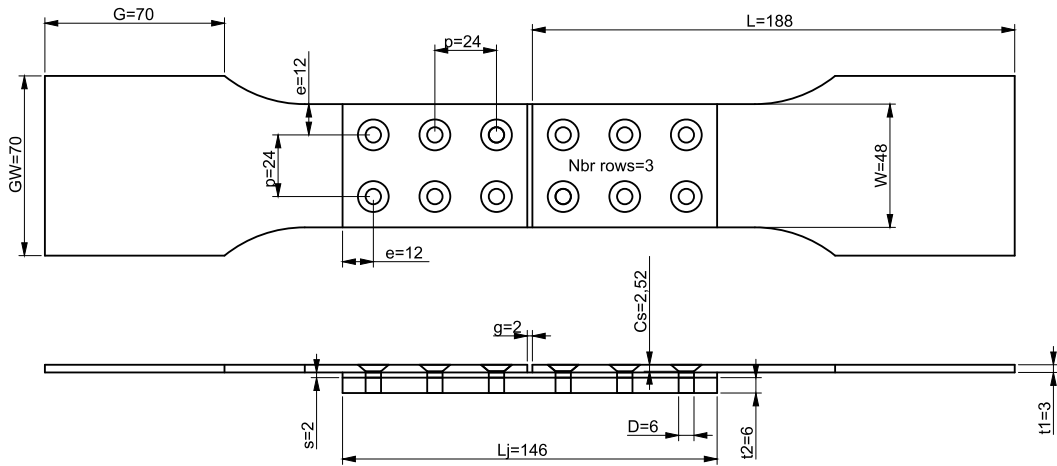


Figure 47: Drawing of specimen type D-S. Figure courtesy of Saab Aeronautics.

2.3.4.3 Test setup

The testing was performed at room temperature at a maximum load frequency of 10 Hz. The same tension dominated load spectrum L28E2 as in [34] was used on all specimens. It consisted of ~60 cycles/flight hour. All specimen types were tested at two maximum spectrum gross stress levels, referred to as low level and high level.

The same uniaxial testing machine as in [34] was used in this test programme. The secondary bending was reduced by use of a lateral support device specifically designed for the specimens, see **Figure 48**.

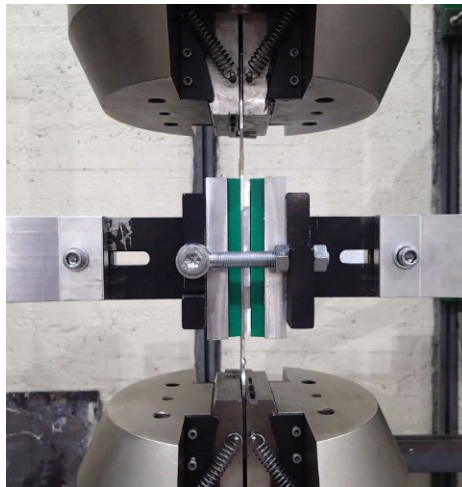


Figure 48: Test machine with lateral support. Figure courtesy of VTT.

2.3.4.4 Test results

The first three specimens that were tested, D:1, D:3 and D:4, had surprisingly low lives (~5000 flight hours). Upon inspection, it was noted that none of the specimens of specimen types D, D-S and C had any washers installed under the nuts. In further examination of the specimens, it was observed that the nuts were torqued to the end of the bolt thread without properly clamping the joint. The specimens were then properly reassembled with washers and the testing was continued. A significant increase of fatigue life (~5 times longer) was achieved on the reassembled D specimens and the remaining specimens were tested without any interruptions. This unintentional mistake has confirmed the importance of the clamping for the fatigue life of a joint.

All specimens failed due to fatigue in macroscopic mode I or I*, see **Figure 49** for definition of the failure modes, except specimen D-S:6, which failed in mode II.

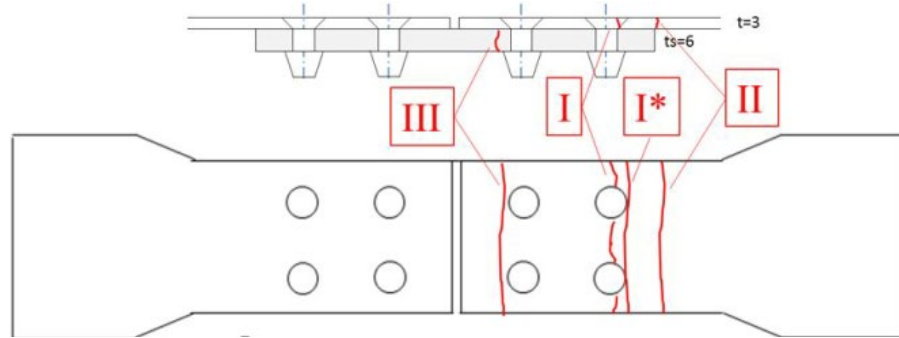


Figure 49: Failure modes. Figure courtesy of Saab Aeronautics.

2.3.4.5 Comparison of predictions and test results

Predictions of fatigue life of the test specimens were performed using the method in [34]. Cumulative damage was assumed equal to 1 at failure, and Haigh diagrams for both normal clamping (NC) and low clamping (LC) were used in the calculations. **Figure 50** shows the comparison for D and D-S specimens and **Figure 51** for C, C-B, C-V and C-Z specimens.

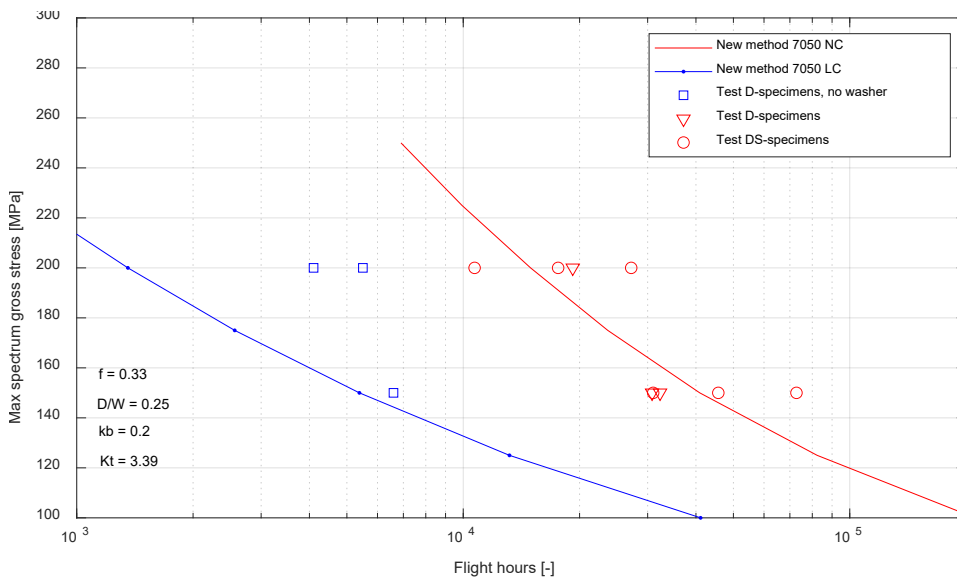


Figure 50: Test and prediction results for D and D-S specimens. NC = Normal Clamping, LC = Low Clamping. Figure courtesy of Saab Aeronautics.

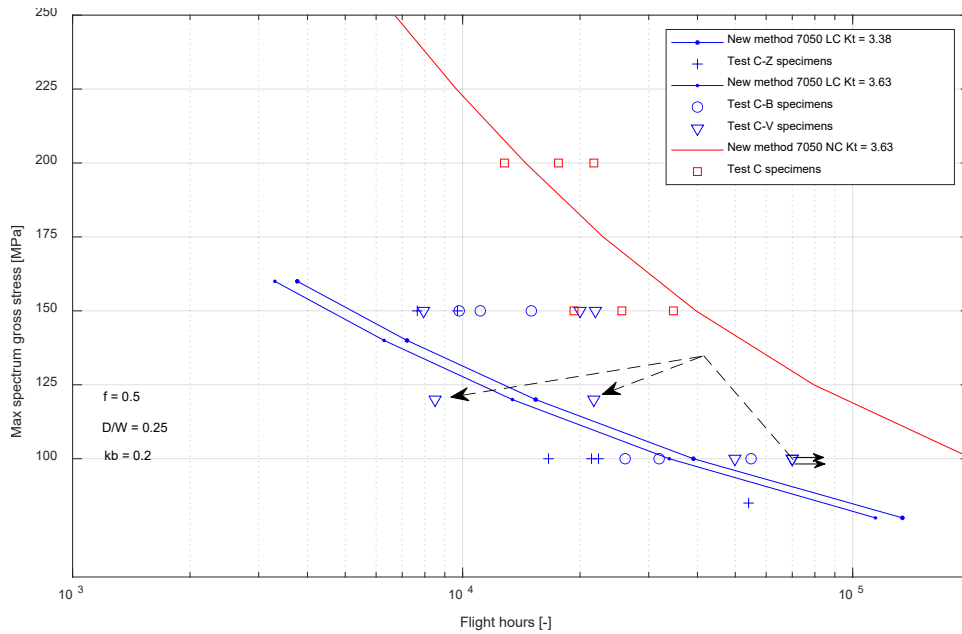


Figure 51: Test and prediction results for C, C-B, C-V and C-Z specimens. NC = Normal Clamping, LC = Low Clamping. Small arrows denote run-outs and dashed arrows denote re-runs. Figure courtesy of Saab Aeronautics.

Comments regarding specimens C, C-B, C-V and C-Z, **Figure 51:**

- The reference specimens C have significantly longer average fatigue lives than C-B, C-V and C-Z specimens although there is a slight overlap of the data at 150 MPa stress level. Specimen type C failed mostly in mode I* while the blind fastener specimens failed only in mode I, see **Figure 52** and **Figure 53**, which indicates the presence of higher clamping load in specimen type C.
- The NC prediction curve is close to the C-specimen data with an over-prediction of a maximum factor of 2, which is in the range of scatter, cf. [34].
- The LC prediction curves goes thru the C-B, C-V and C-Z data at 100 MPa but under predicts it somewhat at 150 MPa. The reason for the latter might be that the blind fastener specimens do have some clamping.

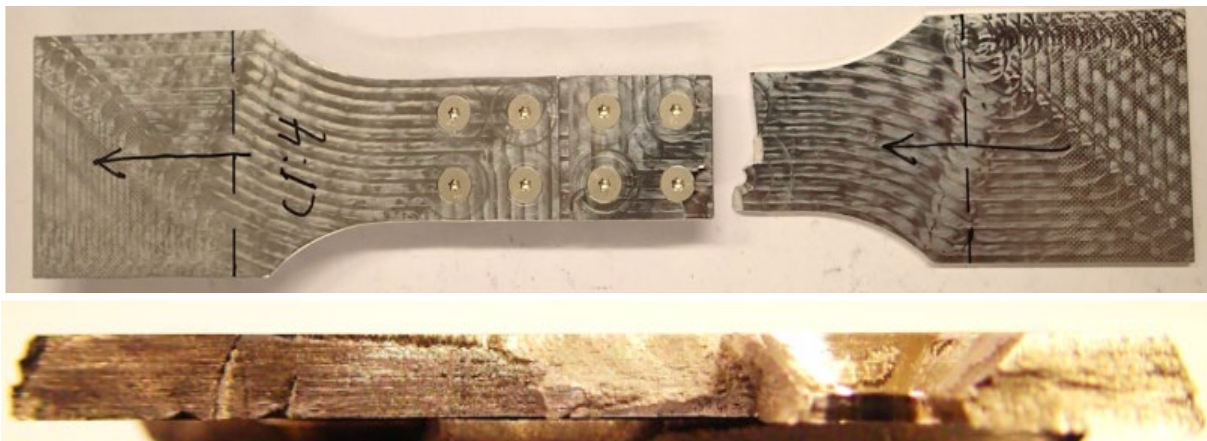


Figure 52: Failure mode I* in C specimen. Figure courtesy of Saab Aeronautics.



Figure 53: Failure mode I in C-B specimen. Figure courtesy of Saab Aeronautics.

2.4 Structural integrity of composite materials

2.4.1 Structural integrity of composite structures and adhesively bonded joints

In the field of structural integrity of composite structures, Tampere University (TAU) focuses on both numerical and experimental analysis of composite structures and adhesively bonded joints. The work has mainly focused on adhesive bonding, and especially on bonded repairs, in the season 2019-2021. The research and development work has included the use of experimental and numerical methods of stress, fracture, and fatigue analysis.

The interest in the stress analysis has been related to shear properties in general. Presumably, the most common test method for determining the mechanical properties of adhesives in shear is the thick adherend lap shear (TALS) method [14]. In TALS, the loading and specimen geometry are relatively simple but a specific extensometer (KGR) to measure the shear strain at the bond line is needed. The specific extensometer measures deflections of three points on the both substrates of specimen, and the data are post-processed for defining the shear strain of the adhesive. Tampere University has used the digital image correlation (DIC) method in various kinds of measurements [36]. DIC is based on the image data of the specimen surface during a test. These images are post-processed with specific correlation algorithms, which provides the deformation field in the imaged region. The full displacement field allows, for example, the evaluation of the strain field in the measurement region (**Figure 54**). This additional information can be applied to compare with finite element analysis (FEA) and the TALS test. The usage of DIC within the TALS testing was trialled when determining the properties of epoxy adhesive FM 300-2 in shear. The DIC method was shown to be feasible for specifying displacements, which can be post-processed to provide comparable shear properties to the properties based on the KGR extensometer.

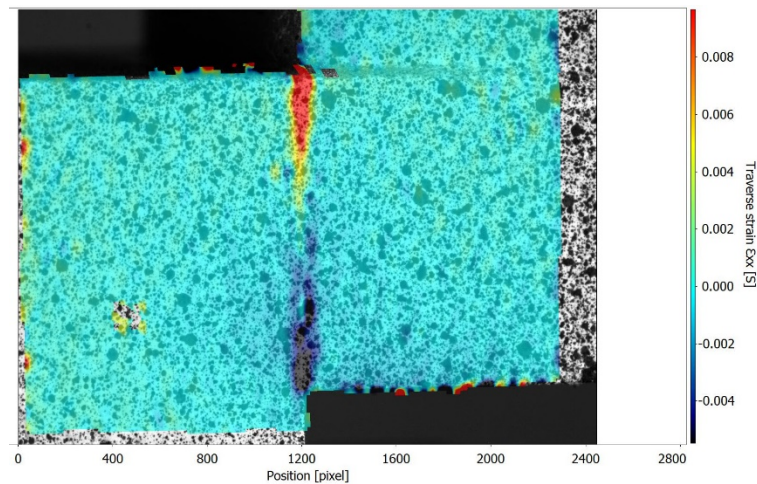


Figure 54: The thick adherend lap shear specimen's transverse (horizontal) strain in the measurement region. Figure courtesy of Tampere University.

The previous fracture testing by Tampere University and Aalto University has determined mode I and II fracture toughness values, G_{IC} and G_{IIC} respectively, for the epoxy adhesive film FM 300-2. The testing was performed for one and two film layers of FM 300-2 forming the bond line [37]. Mode I and II fracture toughness values are applicable when pure mode loading exists at the crack tip. In the mixed-mode case, the so-called fracture criterion is needed for the analysis of fracture. For developing the criterion, also mixed-mode loading cases (tests) are needed. A new concept for the mixed-mode loading test was developed at Tampere University [39]. The developed concept is based on flexural testing, which provides two different mixed-mode (mode ratios) with the single specimen

design. This simplifies adhesive testing when the complex testing jig and awkward loadings are not needed to introduce for the tests. Also, the specimen design and manufacturing should remain straightforward to minimize errors. The new concept is based on the single leg bending specimen, as shown in **Figure 55**. The achieved experimental results and the solved criterion are shown in **Figure 56**.

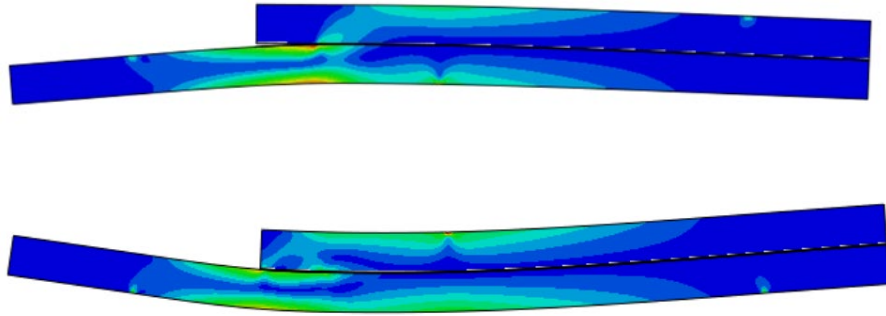


Figure 55: The single-leg bending specimen’s deformation, characterized via simulation when two different mixed-mode ratios are produced by changing the side of the specimen. Figure courtesy of Tampere University.

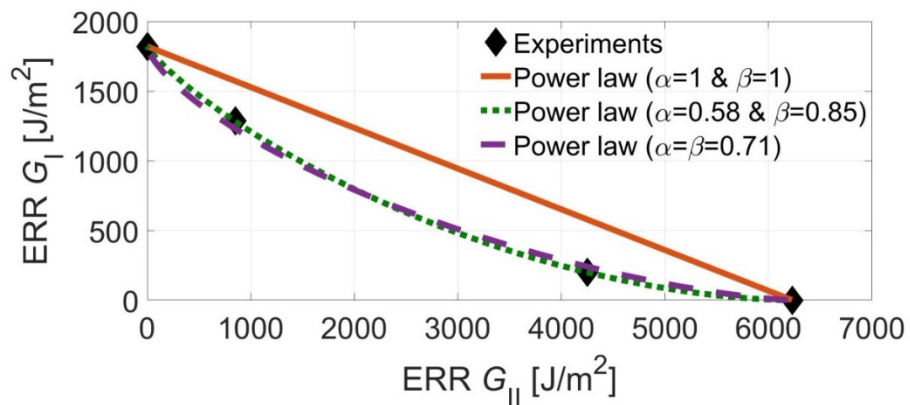


Figure 56: The resolved mixed-mode fracture criterion for the epoxy adhesive FM 300-2. [39]

The work of the season related to the adhesive’s mode II fatigue (crack) growth, as already discussed in the previous ICAF national review (Chapter 2.4.1 of Ref. [34]), was continued further. The crack length observation in general during the experimental testing of mode II bond line fracture is challenging. The difficulty in the visual observation is the consequence of the cracked surfaces sliding against to each other. For that reason, the compliance based methodologies are common in static and fatigue testing of mode II fracture. In the experimental work performed now, the usage of DIC for the crack length monitoring was studied (**Figure 57**). DIC does not require continuous user presence when - noting that one fatigue test takes hours at a minimum. The data post processing related to DIC can also be automated and that minimizes the user-dependency of the results. The development work’s results are to be published in an international article to spread the knowledge and lessons learned. The research work has included negative load ratios ($R<0$) for fatigue testing and the testing setup has required significant amounts of development.

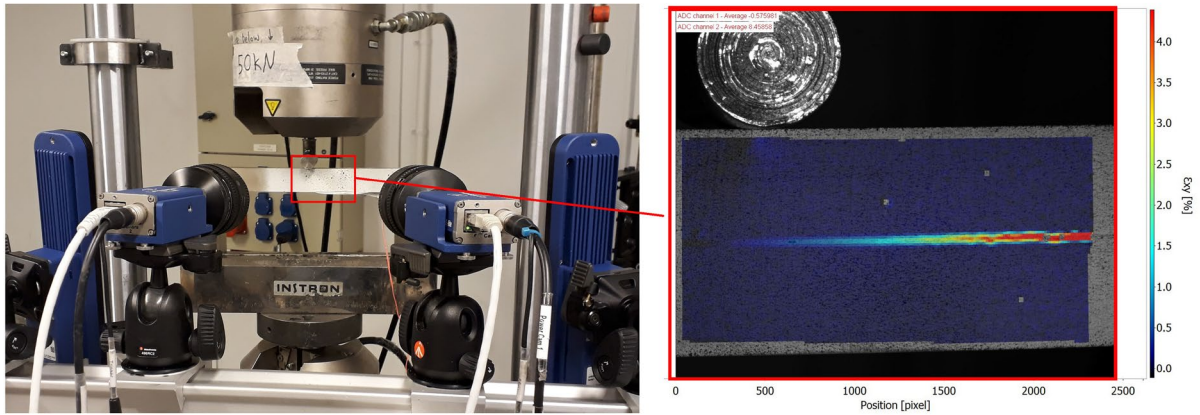


Figure 57: The crack length measurement based on DIC. Figure courtesy of Tampere University.

During this season, the numerical analysis, fracture mechanics and continuum damage modelling, have also been improved actively in the research and development projects. The numerical analyses have been used for supporting and analysing experimental work and data, but also for separate analysis studies have been made. The F/A-18's trailing edge flap and related multi-delamination analysis [40] have been performed (Figure 58) to understand interaction between delamination growth in realistic aircraft structures. The numerical analysis was additionally applied for studying bonded repair patches and their (geometry) adjustments [38]. The target was to analyse if the repair's damage and its visual observation can be achieved before the fast (unstable) ultimate failure occurs. This could be beneficial for the certification of bonded repairs on primary structures. An example of the studied adjustment of a patch shape is shown in Figure 59.

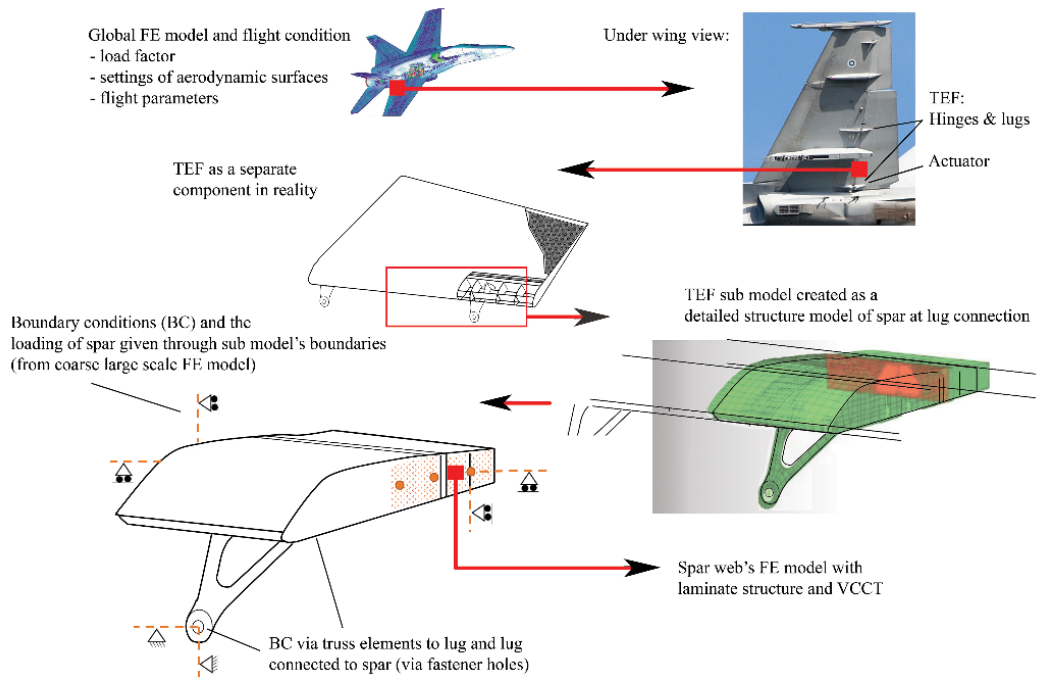


Figure 58: The F/A-18 trailing edge flap's sub-model analysis as an approach for multi-site delaminations study. [40]

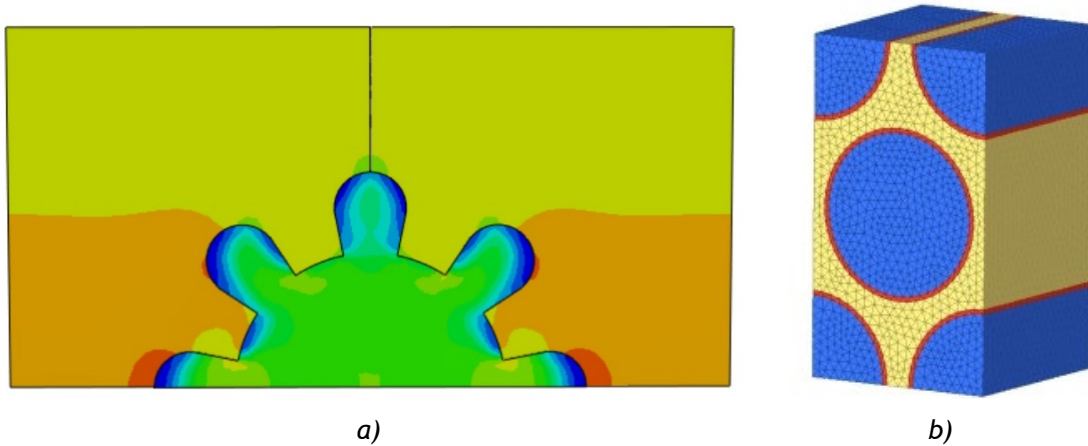


Figure 59: The adjusted bonded repair patch stress distribution under tensile loading (a), RVE-based simulation of AS4/3501-6 composites (b). Figure courtesy of Tampere University.

Other numerical analysis performed in the research group has covered the topics of composite laminate's aging [61], fibre/matrix interfacial fracture [20], and crack nucleation and propagation of bonded joints [35]. Also, the numerical analysis work covered the initial academic research of representative volume element (RVE) based finite element models. The commercial Altair's Multiscale Designer package for finite element methods was studied to evaluate the usability of the RVE based laminate modelling of AS4/3501-6 composites under impact loads and in terms of computational efficiency and operator efforts [18].

The theme of the bonded repair's certification and related damage tolerance is currently under work in the project by European Defence Agency (EDA) - called Patchbond II (Certification of adhesive bonded repairs for Primary Aerospace composite structures). The project Patchbond II focuses on the damage tolerance of bonded repairs, which are studied both experimentally and numerically to have a thorough understanding of the challenges and solutions. This four-year project is a multinational collaboration consisting of six countries and 15 different partners; Tampere University is the leader of the work package of numerical analysis, and coordinating the project nationally. The other Finnish partners involved are Patria Aviation and VTT.

2.5 Repair technologies

2.5.1 Composite repair of the Wing Root Step Lap Joint

The inner wing root of the F/A-18 fighter aircraft is a double-sided titanium-composite stepped lap bonded joint. A repair concept for a case where two innermost steps are damaged was developed and analysed (Chapter 2.5.1 of Ref. [34]). The basic principle of the repair concept is to remove the damaged steps and bond a customized CRFP patch with a film adhesive as schematically illustrated in **Figure 60**. The validation of the repair concept follows a building block approach. [82]

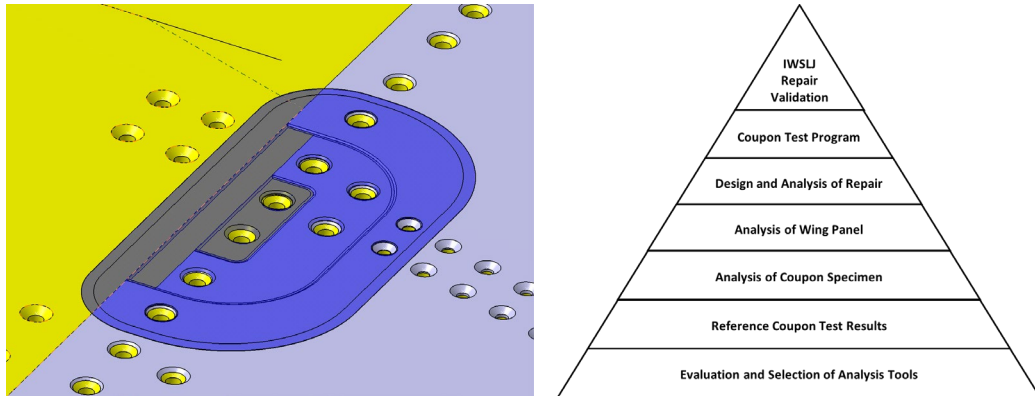


Figure 60: The IWSLJ repair concept and building block approach for the repair validation. Figure courtesy of Patria Aviation.

The design and analysis of the repair was performed using the tools and modelling approach selected during the work. The analysis model with the repair patch and an example of the analysis results are shown in **Figure 61**.

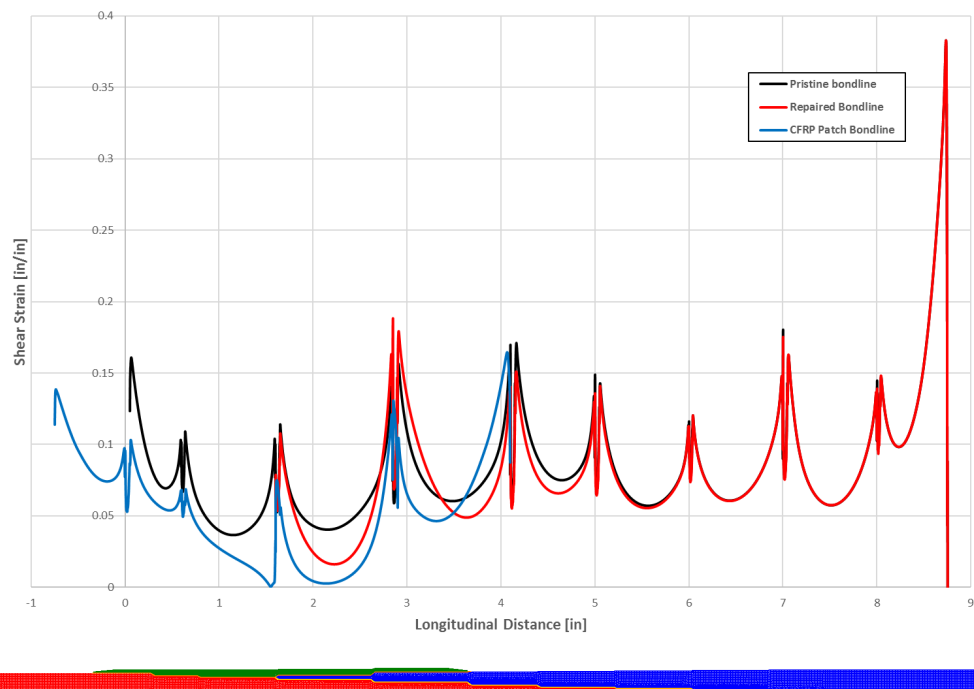


Figure 61: IWSLJ analysis model with repair patch and example of the results. Figure courtesy of Patria Aviation.

The repair concept validation program is continued by accomplishing four separate repairs on an actual wing that is removed from service. The repairs are performed on outer mold line (OML) of the lower skin. The custom designed CFRP patch was made of same prepreg material as used in the original wing skin (AS4/3501-6). This patch was then secondary bonded to the wing panel using FM300-2 film adhesive. The heat to the repair was applied using regular heat blankets. The main challenge in the repair is to provide sufficient heat to the repair area because of several heat sinks in the wing. Several additional heat blankets were used to provide additional heating to ribs and spars. The upper skin was removed to have the access also to the inner mold line (IML) of the lower skin. Insulation was used throughout the repair area in the IML to reduce the heat loss. Four patches were bonded in three different repair cycles. The completed repairs on the wing are shown in **Figure 62**.

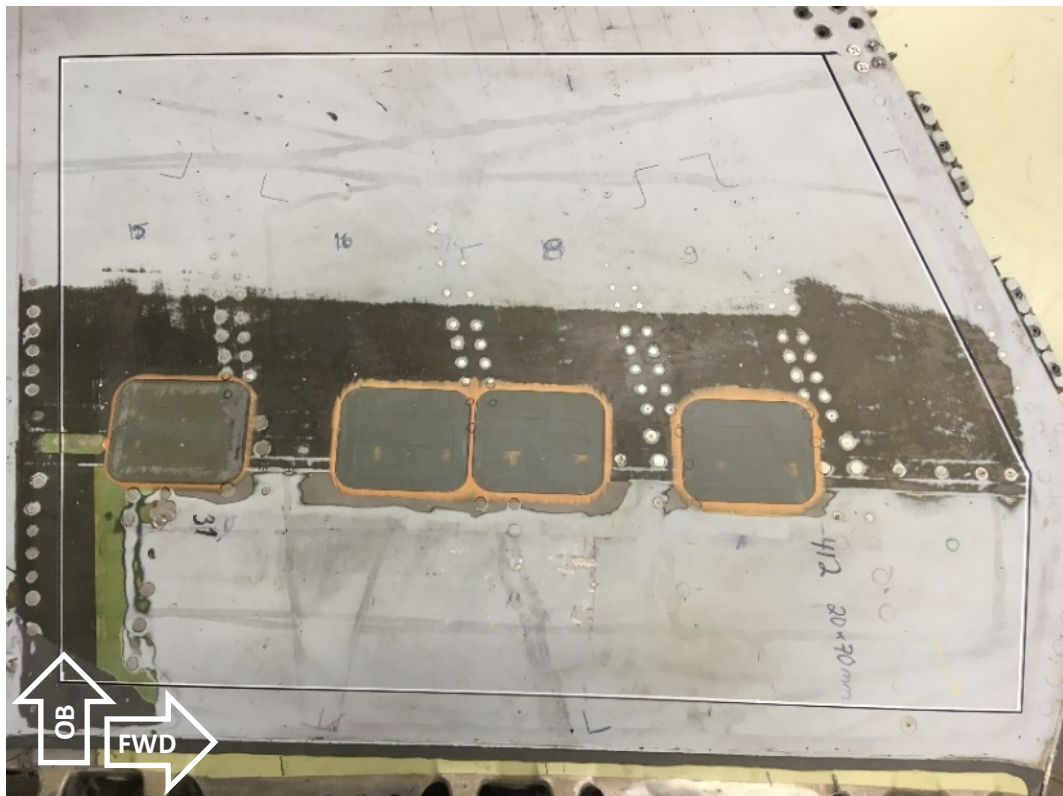


Figure 62: The F/A-18 lower inner wing skin panel with four repairs. Figure courtesy of Patria Aviation.

To proceed with the coupon test program, the panel from the wing was then cut using water jet cutter. Once having full access to the IML of the panel, the positions of the test specimens were finalized. The specimens were again water jet cut from the panel. The geometry of the specimens was the same as used in original OEM qualification testing of the joint. Altogether seven specimens were obtained from the wing panel. One additional test specimen was obtained from CREDP (The F/A-18 Composite Repair Engineering Development Program) collaboration and will be used as one of the reference specimens although it does not have exactly same configuration as the other specimens. The purpose is to perform both static and fatigue tests. Three different configurations are used in static tests: reference specimens, repaired specimens and fail-safe specimens. The fail-safe specimen is similar to the repaired specimen but without the patch. In fatigue tests only repaired specimens are used. The finalized test specimens are shown in **Figure 63**. The static tests are scheduled for spring 2021 and fatigue tests to be finished during autumn 2021.



Figure 63: Finalized test specimens. Figure courtesy of Patria Aviation.

2.5.2 VCCT analysis of the Step Lap Joint

To enhance the knowledge about the criticality of various possible damages within bonded step lap joint, several cases were analyzed using VCCT (Virtual Crack Closure Technique) implemented in FEM. The analysis tool was MSC/Marc. The analysis is based on 2D models with plane strain elements. Similar analysis approach and test results are published in References [35], [39], [41]. Two major types of disbonds were studied: disbond at joint end with free edge and embedded crack at the radius of the steps. The analysis cases are illustrated in **Figure 64**.

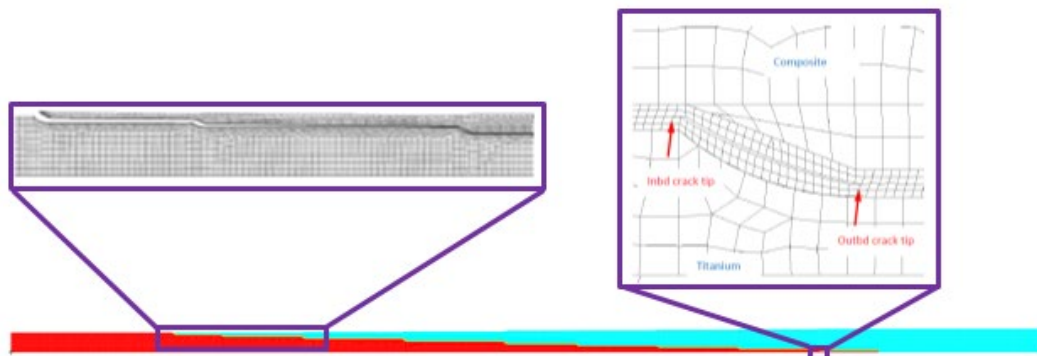


Figure 64: Analysis model and examples of damages. Figure courtesy of Patria Aviation.

To account for mixed modes at crack tip, the criticality of the loading is evaluated using a power law. The exponent used in the power law equation were defined in Ref. [39]. In

principle, the analysis is based on static tension or compression. Several knock down factors were used to take into account other parameters affecting the criticality: statistical factor for reference test results, fatigue retention factor, elevated temperature factor and additional factor for multiaxial loadings. Currently only one crack front can be used in a single analysis. Therefore, each crack case was analyzed separately.

The strain energy release rate for joint end disbond is shown in **Figure 65** (left). The graph presents G_I and G_{II} component together with G_{tot} which is a summation of the two components. With the dotted lines are shown estimated failure load (red) obtained with the power law and ultimate load level for the joint (black). The results reveal that the load required for the crack to grow is clearly higher than the ultimate load level for the joint.

The results for embedded crack at the radius are shown in **Figure 65** (right). The results are obtained for the outboard crack tip in tension loading. In addition to the estimated static failure load, several other load levels are indicated. The load levels to propagate the crack are higher than ultimate load level for the join as well as tested specimen strength and yielding or rupture of the titanium part of the joint. According to these analysis results it is not likely to observe damage propagation with in-service loads. It was also seen in the analysis that when extending the size of the embedded crack the load level to propagate the crack becomes higher.

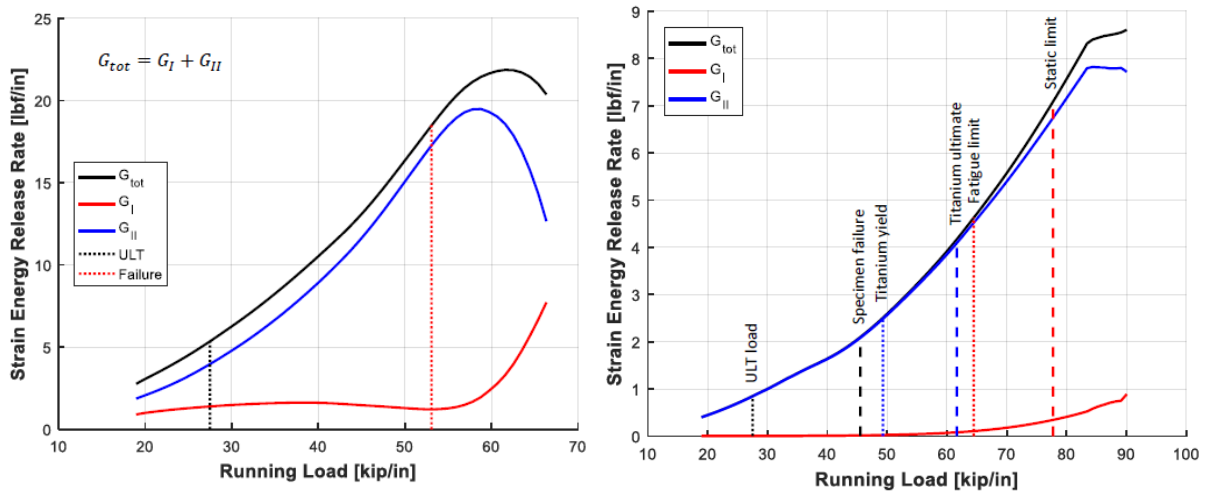


Figure 65: Analysis results for end disbond (left), and embedded crack at step radius (right). Figure courtesy of Patria Aviation.

3 Related activities

3.1 EDA Patchbond I project

The four-year “Bolt free battle and operational damage repairs of metal and composite primary aircraft structures (PATCHBOND I)” project under the framework of the European Defence Agency (EDA) R&T Category B projects was highlighted in Chapter 3.2 of Ref [34], and completed in 2019.

The project concentrated on the permanent bonded-only composite patch repair of damaged composite primary structures on a rotary wing platform, having the horizontal stabilizer of the NH90 helicopter as a demonstrator. The primary goal was to specify a certification approach that could fulfil the airworthiness requirements for a bonded composite patch repair in a highly loaded primary structure. The secondary goal was to investigate and define materials and repair processes capable of repairing the composite structure and to comply with the required operational capability.

The work was performed by an international consortium consisting of 14 industrial and scientific partners from five European countries enabled to participate in EDA’s projects (alphabetically: Finland: Aalto University (until 2017), Patria Aviation, VTT Technical Research Centre of Finland Ltd.; Germany: Airbus Defence and Space, Bundeswehr Research Institute for Materials, Fuels and Lubricants (WIWeB); the Netherlands: NLR, Fokker Services B.V., KVE Composites Repair; Norway: Norwegian Defence Research Establishment (FFI), Norwegian Defence Logistics Organization (NDLO), DolphiTech, FiReCo, Light Structures; and Spain: Spanish Institute for Aerospace Research (INTA). Project Lead Contractor was NLR (the Netherlands), and Patria Aviation was the Finnish coordinator of the project. The Finnish Defence Forces Logistics Command (FDFLOGCOM) was the national bill paying authority of the project.

The activities of the Finnish partners supported the certified repair process involving in analytical and numerical analysis, repair design procedures, materials and processes, NDI, and structural health monitoring based on Acousto Ultrasonics (AU).

Despite of industrially accepted repairs realized for the test specimens of various scales, the project as such was not able to meet all the objectives. The stable damage growth was not achieved in the experimental tests performed, thus the applicability of the SHM-technology as part of certification was not fully demonstrated. Another major drawback of was that a complete loss of the adhesive bonded patch could not be prevented.

3.2 EDA Patchbond II project

The four-year “Certification of adhesive bonded repairs for Primary Aerospace composite structures” (PATCHBOND II) project began in 06/2020 under the framework of the European Defence Agency (EDA) R&T Category B projects. The PATCHBOND II project is a follow-on project to PATCHBOND I. It focuses on establishing certifiable procedure for bolt free adhesively bonded composite repairs to ensure the damage tolerant design philosophy in aerospace primary structures - having the NH90 helicopter still as a demonstrator platform.

It can be considered that the level of ambition in the Patchbond I was originally set too high, and the fundamental understanding of the complicated failure mechanisms was not thoroughly studied. However, the results of the PATCHBOND I project can be used as first steps towards certification of adhesively bonded repairs of primary composite structures aimed at overcoming the Bonding Repair Size Limit (BRSL). In the follow-up project, PATCHBOND II, the work will be continued concentrating on improved repair processes and repair strategies to enable beyond the BRSL composite repairs. The key element in overcoming current repair size limits and to ensure the damage tolerance of damaged structures for bonded repairs is to understand the damage propagation in composite structures and especially in the bondline. From manufacturing point of view the hard patch and co-bonded patch methods with applicable adhesives will be in question.

The entire project falls into two major Work Packages (WP): In the design/analyses WP, the objective is to understand the fundamental principles of adhesive bonding, to analytically/numerically find out the conditions for defect growth threshold after which the crack starts to grow and from that establish basis for larger repair procedures. In the SHM WP, the project work focuses on the use of structural health monitoring (SHM) systems to support the monitoring and overall maintenance of the composite repair.

The work will be performed by an international consortium consisting of 15 industrial and scientific partners from six European countries enabled to participate in EDA's projects, countries alphabetically: Czech Republic: Czech Aerospace Research Centre (VZLU); Finland: Tampere University (TAU), Patria Aviation, VTT Technical Research Centre of Finland; Germany: Bundeswehr Research Institute for Materials, Fuels and Lubricants (WIWeB), Airbus Defence and Space, University of Stuttgart (USTUTT); Italy: Politecnico di Milano (POLIMI); the Netherlands: NLR, KVE Composites Repair, Fokker Services B.V; Norway: Norwegian Defence Materiel Agency (NDMA), Norwegian Defence Research Establishment (FFI), FiReCo, Light Structures. Project Lead Contractor is NLR (the Netherlands). Tampere University is the Finnish national coordinator of the project (see also Chapter 2.4.1) and the Finnish Defence Forces Logistics Command (FDFLOGCOM) is the national bill paying authority of the project.

3.3 Quantification of optical distortions near industrialization and the follow-on project to quantify scratches and dents on aircraft transparencies and their repair instructions near successful completion

The need to automatically characterize and quantify optical distortions transparencies has been studied since 1960 [12] and methods has been developed for film photography e.g. the double exposure method, ASTM F733-09 [16] and Grid Line Slope method, ASTM F2156-11 [17]. Also fully automated systems based on digital imaging and machine learning have been developed [19], [64].

The FINAF expressed an interest to have a fully automated capability for measuring and quantifying optical distortions on aircraft transparencies with the following FINAF-specific requirements:

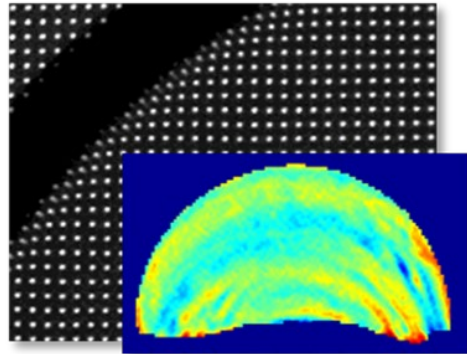
- Systematic, reproducible results
- Remove subjectivity related to human observers with an automated system
- Measure distortions and classify transparencies to pre-defined categories regarding their usability (pass / fail / subject to repair)
- Provide information for maintenance
- Track changes in transparencies (service history in view of sustainment aspects)
- Measure transparencies without removing them from aircraft.

Thus, the FINAF tasked VTT to develop a fully automated optical distortion detection system for measuring and quantifying optical distortions on the FINAF F/A-18C transparencies. VTT executed the XPARENCY project in two phases in close collaboration with the FINAF and Patria Aviation:

- XPARENCY Phase 1 (an “off-aircraft” laboratory-level demo system, in which the F/A-18 windshield could be inspected in a controlled laboratory environment, including additional ideas on how to develop the system further, **Figure 66**).
- XPARENCY Phase 2 (an “on-aircraft” proof-of-concept system, in which the F/A-18C windshield and canopy could be inspected in normal hangar environments while these transparencies were installed “mission ready” in the aircraft).

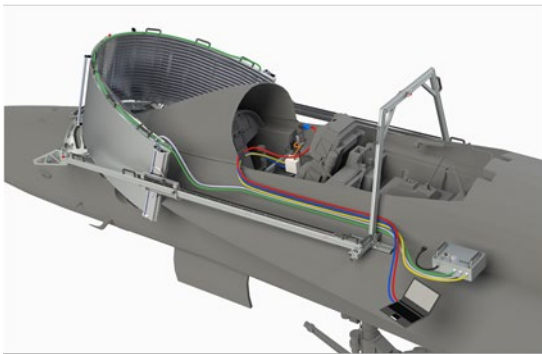


XPARENCY Phase 1 Lab system
ASTM F733 & F2156

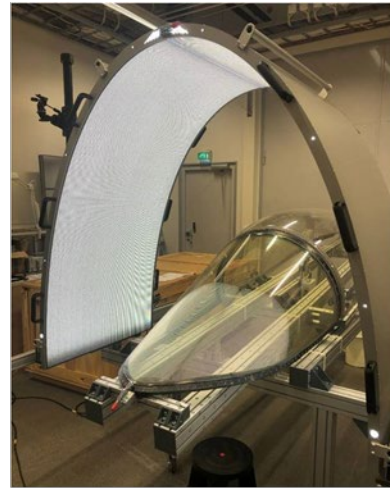


XPARENCY Phase 1 Lab system
Projector-based Approach (new)

Figure 66: An overview of the XPARENCY's "off-aircraft" Phase 1 transparency optical distortion detection system [59]. Figure courtesy of VTT.



Finalized XPARENCY design



Functional XPARENCY prototype at Insta



XPARENCY fitting to F/A-18

Figure 67: XPARENCY development from drawing board to reality by Insta ILS Oy. Figure courtesy of Insta ILS Oy and the FDF.

Following VTT's successful demonstration of the "on-aircraft" optical distortion detection system's functional prototype, a Finnish company Insta ILS Oy started upgrading the Technology Readiness Level (TRL) to define a new product (**Figure 67**). The XPARENCY1 on-aircraft measurement system based on the VTT built prototype is now fully functional at Insta's facilities and ready for the Final Acceptance Tests by the FDFLOGCOM who is the launch customer with its F/A-18 fleet. The XPARENCY1 may be easily adapted to any other aircraft windshield and canopy measurement needs.

Parallel to the above industrialization activities of the XPARENCY Phase 2, the FDFLOGCOM JSC tasked VTT to develop the system further, to build upon the existing XPARENCY proof-of-concept and expand to the detection and quantifying of scratches, dents and haze in the F/A-18C windshields and canopies. This follow up project, named XPARENCY2, is near its successful completion with three resulting prototypes for the consecutive measurements tasks listed in **Figure 68**:

- Task A aims for automatic mapping and detection of all scattering defects in both windshield and canopy.
- Task B continues by measuring the accurate dimensions of individual defects.
- Finally, task C uses the distortion information measured with XPARENCY Phase 2 -system with the defect information gathered from tasks A-B and simulates the repair and its effect to the optical distortion for optimisation. VTT developed repair simulation tools to verify if simulations of repair effects work in real life in view of resulting (new, anticipated) optical distortions. In other words, the repair can be simulated to see if the transparency's actual repair is feasible.

Several technologies were screened and ranked by VTT for the tasks, from which camera based methods were selected for the above tasks A and B. The optical simulation in task C builds upon the tools, methods and knowledge on optical simulation of VTT's Optical Measurements Team. VTT developed the methods for all the tasks A-C in close collaboration with the FDF experts. The chosen methods were confirmed with real F/A-18C transparency samples and validated with laboratory measurements.

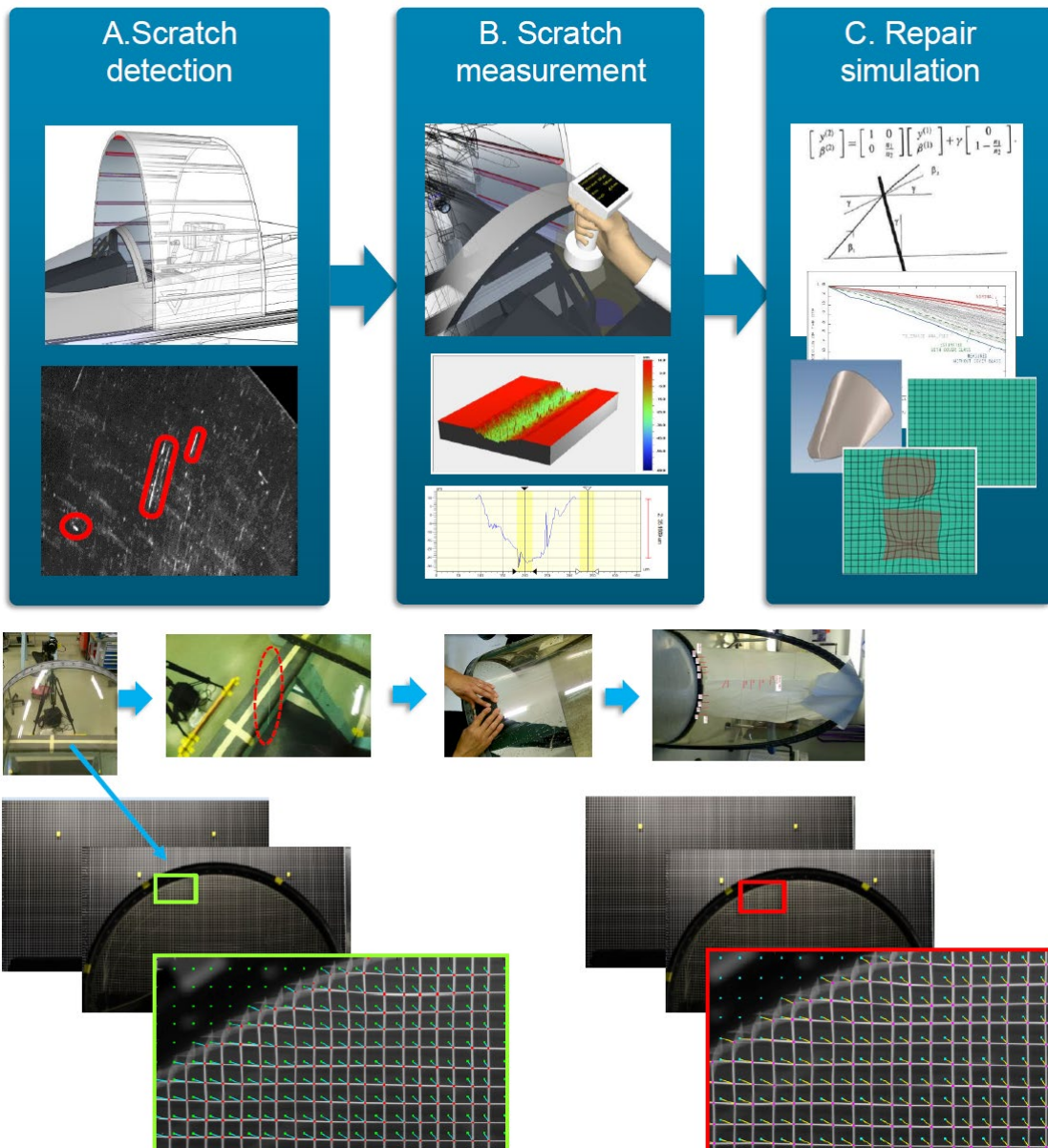


Figure 68: An overview of the XPARENCY2 “on-aircraft” system to detect and quantify scratches, dents, and haze in the F/A-18C windshields and canopies [60]. Figure courtesy of VTT.

References

- [1] **From Observation Sorties to Multi-Role Fighters.** 2019. The Finnish Air Force web page. Retrieved from <https://ilmavoimat.fi/en/history>
- [2] **Valmet L-70 Vinka.** 2021. The Finnish Defence Forces web page. Retrieved from <https://puolustusvoimat.fi/en/equipment#/asset/view/id/207>
- [3] **Grob G 115E.** 2021. The Finnish Defence Forces web page. Retrieved from <https://puolustusvoimat.fi/en/equipment#/asset/view/id/205>
- [4] **BAE Systems Hawk.** 2021. The Finnish Defence Forces web page. Retrieved from <https://puolustusvoimat.fi/en/equipment#/asset/view/id/202>
- [5] **Boeing F/A-18 Hornet.** 2021. The Finnish Defence Forces web page. Retrieved from <https://puolustusvoimat.fi/en/equipment#/asset/view/id/201>
- [6] **All Finnish Air Force's Hornets Upgraded to MLU 2.** 2017. The Finnish Air Force web page. Retrieved from http://ilmavoimat.fi/en/article/-/asset_publisher/kaikki-ilmavoimien-hornetit-on-nyt-paivitetty-mlu-2-tasoon. Published in English on 5.1.2017 at 10.21.
- [7] **Long-Term Development Key to Sustained Air Defence Capability.** 2021. The Finnish Air Force web page. Retrieved from https://ilmavoimat.fi/en/development_of_finlands_air_defense_capability.
- [8] **Preliminary Assessment for Replacing the Capabilities of the Hornet Fleet, Final Report.** 2015. Helsinki: Ministry of Defence. ISBN 978-951-25-2680-2. Available as pdf from https://www.defmin.fi/files/3178/Preliminary_Assessment_for_Replacing_the_Capabilities_of_the_Hornet_Fleet.pdf.
- [9] **HX Program - new fighters for Finland by 2025.** 2021. Ministry of Defence web page. Retrieved from https://www.defmin.fi/en/frontpage/administrative_branch/strategic_capability_projects/hx_fighter_program/hx_fighter_program#6e21980d
- [10] **HX Challenge completed successfully.** 2020. The Finnish Air Force web page. Retrieved from <https://ilmavoimat.fi/en/-/hx-challenge-completed-successfully>
- [11] **Final Quotations for HX Fighter Programme Received.** 2021. Ministry of Defence web page. Retrieved from https://www.defmin.fi/en/topical/press_releases_and_news/final_quotations_for_hx_fighter_programme_received.11940.news#6e21980d
- [12] Amosov, N. I. 1958. **Estimating the optical distortion from curved automobile glass.** Glass and Ceramics, 15 (1958), 427-429, <https://doi.org/10.1007/BF00678735>.
- [13] **AFGROW - Fracture Mechanics and Fatigue Crack Growth Analysis software tool.** 2021. Ohio: LexTech, Inc. Available at: <https://www.afgrow.net/>
- [14] **ASTM D5656-10.** 2017. **Standard Test Method for Thick-Adherend Metal Lap-Shear Joints for Determination of the Stress-Strain Behavior of Adhesives in Shear by Tension Loading.** ASTM International, West Conshohocken, PA, USA. <https://doi.org/10.1520/D5656-10R17>.
- [15] **ASTM E2862-18.** 2018. **Standard Practice for Probability of Detection Analysis for Hit/Miss Data.** ASTM International, West Conshohocken, PA, USA. <https://doi.org/10.1520/E2862-18>.

- [16] ASTM F733-09. 2009. **Standard Practice for Optical Distortion and Deviation of Transparent Parts Using the Double-Exposure Method**. ASTM International, West Conshohocken, PA, USA. <https://doi.org/10.1520/F0733-09>.
- [17] ASTM F2156-11. 2011. **Standard Test Method for Measuring Optical Distortion in Transparent Parts Using Grid Line Slope**. ASTM International, West Conshohocken, PA, USA. <https://doi.org/10.1520/F2156-11>.
- [18] Colmenero Diaz, O. **Multi-scale simulation of low-speed impact loads on Carbon Fibre Reinforced Polymer (CFRP) panels - An application to a thin rigid aerospace panel**. M.Sc. thesis. Aalto University, Finland. Submitted (2021).
- [19] Dixon, M., Glaubius, R., Freeman, P. et al. 2011. **Measuring optical distortion in aircraft transparencies: a fully automated system for quantitative evaluation**. Machine Vision and Applications, 22 (2011), 791-804, <https://doi.org/10.1007/s00138-010-0258-z>.
- [20] Dsouza, R., Antunes, P., Kakkonen, M., Jokinen, J., Sarlin, E., Kallio, P. and Kanerva, M. 2020. **3D interfacial debonding during microbond testing: Advantages of local strain recording**. Composites Science and Technology, 195 (2020), <https://doi.org/10.1016/j.compscitech.2020.108163>.
- [21] Hoffren, J. 2019. **Interface load modelling for Hornet wing**. Report № HN-L-0320 (in Finnish, classified). Tampere: Patria Aviation Oy.
- [22] Hoffren, J. 2020. **Flow study for Hornet engine inlet duct**. Report № HN-A-0003 (in Finnish, classified). Tampere: Patria Aviation Oy.
- [23] Hukkanen, T. 2019. **Risk Analysis of Changes in Hornet SSP Modification Program**. Technical Report № HN-L-0316 (in Finnish, classified). 101 p. Halli: Patria Aviation Oy.
- [24] Hukkanen, T. 2019. **Analysis Method for Risk Level Assessment in Structural Integrity Program**. Technical Report № HN-L-0341 (in Finnish, classified). 46 p. Halli: Patria Aviation Oy.
- [25] ICAF. 2001. **A Review of Recent Aeronautical Fatigue Investigations in Finland until March 2001**. (A. Siljander, Ed.). Research Report № BVAL33-011139. Espoo: VTT Technical Research Center of Finland. Available at: http://www.vtt.fi/inf/julkaisut/muut/2001/icaf_2001_finland_review.pdf.
- [26] ICAF. 2003. **A Review of Aeronautical Fatigue Investigations in Finland during the Period February 2001 - March 2003**. (A. Siljander, Ed.). Research Report № BTUO33-031123. Espoo: VTT Technical Research Center of Finland. Available at: http://www.vtt.fi/inf/julkaisut/muut/2003/icaf_2003_finland_review.pdf.
- [27] ICAF. 2005. **A Review of Aeronautical Fatigue Investigations in Finland during the Period April 2003 - April 2005**. (A. Siljander, Ed.). Research Report № BTUO33-051366. Espoo: VTT Technical Research Center of Finland. Available at: http://www.vtt.fi/inf/julkaisut/muut/2005/icaf_2005_finland_review_issue1.pdf.
- [28] ICAF. 2007. **A Review of Aeronautical Fatigue Investigations in Finland during the Period May 2005 - April 2007**. (A. Siljander, Ed.). ICAF Doc № 2410 (Research Report № VTT-R-03406-07). Espoo: VTT Technical Research Center of Finland. Available at: http://www.vtt.fi/inf/julkaisut/muut/2007/ICAF_FinlandReview_2007.pdf.
- [29] ICAF. 2009. **A Review of Aeronautical Fatigue Investigations in Finland May 2007 - April 2009**. (A. Siljander, Ed.). ICAF Doc № 2418 (Research Report № VTT-R-02540-09). Espoo: VTT Technical Research Center of Finland. Available at: http://www.vtt.fi/inf/julkaisut/muut/2009/ICAF_Doc2418.pdf.

- [30] ICAF. 2011. **A Review of Aeronautical Fatigue Investigations in Finland May 2009 - March 2011.** (E. Peltoniemi, A. Siljander, Eds.). ICAF Doc № 2427 (Research Report № VTT-R-02827-11). Espoo: VTT Technical Research Center of Finland. Available at: https://cris.vtt.fi/ws/portalfiles/portal/45002287/ICAF_Doc2427_FinlandReview_2011.pdf.
- [31] ICAF. 2013. **A Review of Aeronautical Fatigue Investigations in Finland April 2011 - February 2013.** (A. Siljander, Ed.). ICAF Doc № 2428 (Research Report № VTT-R-02105-13). Espoo: VTT Technical Research Center of Finland. Available at: https://cris.vtt.fi/ws/portalfiles/portal/45002373/ICAF_FinlandReview_2013_issue1_3April13.pdf.
- [32] ICAF. 2015. **A Review of Aeronautical Fatigue Investigations in Finland March 2013 - February 2015.** (A. Siljander, P. Varis, Eds.). ICAF Doc № 2432 (Research Report № VTT-CR-01811-15). Espoo: VTT Technical Research Center of Finland Ltd. Available at: http://www.vtt.fi/inf/julkaisut/muut/2015/ICAF_Doc_No_2432_FinlandReview_2015_issue_1_21May15.pdf.
- [33] ICAF. 2017. **A Review of Aeronautical Fatigue Investigations in Finland March 2015 - March 2017.** (T. Viitanen, P. Varis, A. Siljander, Eds.). ICAF Doc № 2433 (Research Report № VTT-CR-02002-17). Espoo: VTT Technical Research Center of Finland Ltd. Available at: http://www.vtt.fi/inf/julkaisut/muut/2017/ICAF_Doc2433_Finland_Review_2017.pdf.
- [34] ICAF. 2019. **A Review of Aeronautical Fatigue Investigations in Finland April 2017 - March 2019.** (T. Viitanen, A. Siljander, Eds.). (Research Report № VTT-CR-00352-19). Espoo: VTT Technical Research Center of Finland Ltd. Available at: https://cris.vtt.fi/ws/portalfiles/portal/24743703/ICAF_Finland_Review_2019.pdf.
- [35] Jokinen, J. 2019. **Numerical crack nucleation and propagation analyses of bonded joints.** Doctoral dissertation, Espoo: Aalto University, School of Engineering, Department of Mechanical Engineering, 135 p. Available at: <http://urn.fi/URN:ISBN:978-952-60-8825-9>.
- [36] Jokinen, J., Orell, O. and Kanerva, M. 2021. **Experimental inspections of materials and structures using DIC.** In: Koivisto, J. and Nousiainen, M. (Eds.) Annual Book of Defence Research 2021 (in Finnish). Riihimäki: The Finnish Defence Forces, pp. 50-52. ISBN 978-951-25-3171-4. Available at: <https://puolustusvoimat.fi/-/puolustustutkimuksen-vuosikirja-2021>.
- [37] Jokinen, J., Wallin, M. and Kanerva, M. 2020. **The influence of the number of adhesive plies (FM 300-2) on fracture properties.** The 32nd Congress of the International Council of the Aeronautical Sciences (ICAS2020), *Accepted for publication*.
- [38] Jokinen, J., Wallin, M. and Kanerva, M. 2020. **Adjusted shapes of adhesively bonded repair patches of the early indication of debonding in fighter aircraft structures.** The 32nd Congress of the International Council of the Aeronautical Sciences (ICAS2020), *Accepted for publication*.
- [39] Jokinen, J., Orell, O., Wallin, M. and Kanerva, M. 2020. **A concept for defining mixed-mode behaviour of tough epoxy film adhesives by single specimen design.** Journal of Adhesion Science and Technology, 34:18, 1982-1999, <https://doi.org/10.1080/01694243.2020.1746606>.
- [40] Jokinen, J., Wallin, M., Kanerva, M. and Saarela, O. 2020. **Analyses of criticality for multiple site delaminations in the flap spar of Finnish F/A-18 aircraft.** The Aeronautical Journal, Volume 125, Issue 1285, March 2021, pp. 556 - 577, <https://doi.org/10.1017/aer.2020.69>.
- [41] Jokinen, J., Wallin, M. and Saarela, O. 2015. **Applicability of VCCT in mode I loading of yielding adhesively bonded joints - a case study.** International Journal of Adhesion and Adhesives, Volume 62, October 2015, pp. 85 - 91, <https://doi.org/10.1016/j.ijadhadh.2015.07.004>.

- [42] Kaikkonen, J. 2021. **Detailed FE model of Hornet Dorsal Deck Y453-Y557.5**. Report № HN-L-0294 (in Finnish, classified). Tampere: Patria Aviation Oy.
- [43] Koski, K. 2020. **Small crack growth in Al 7050-T745**. Research Report № VTT-R-00528-20 (in Finnish, classified). Espoo: VTT Technical Research Center of Finland Ltd.
- [44] Koski, K. 2020. **Boltjoints2**. Memorandum № VTT-R-00208-20 (classified). Espoo: VTT Technical Research Center of Finland Ltd.
- [45] Laakso, R. 2021. [In preparation] **Rudder Tests. Issue 1, Rev0.90**. Customer Report № VTT-CR-00133-20 (classified). Espoo: VTT Technical Research Centre of Finland Ltd
- [46] Laakso, R. 2021. **SHM quality**. Memorandum № VTT-M-00492-20 (in Finnish, classified). Espoo: VTT Technical Research Center of Finland Ltd.
- [47] Laatikainen, Y., Hukkanen, T. and Vuori, M. 2020. **GO Mini-OLM flight preparations**. Technical Report № GO-S-0011 (in Finnish, classified). Halli: Patria Aviation Oy.
- [48] **LifeWorks User's Manual**, Finland Air Force Version. 2004. The Boeing Company, July 26, 2004, Revision A.
- [49] Liius, M. 2021. **Life estimation with crack initiation and crack growth analysis of Hornet Inner Wing Front Spar Fasteners 178, 184, 1438 and 1439**. Report № HN-L-0342 (in Finnish, classified). Tampere: Patria Aviation Oy
- [50] Liius, M. 2020. **Life estimation with crack initiation and crack growth analysis of Hornet dorsal longeron fastener hole #45 and splice plate -2005-2007**. Report № HN-L-0337 (in Finnish, classified). Tampere: Patria Aviation Oy.
- [51] Liukkonen, S. 2020. **HN-432 Onboard HOLM System's Electrical Calibration 2020**. Research Report № VTT-R-00059-20 (in Finnish, classified). Espoo: VTT Technical Research Center of Finland Ltd.
- [52] Liukkonen, S. 2020. **Grob Mini-OLM - GO-12 strain sensor installations**. Research Report № VTT-R-00829-20 (in Finnish, classified). Espoo: VTT Technical Research Center of Finland Ltd.
- [53] Malmi, S. 2021. **F/A-18 Hornet, SAFE Fatigue Tracking of Structures, Management Report, Period 3, 2020**. Report № HN-L-1070 (in Finnish, classified). Tampere: Patria Aviation Oy.
- [54] Malmi, S. 2021. **Shear force fatigue spectrum comparison of Hornet former Y508 wing shear tie**. Report № HN-L-0335 (in Finnish, classified). Tampere: Patria Aviation Oy.
- [55] Malmi, S. 2019. **Hawk Mk.66, Development of Neural Network (NN) -based fatigue tracking environment and fatigue tracking of the Tail**. Report № HW-S-0035 (in Finnish, classified). Tampere: Patria Aviation Oy.
- [56] Malmi, S. and Hoffren, J. 2020. **Operational spectra for Hornet wing interface loads**. Report № HN-L-0332. (in Finnish, classified). Tampere: Patria Aviation Oy.
- [57] Malmi, S. and Liius, M. 2020. **Fatigue analysis and critical crack size estimation of Hornet former Y508 wing shear tie**. Report No HN-L-0266 rev A (in Finnish, classified). Tampere: Patria Aviation Oy.
- [58] Nieminen, V. 2019. **Modal Testing of Vertical Tail of F/A-18 Hornet**. Research Report № VTT-R-01234-19 (classified). Espoo: VTT Technical Research Center of Finland Ltd.
- [59] Okkonen, M. et al. 2016. **XPARENCY final report**. Customer Report № VTT-CR-00840-16 (in Finnish, classified). Oulu: VTT Technical Research Center of Finland Ltd.

- [60] Okkonen, M. and Mäyrä, A. 2018. **Optical Simulation of Scratch Repair in F/A-18's**. ASTM Committee F07.08 on Aerospace Transparent Materials and Enclosures, Washington DC, USA. 7 November, 2018.
- [61] Roderer, O., Pärnänen, T., Jokinen, J., Lindgren, M., Sarlin, E. and Kanerva, M. 2021. **Chemical ageing effects on the ply and laminate strength of a filament wound cross-ply GFRP**. Composite Structures (260), <https://doi.org/10.1016/j.compstruct.2020.113508>.
- [62] Tikka, J. and Salonen, T. 2007. **Parameter Based Fatigue Life Analysis of F18 Aircraft**. In: Lazzeri, L. and Salvetti, A. (Eds.) Durability and Damage Tolerance of Aircraft Structures: Metals vs. Composites, Volume I, Proceedings of the the 24th Symposium of the International Committee on Aeronautical Fatigue, Naples, Italy. 16-18 May 2007. Pisa, Italy: Pacini Editore, 2007, pp. 412-426. ICAF-Doc. 2417.
- [63] Tikka, J. and Salonen, T. 2015. **Practical Experience of Neural Network Based Fatigue Life Monitoring**. In: Siljander, A. (Ed.) Embracing the future - respecting the past; supporting aging fleets with new technologies, Proceedings of the 34th Conference and the 28th Symposium of the International Committee on Aeronautical Fatigue and Structural Integrity, Helsinki, Finland. 1-5 June 2015, pp. 879-888. ISBN 978-951-38-7442-1.
- [64] TOPINS. 2021. Retrieved from <http://www.topinnsolution.com/>
- [65] Varis, P., Juntunen, J., Isotahdon, E., Marja-aho, M., Siljander, A., Metsäjoki, J. and Koski, K. 2019. **Small crack growth study**. Customer Report № VTT-CR-03255-18 (in Finnish, classified). Espoo: VTT Technical Research Center of Finland Ltd.
- [66] Viitanen, T. 2019. **HUTFLY2 Flight Simulation Software - Update for the F/A-18C mass model**. Research Report № VTT-R-00560-19 (in Finnish, classified). Espoo: VTT Technical Research Center of Finland Ltd.
- [67] Viitanen, T. 2019. **F/A-18C Hornet Landing Simulations, Phase 3**. Research Report № VTT-R-00697-19 (classified). Espoo: VTT Technical Research Center of Finland Ltd.
- [68] Viitanen, T. 2019. **Store Configurations of the FINAF BOS2 flight data set**. Memorandum VTT-M-01115-19 (classified). Espoo: VTT Technical Research Center of Finland Ltd.
- [69] Viitanen, T. 2019. **HN-416 Onboard HOLM System's Electrical Calibration 2019**. Research Report № VTT-R-00678-19 (in Finnish, classified). Espoo: VTT Technical Research Center of Finland Ltd.
- [70] Viitanen, T. 2020. **The F/A-18 fatigue cracks database v5.0: Part number specific fatigue cracking observations**. VTT Research Report № VTT-R-01441-20 (in Finnish, classified). Espoo: VTT Technical Research Center of Finland.
- [71] Viitanen, T. 2020. **Trajectory comparisons for the JDAM Mk82 store**. Research Report № VTT-R-00837-20 (in Finnish, classified). Espoo: VTT Technical Research Center of Finland Ltd.
- [72] Viitanen, T. 2021. **FINAF data package 3, Rev. A**. Memorandum № VTT-M-00091-21 (classified). Espoo: VTT Technical Research Center of Finland Ltd.
- [73] Viitanen, T. 2021. **HN-416 Onboard HOLM System's Electrical Calibration 2021**. Research Report № VTT-R-00167-21 (in Finnish, classified). Espoo: VTT Technical Research Center of Finland Ltd.
- [74] Viitanen, T. 2021. **HN-432 Onboard HOLM System's Electrical Calibration 2021**. Research Report № VTT-R-00168-21 (in Finnish, classified). Espoo: VTT Technical Research Center of Finland Ltd.

- [75] Viitanen, T., Laakso, R. and Mäkinen, J. 2019. **HOLM Analyses Database, HOLM_BASE v5.0.0**. Research Report № VTT-M-03240-18 (in Finnish, classified). Espoo: VTT Technical Research Center of Finland Ltd.
- [76] Viitanen, T., Laakso, R. and Mäkinen, J. 2020. **HOLM fatigue analyses, Annual Report 2019**. Research Report № VTT-R-01273-19 (in Finnish, classified). Espoo: VTT Technical Research Center of Finland Ltd.
- [77] Viitanen, T., Koski, K., Laakso, R. (VTT) and Janhunen, H. (Trano Oy). 2020. **The effect of air-to-ground (A/G) training on the structure of the FINAF F/A-18C Hornet**. Research Report № VTT-R-01207-20 (in Finnish, classified). Espoo: VTT Technical Research Center of Finland Ltd.
- [78] Virkkunen, I. 2021. **The "Small crack problem" in hit/miss Probability of Detection**, to be published. Espoo: Trueflaw Ltd.
- [79] Virkkunen, I. 2020. **Finnish POD round robin study final results**. Report № 310CAQ510v2 (classified). Espoo: Trueflaw Ltd.
- [80] Virkkunen, I., Koskinen, T., Papula, S. et al. 2019. **Comparison of \hat{a} Versus a and Hit/Miss POD-Estimation Methods: A European Viewpoint**. *J Nondestruct Eval* 38, 89 (2019). <https://doi.org/10.1007/s10921-019-0628-z>
- [81] Vos, J. B., Charbonnier, D., Siikonen, T., Salminen, E., Hoffren, J., Gehri, A., and Stefani, P. 2018. **Swiss/Finnish Collaboration on Aero-elastic simulations for the F/A-18 fighter**. In *2018 Applied Aerodynamics Conference* (p. 3642).
- [82] Wallin, M. 2019. **Test Specification for Step Lap Joint Repair Validation**. Technical Report № HN-K-0037 (classified). 27 p. Halli: Patria Aviation Oy.

Report's title	
A REVIEW OF AERONAUTICAL FATIGUE INVESTIGATIONS IN FINLAND APRIL 2019 - APRIL 2021	
Customer, contact person, address	
Finnish Defence Forces Logistics Command, Joint System Centre, Air Systems Division Mr. Ari Kivistö P. O. Box 69; FI-33541 Tampere; Finland	
Project name	Project number
PIIKKI_2020-2021 - 1.5 TA4_ICAF2021_NR	128638 - 1.5
Editors	Pages
Tomi Viitanen, Aslak Siljander	73
Keywords	Report identification code
ICAF, aeronautical fatigue, military aircraft, fixed wing, structural integrity, FDF, FINAF, Finland	VTT-CR-00448-21/ 24.6.2021
Summary	
<p>This document was prepared for the delivery to the International Committee on Aeronautical Fatigue and Structural Integrity (ICAF) webinar scheduled to be held on 30 June 2021.</p> <p>A review is given of the aircraft structural fatigue research and associated activities which form part of the programs within the Air Force Command Finland (AFCOMFIN), the Finnish Defence Force Logistics Command, Joint Systems Centre (FDFLOGCOM JSC), Air Systems Division; Army Command Finland (ARCOMFIN); Aalto University; Arecap Ltd; Elomatic Ltd; Emmecon Ltd; Eurofins Expert Services Oy; Insta ILS Oy; Patria Aviation Oy; Tampere University; Trano Oy; Trueflaw Ltd; and VTT Technical Research Centre of Finland Ltd (VTT).</p> <p>The review summarizes fatigue related research programs and investigations on specific military aircraft since the previous Finnish National Review (presented in the 36th Conference, ICAF, Krakow, Poland) up to March 2019.</p>	
Confidentiality	Public
Espoo 24 June 2021	
<p>Tomi Viitanen Senior Scientist (VTT), ICAF National Delegate Finland</p> <p>Aslak Siljander Principal Scientist (VTT)</p>	
Editors' contact address	
VTT, P. O. Box 1000, FI-02044 VTT, Finland (Street: Kivimiehentie 3, Espoo, Finland)	
Distribution	
Unclassified. Distribution unlimited. This document has been authorized by the FDFLOGCOM JSC for unlimited public release [Permission № BR10751 / 24.06.2021].	